

**MULTIPLE SCLEROSIS INDUCED  
NEUROPATHIC PAIN**

by

**Farhana Begum**

A Thesis submitted to the Faculty of Graduate Studies of

The University of Manitoba

in partial fulfilment of the requirements of the degree of

**Master of Science**

Department of Human Anatomy and Cell Science

University of Manitoba

Winnipeg

## **ABSTRACT**

Multiple Sclerosis (MS) is an autoimmune disease of the central nervous system (CNS). Antigen induced activation of Th1 cells in the peripheral blood leads to elevated production of inflammatory cytokines such as tumor necrosis factor alpha (TNF- $\alpha$ ) that have been directly linked to disease induction and neuropathic pain. It was hypothesized that following antigenic induction, cytokines gain access to the spinal cord and participate in direct cellular interaction with dorsal horn neurons. Using an animal model of MS, we show that TNF- $\alpha$  gene and protein expression in the dorsal root ganglia (DRG) and spinal cord tissue is increased in the active group. In addition, our findings show TNF- $\alpha$  mRNA expression in the dorsal root entry point. Therefore, our results support the hypothesis that antigen induced DRG derived TNF- $\alpha$  can transport to the spinal cord via the dorsal roots and is involved in the underlying pathogenesis of MS induced neuropathic pain.

## ACKNOWLEDGEMENTS

It is a great pleasure to take this opportunity to convey my sincere thanks to those people who made this thesis possible.

First, I thank my supervisor Dr. Mike Namaka for his continuous support in the Master program. Dr. Namaka was always there to listen and to give advice. His enthusiasm, inspiration, and great efforts especially in explain things adequately helped me gain an appreciation for my research. He taught me how to ask questions and express my ideas. He showed me different ways to approach a research problem and the need to be persistent to accomplish any goal. This paper would not have been possible without his endless support.

A special thanks goes to my co-supervisor, Dr. Emma Frost, who has put in the most effort in helping me complete my research and dissertation. Dr. Frost has been a friend and mentor. She taught me how to write academic papers, made me a better researcher, had confidence in me when I doubted myself, and brought out the good ideas in me (More importantly, she taught me how to work hard and play hard, and how to ski to reduce stress!). Without her encouragement and constant guidance, I could not have finished this dissertation. Best wishes to you Dr. Frost.

Besides my advisors, I would like to thank the rest of my advisory committee: Dr. Thomas Klonisch, for the guiding questions and for rescuing me from various crises. He also gave insightful comments and reviewed my work.

I wish to express my sincere gratitude to Dr. Jean Paterson for her guidance as well as for teaching me different histological staining.

I wish to thank other team members of the Cellular Neuroscience Research Team for their friendly support, interesting discussions and being fun to be with. Thanks, Cellular Neuroscience Research Team!

I am also greatly indebted to Human Anatomy and Cell Sciences Department for their contribution to this long journey. I would also like to thank the HSC Toast Master Club for providing a loving environment.

Last, but not least, I thank my family: my parents, for unconditional support and encouragement to pursue my interests. I am indebted to my siblings for reminding me that my research should always be useful and serve good purposes for all humankind. I wish to thank my husband for his continuous support, encouragement and enthusiasm to complete my research work.

This work was supported through the funding provided by the Biogen Idec, Manitoba Institute of Child Health (MICH) travel award, Faculty of Graduate Studies (FGS) travel award, GSA conference grant, FGS Top Up award and Manitoba Health Research Council (MHRC) studentship award.

# TABLE OF CONTENTS

<b>ABSTRACT</b> .....	<b>i</b>
<b>ACKNOWLEDGEMENTS</b> .....	<b>ii</b>
<b>LIST OF ABBREVIATIONS</b> .....	<b>ix</b>
<b>CHAPTER 1: INTRODUCTION</b> .....	<b>1</b>
<i>THE NERVOUS SYSTEM</i> .....	<b>1</b>
<i>THE BRAIN</i> .....	<b>1</b>
<i>THE SPINAL CORD</i> .....	<b>2</b>
<i>ASCENDING PATHWAYS</i> .....	<b>3</b>
<i>DESCENDING PATHWAYS</i> .....	<b>5</b>
<i>DORSAL ROOT GANGLIA (DRG)</i> .....	<b>6</b>
<i>THE GREY MATTER</i> .....	<b>8</b>
<i>THE WHITE MATTER</i> .....	<b>9</b>
<i>MULTIPLE SCLEROSIS (MS)</i> .....	<b>9</b>
<i>MYELIN</i> .....	<b>10</b>
<i>EPIDEMIOLOGY OF MS</i> .....	<b>12</b>
<i>CLINICAL PRESENTATION OF MS</i> .....	<b>13</b>
<i>ETIOLOGY OF MS</i> .....	<b>14</b>
<i>AUTOIMMUNITY AND MS</i> .....	<b>16</b>
<i>BLOOD BRAIN BARRIER (BBB)</i> .....	<b>17</b>
<i>SYMPTOMS OF MS</i> .....	<b>18</b>
<i>MS ASSOCIATED PAIN</i> .....	<b>19</b>
<i>NEUROPATHIC PAIN</i> .....	<b>19</b>
<i>PAIN TRANSMISSION</i> .....	<b>21</b>
<i>PAIN PROCESSING LOOP</i> .....	<b>21</b>

<i><b>PATHOPHYSIOLOGY OF NEUROPATHIC PAIN</b></i> .....	<b>22</b>
<i><b>IONIC MECHANISM</b></i> .....	<b>22</b>
<i><b>SODIUM CHANNEL</b></i> .....	23
<i><b>POTASSIUM CHANNEL</b></i> .....	23
<i><b>HYPERPOLARIZATION-ACTIVATED CYCLIC NUCLEOTIDE GATED CHANNEL</b></i> .....	23
<i><b>CALCIUM CHANNEL</b></i> .....	24
<i><b>NEUROTRANSMITTER MECHANISMS</b></i> .....	<b>24</b>
<i><b>CYTOKINES</b></i> .....	<b>26</b>
<i><b>TUMOR NECROSIS FACTOR ALPHA (TNF-<math>\alpha</math>)</b></i> .....	<b>27</b>
<i><b>TNF-<math>\alpha</math> RECEPTORS</b></i> .....	27
<i><b>THE FUNCTION OF TNF-<math>\alpha</math></b></i> .....	28
<i><b>NEUROTROPHINS</b></i> .....	<b>29</b>
<i><b>NEUROTROPHIN RECEPTORS</b></i> .....	30
<i><b>NERVE GROWTH FACTOR (NGF)</b></i> .....	30
<i><b>BRAIN DERIVED NEUROTROPHIC FACTOR (BDNF)</b></i> .....	31
<i><b>GLIAL CELL LINE-DERIVED NEUROTROPHIC FACTOR (GDNF)</b></i> .....	32
<i><b>EFFECTS OF NEUROTROPHINS AND CYTOKINES ON OLIGODENDROCYTES</b></i> .....	<b>32</b>
<i><b>NEUROTROPHIN INTERACTIONS</b></i> .....	<b>33</b>
<i><b>DRG/SPINAL CORD MODEL OF MS INDUCED NEUROPATHIC PAIN</b></i> .....	<b>34</b>
<i><b>HYPOTHESIS AND AIMS</b></i> .....	<b>36</b>
<i><b>HYPOTHESIS</b></i> .....	36
<i><b>SPECIFIC AIMS</b></i> .....	36
 <i><b>CHAPTER 2: MATERIALS AND METHODS</b></i> .....	 <b>37</b>
<i><b>ANIMAL MODEL</b></i> .....	<b>37</b>
<i><b>EXPERIMENTAL ANIMALS</b></i> .....	<b>38</b>
<i><b>INDUCTION OF EAE</b></i> .....	<b>38</b>
<i><b>CLINICAL ASSESSMENT</b></i> .....	<b>40</b>
<i><b>BEHAVIORAL ASSESSMENTS</b></i> .....	<b>40</b>
<i><b>THERMAL SENSORY TESTING</b></i> .....	40
<i><b>MECHANICAL ALLODYNIA</b></i> .....	41
<i><b>TISSUE COLLECTION</b></i> .....	<b>41</b>
<i><b>ANIMAL PERFUSION</b></i> .....	<b>41</b>

<i>DECALCIFICATION OF SPINAL COLUMN</i> .....	43
<i>TISSUE PREPARATION AND FROZEN SECTIONS</i> .....	44
<i>TISSUE COLLECTION FOR QUANTITATIVE REAL-TIME PCR (qRT PCR)</i> .....	44
<i>IMMUNOHISTOCHEMICAL (IHC) CYTOKINE ANALYSIS</i> .....	45
<i>QUANTIFICATION OF IMMUNOHISTOCHEMISTRY</i> .....	46
<i>IN SITU HYBRIDIZATION (ISH)</i> .....	46
<i>IMAGE ANALYSIS</i> .....	48
<i>QUANTITATIVE REAL- TIME POLYMERASE CHAIN REACTION (qRT-PCR)</i> .....	48
<i>TOTAL RNA ISOLATION</i> .....	49
<i>REVERSE TRANSCRIPTASE (RT)</i> .....	50
<i>AMPLIFICATION</i> .....	50
<i>PURIFICATION OF DOUBLE-STRANDED DNA</i> .....	53
<i>STANDARD CURVES FOR QUANTIFICATION OF DNA</i> .....	53
<i>AMPLIFICATION OF SAMPLES</i> .....	56
<i>STATISTICAL ANALYSIS</i> .....	57
<b>CHAPTER 3: RESULTS</b> .....	<b>58</b>
<i>IMMUNOHISTOCHEMICAL (IHC) ANALYSIS OF TNF- <math>\alpha</math> EXPRESSION</i> .....	58
<i>IN SITU HYBRIDIZATION (ISH)</i> .....	58
<i>QUANTITATIVE REAL-TIME PCR (qRT-PCR)</i> .....	58
<i>NEUROLOGICAL DISABILITY ASSESSMENTS</i> .....	59
<i>BEHAVIORAL ASSESSMENTS</i> .....	59
<i>ASSESSMENT OF SENSITIVITY TO NOXIOUS HEAT (THERMAL HYPOALGESIA/THERMAL HYPERALGESIA)</i> .....	59
<i>ASSESSMENT OF SENSITIVITY TO TOUCH (MECHANICAL ALLODYNIA)</i> .....	60
<i>CELLULAR SOURCE OF TNF-<math>\alpha</math></i> .....	60
<b>CHAPTER 4: FIGURES AND TABLES</b> .....	<b>61</b>
<i>Figure 1: Classification of spinal cord neurons involved in afferent pain transmission</i> .....	61
<i>Figure 2: Classification of Interneuron</i> .....	62
<i>Figure 3: Evolutionary Classification of Dorsal Root Ganglia (DRG)</i> .....	63
<i>Figure 4: Classification of sensory afferent fibers involved in pain transmission</i> .....	65

<i>Figure 5: Development of lymphocytes and subtypes of T cells.</i> .....	66
<i>Figure 6: Pathway of pain impulse transmission (PNS to CNS).</i> .....	68
<i>Figure 7: Model of MS associated neuropathic pain &amp; demyelination.</i> .....	70
<i>Figure 8: Cross section of the 6% TCA decalcified spinal cord stained with hematoxylin and eosin (H&amp;E) stain.</i> .....	72
<i>Figure 9: Rat spinal cord myelin structure after 6% TCA solution decalcification of the vertebral column.</i> .....	74
<i>Figure 10: TNF-<math>\alpha</math> double immunohistochemistry.</i> .....	76
<i>Figure 11: TNF-<math>\alpha</math> immunoreactivity in the DRG.</i> .....	77
<i>Figure 12: TNF-<math>\alpha</math> immunoreactivity in the spinal cord.</i> .....	78
<i>Figure 13: In situ hybridization for detection of TNF-<math>\alpha</math> mRNA.</i> .....	79
<i>Figure 14: In situ hybridization for detection of TNF-<math>\alpha</math> mRNA within the spinal cord.</i> .....	80
<i>Figure 15: Real-time PCR results of TNF-<math>\alpha</math> expression within DRG.</i> .....	81
<i>Figure 16: Normalized Real-time PCR results of TNF-<math>\alpha</math> expression within spinal cord.</i> .....	82
<i>Figure 17: Global Neurological Disability Score for animals induced to a state of EAE.</i> .....	83
<i>Figure 18 (A-G): Detailed Neurological Disability Scores for active EAE animals.</i> .....	84
<i>Figure 19: Normalized thermal withdrawal latencies in EAE15 rats for tail relative to time of disease onset.</i> .....	87
<i>Figure 20: Thermal withdrawal latencies normalized to baseline responses (average of Day -4 to Day -1).</i> .....	88
<i>Figure 21: Mechanical withdrawal thresholds normalized to baseline responses (average of Day -4 to Day -1).</i> .....	89
<i>Figure 22: Percentage of TNF-<math>\alpha</math> positive neurons in DRG.</i> .....	90
<i>Figure 23: Cell size distribution of TNF-<math>\alpha</math> positive neurons in DRG.</i> .....	91
<i>Table1: Afferent fibers innervation into the spinal cord laminae (Millan, 1999).</i> .....	92
<i>Table 2: Animal usage: N=66.</i> .....	92
<i>Table 3: Neurological Disability Clinical Scoring System for animals induced to a state of EAE.</i> .....	93
<i>Table 4: Summary of tissue analysis.</i> .....	93

<b>CHAPTER 5: DISCUSSION .....</b>	<b>94</b>
<i>TNF-<math>\alpha</math> PROTEIN AND GENE EXPRESSION .....</i>	<i>94</i>
<i>NEUROLOGICAL DISABILITY ASSESSMENTS .....</i>	<i>98</i>
<i>BEHAVIORAL ASSESSMENTS .....</i>	<i>98</i>
<i>CELLULAR SOURCE OF TNF-<math>\alpha</math> EXPRESSION.....</i>	<i>100</i>
<b>CHAPTER 6: LIMITATIONS AND FUTURE RESEARCH CONSIDERATIONS .....</b>	<b>101</b>
<b>CHAPTER 7: SUMMARY AND CONCLUSIONS .....</b>	<b>103</b>
<b>CHAPTER 8: REFERENCES .....</b>	<b>105</b>
<b>CHAPTER 9: APPENDIX.....</b>	<b>117</b>

## LIST OF ABBREVIATIONS

AC= active control  
BBB= blood brain barrier  
BDNF= brain-derived neurotrophic factor  
CNS= central nervous system  
CGRP= calcitonin gene related peptide  
DH= dorsal horn  
DRG= dorsal root ganglia  
Dpi= post disease induction  
EAE= experimental autoimmune encephalomyelitis  
GABA= gamma aminobutyric acid  
HCN= hyperpolarization-activated cyclic nucleotide gated  
IL-12= interleukin-12  
IFN- $\gamma$ = interferon gamma  
IHC= immunohistochemistry  
ISH= in situ hybridization  
K+= potassium ion  
MBP= myelin basic protein  
MOG= myelin oligodendrocyte glycoprotein  
NE= norepinephrine  
Na+= sodium ion  
NPY= neuropeptide Y  
NC=Naïve control  
NGS=normal goat serum  
NGF= nerve growth factor  
NT-3= neurotrophin-3  
NT-4/5= neurotrophin-4/5

NDS=normal donkey serum  
OL= oligodendrocyte  
PLP=proteolipid protein  
PNS= peripheral nervous system  
PAG= peraqueductal grey  
PBS= phosphate buffer saline  
qRT-PCR= quantitive real time polymerase chain reaction  
RT= room temperature  
SP = substance P  
SNL= spinal nerve ligation  
STT= spinothalamic tract  
SRT= spinoreticular tract  
SMT=spinomesencephalic tract  
TNF- $\alpha$ = tumor necrosis factor alpha  
TNFR1= tumor necrosis factor alpha receptor 1  
TNFR2=tumor necrosis factor alpha receptor 2  
Th0= naïve helper T cell  
Th1= type 1 helper T cell  
TrkA= tyrosine kinase A  
TrkB= tyrosine kinase B  
TrkC= tyrosine kinase C  
WM= white matter

## **CHAPTER 1: INTRODUCTION**

### ***THE NERVOUS SYSTEM***

The nervous system is a very complex system in the body which monitors and controls a variety of organ systems through positive or negative feedback loops. The two main divisions of the nervous system are: the CNS which encompasses the brain and spinal cord and the peripheral nervous system (PNS) which encompasses the receptors and effector targets of the body, the peripheral ganglia, and the nerve processes. The PNS directly connects to the CNS and together they regulate normal physiological functioning within the body.

### ***THE BRAIN***

The brain is a very complex organ, composed of two broad classes of cells: neurons and glia. The mature brain contains 100 billion neurons and about 10 times more glial cells (Noctor et al., 2007; Azevedo et al., 2009). Neurons are highly specialized, excitable cells, capable of receiving information from other cells for subsequent integration and transmission to other neurons and a variety of non-neuronal cells of the CNS. Glial cells represent the second main class of cells which function to provide support and nutrition via paracrine mechanisms to neurons. In addition, these non-neuronal cell types are also involved in executing the critical nervous system functions of information processing, plasticity, learning and memory (Temburni and Jacob, 2001). The major subtypes of CNS glial cells are astrocytes, oligodendrocytes, microglia and ependymal cells.

## ***THE SPINAL CORD***

The spinal cord is the second major component of the CNS which represents the main pathway for conveying information between the PNS and the brain. It originates below to the brainstem and extends down to the space between first and second lumbar vertebrae.

Based on cross-sectional structural analysis of the spinal cord, it is divided into grey matter located around the deeper central core and white matter located primarily in the outer external layers of the cord. The grey matter of the spinal cord is divided into 10 laminae (Wall, 1967). Based on the type of sensory stimulus conducted from the periphery, different types of sensory afferent fibers terminate their projections into specific spinal cord laminae. The 10 laminae are divided into specific sections as follows: laminae I (marginal layer), II (substantia gelatinosa), III and IV (nucleus proprius) and V and VI (deep layers) comprise the dorsal horn (DH). Lamina VII corresponds to the intermediate grey matter, laminae VIII and IX comprise the medial and lateral ventral horn (VH), respectively, while lamina X is the region surrounding the central canal (Millan, 1999).

In general the spinal cord is composed of 3 main areas that include the dorsal horn (DH), the lateral horn and the ventral horn. The DH receives several types of sensory information from the afferent fibers of the periphery. One of the principle effector targets of the pre-synaptic afferent fibers are spinal cord DH neurons (Figure 1) (Millan, 1999). As a neuronal class, neurons are further subdivided into 6 types: i) Nociceptive-Specific (NS) neurons which are activated exclusively by high intensity, noxious stimuli mediated by C and A $\delta$  fibres. ii) Wide dynamic range (WDR) neurons which are activated by C, A $\delta$ , and A $\beta$  fibers iii) Non-nociceptive (NON-N) neurons, activated by A $\beta$  fiber iv)

Excitatory interneuron v) Inhibitory interneurons vi) Both Excitatory and Inhibitory interneurons. Interneurons are spinal cord neurons which reside between the pre-synaptic terminal and post-synaptic neurons within the spinal cord. Interneurons mediate their actions by secreting neurotransmitters that interact with pre-synaptic primary afferent terminals or postsynaptic DH neurons to regulate nociceptive input (Figure 2) (Millan, 1999). The spinal cord utilizes specific ascending tracts to convey information from the spinal cord to the brain. Once this information is received by the brain and processed, the brain then in turn activates a variety of descending tracts that ultimately regulate the afferent input at the spinal cord level.

In summary, the interaction between pre-synaptic afferents with inter-neurons and DH neurons in the spinal cord followed by message transmission via ascending paths to the brain that ultimately activate descending control of the spinal cord represents the normal processing loop for signal transmissions such as pain.

### ***ASCENDING PATHWAYS***

Incoming primary peripheral afferent fibres enter the spinal cord via the dorsal root ganglia (DRG), where they synapse in the DH. This sensory afferent information is then conveyed via two main pathways or systems to higher centres in the brain. These systems include the posterior column-medial lemniscal system and the anterolateral systems. The large diameter A $\beta$  fibers make up the posterior column-medial lemniscal system and carries non nociceptive sensory information. The afferents to the anterolateral systems have small diameter fibers compared to postero medial systems. The fibers are mainly A $\delta$  and C fibers and carry noxious information. Three major pathways of the anterolateral

systems are: the spinothalamic tract (STT), the spinoreticular tract (SRT), and the spinomesencephalic tract (SMT). Other pathways of the ascending system include spinoparabrachio-amygdaloid tract, spinoparabrachio-hypothalamic tract, spinohypothalamic tract, spinocervical tract.

The STT is the classical pathway for pain transmission (Fields and Basbaum, 1978). STT originate from lamina I, II, IV, V/VI, VII/VIII, LSN of spinal cord and terminate into the thalamus, also periaqueductal grey (PAG) and collaterals (Millan, 1999).

The second major pathway of nociceptive transmission is the SRT. This pathway constitutes a major sub-component of the fibers of anterolateral system, and is therefore considered an alternative route of pain transmission (Fields and Basbaum, 1978). SRT originate from laminae I, V/VI, VII/VIII, X (few) of the spinal cord and terminate into the lateral reticular nucleus of brainstem reticular formation, projects into the medial thalamus and dorsal raphe nuclei (DRN) (Millan, 1999). SRT plays a critical role in relaying and integrating nociceptive information contributing to the aversive-motivational responses aspects of pain (Fields and Basbaum, 1978).

The SMT neurons originate from laminae I, II, IV, V, VII, X, and the Lateral Spinal Nucleus (LSN). Mesencephalic terminal areas from these projections include midbrain, periaqueductal grey (PAG), deeper layers of superior colliculus (SCL), nucleus cuneiformus (NCF), parabrachial nucleus (PBN) and thalamus (Millan, 1999). SMT plays an important role in integrating autonomic, motivational-affective response to pain (Millan, 1999). Activation of these ascending pathways can subsequently activate the descending inhibitory anti-nociceptive pathways which produce endogenous analgesic

agents e.g. endorphins and enkephalons, NPY, and gamma aminobutyric acid (GABA) (Millan, 1999).

### ***DESCENDING PATHWAYS***

Descending pathways can be divided into a dorsolateral system and a ventromedial system. The dorsolateral system includes the rubrospinal tract and the corticospinal tract. The ventromedial system includes the vestibulospinal tract, the reticulospinal tract and the tectospinal tract.

The corticospinal tract also known as the pyramidal tract is the largest and most important descending pathway. The main functions of the pyramidal tracts are to control movement, including fine motor control and maintaining posture. The neurons of the corticospinal tract originate from the cerebral cortex. As the tract descends, approximately 80% of the fibers cross over to the contralateral side in the medulla oblongata. 10% enter the lateral corticospinal tract on the same side. The remaining 10% of the descending fibers cross over at the level that they exit the spinal cord and travel in the anterior corticospinal tract. Most corticospinal tract axons terminated in lamina VI and VII of cervical segments of the spinal cord (Yang and Lemon, 2003).

In humans, 31 pairs of spinal nerves arise along the spinal cord. These are mixed nerves because they contain both sensory and motor axons. Each pair of spinal nerves is associated with a pair of sensory ganglia known as dorsal root ganglia, situated outside of the spinal cord along the entire length of the vertebral column.

### ***DORSAL ROOT GANGLIA (DRG)***

DRG is a sensory ganglia of the PNS. The main function of the ganglia is to regulate and maintain sensory homeostasis. The DRG house a variety of distinct neuronal and non-neuronal cell types e.g. satellite cells, fibroblasts and schwann cells (Fields et al., 1978; van Dorp et al., 1990). The sensory neurons within the DRG are of pseudo-unipolar types that have a single long dendrite, a short axon and smooth rounded cell body. The dendrites are located in the skin, muscles, tendons, joints and internal organs while the axon extends from the dendrites, to the cell body located within the DRG, and subsequently continues to the DH of the spinal cord. The dendrites are structurally and functionally similar to an axon and are myelinated. The single axon makes up the afferent nerve which conveys a variety of sensory information such as pain, touch, temperature, proprioception and vibration from the periphery. The axon bypasses the neuronal cell body, and continues to propagate along the proximal process until reaching the synaptic terminal in the dorsal horn of the spinal cord.

DRG neurons are classified based on their size, diameter of axon, conduction velocity, basic stains, distribution of organelles and several other identifiable factors (Figure 3). In the early 1900's size criteria were used as a means of sub-division. Cells were classified as either small (<25 $\mu\text{m}$ ), medium (25-45 $\mu\text{m}$ ) or large (> 45 $\mu\text{m}$ ). During the same time, a relationship between soma size and axonal diameter was also established. Based on this classification it was noted that large cells give rise to large axons while small cells give rise to small axons (Duce and Keen, 1976). Later, this relationship was extended to include varying degrees of axonal myelination. Small DRG cells were identified to be connected to non-myelinated axons while the large cells tended to be connected to

myelinated axons (Mense, 1990). Since the diameter of myelinated fibres is linearly related to conduction velocity, it was also possible to predict the size of the soma from the conduction velocity of its axon(s) (Lykissas et al., 2007). Thus, by the late 1900's it was generally accepted that conduction velocity served as an excellent estimate for axon size (Yoshida and Matsuda, 1979; Cameron et al., 1986). Early assessment of the DRG cells was also based on basic stains of the neuronal cell bodies. Light microscopy examinations showed two predominant types of DRG cells: lightly stained, clear cells that tended to be large; and intensely stained, dark cells that tended to be small. Thus the cells were defined as 'large light' cells; and 'small dark' cells. Subsequently, additional classifications of DRG cells were divided into 3 types (A, B, C) on the basis of their size and the distribution of their organelles (Duce and Keen, 1977; Rambourg et al., 1983). Following this, the DRG neurons were further subdivided into six subtypes according to the arrangement and three-dimensional organization of the Nissl bodies and Golgi apparatus in the perikarya (Duce and Keen, 1977).

DRG neurons also have been sub-divided according to the various neurotrophic factors which they are known to produce. Neurotrophins are growth factors that regulate the growth, differentiation and survival of neurons. Such neurotrophins include nerve growth factor (NGF), brain-derived neurotrophic factor (BDNF), neurotrophin-3 (NT-3), and neurotrophin-4/5 (NT-4/5) (Takei and Laskey, 2008b).

There are four sub-divisions of sensory afferents: cutaneous, muscle, visceral, and silent (Figure 4) (Millan, 1999). Cutaneous afferent fibers of DRG neurons have been subdivided into A $\beta$ , A $\delta$  and C fibers. These primary sensory afferent fibers have been classified based on sensory neuronal size, structure and conduction velocity. The A $\beta$

fibers contain thick myelinated, large diameter sensory axons with rapid conduction velocity of 30-100m/s. A $\delta$  fibers contain intermediate sized myelinated sensory axons with a conduction velocity of 4-30m/s (Gasser, 1950). The C class fibers contain unmyelinated small diameter sensory axons which have a slow conduction velocity of less than 2.5 m/s (Gasser, 1950). All three classes of cutaneous fibers can transmit non-nociceptive information. Under normal circumstances, only C and A $\delta$ , but not A $\beta$ , fibers transmit nociceptive information (Millan, 1999). Upon exposure to a noxious stimulus, A $\delta$  fibers elicit a first phase of sharp pain, whereas C fibres evoke a second wave of dull persistent pain. In the absence of tissue or nerve injury, A $\beta$  fibers are responsive only to vibration, pressure, touch and other modes of non-noxious, low intensity mechanical stimuli (Millan, 1999). The cutaneous afferents are not only divided by the responsiveness to various sensory stimuli but can also be segregated according to their central projection into the grey matter of the DH within the spinal cord. Cutaneous C fibers project into laminae I, II<sub>0</sub>, V and X. High threshold A $\delta$  fibres terminate into lamina I, II<sub>0</sub> (the outer part of laminae II), and X. In the absence of tissue or nerve injury A $\beta$  fibres mediate non-nociceptive information via relayed projections to laminae I, I I, III, IV, V, VI (Table 1) (Millan, 1999).

### ***THE GREY MATTER***

The grey matter is a major component of the CNS. About 40% of the human brain is made up grey matter. The grey matter contains neuronal cell bodies, in contrast to white matter, which mostly contains myelinated axonal tracts. In addition to housing the neuronal cell bodies, the grey matter also contains dendrites, glial cells and capillaries. In the spinal cord, white matter is at the periphery, the grey matter at the centre. The grey

matter functions to route sensory or motor stimulus to interneurons of the CNS in order to create a response to the stimulus through chemical synapse activity.

### ***THE WHITE MATTER***

The WM is composed of bundles of nerve cell processes, which is sheathed with a lipid rich, multilayered sheath, known as myelin. Following tissue sectioning, the white matter of the CNS appears pinkish white because myelin is composed largely of lipid. It forms the bulk of the deep parts of the brain and superficial parts of the spinal cord. WM is responsible for signal transduction between grey matter areas, and nerve impulse messaging between neurons. Many diseases are associated with the damage or dysfunction (any disturbance in the function of an organ or body part) of the WM, including Multiple Sclerosis, Alzheimer's disease, Parkinson's disease (Scheltens et al., 1992; Sohn and Kim, 1998; Compston and Coles, 2008). Despite the wide variety of WM disorders, MS is recognized as one of the most common diseases affecting myelin(Compston and Coles, 2008). Inflammatory CNS lesions are the hallmark of MS, and about 95% of all MS lesions occur in the WM.

### ***MULTIPLE SCLEROSIS (MS)***

MS is an inflammatory, chronic, neurological disorder that affects nerve impulse conduction in the brain and spinal cord. MS is characterized by targeted destruction of the myelin. The characteristic demyelination of nerve axons associated with the disease causes scarring and hardening (sclerosis) of CNS tissue and slows conduction of nerve impulses, which results in a diverse array of clinical symptoms (Trapp et al., 1999). Inflammation, demyelination and axonal degeneration are major pathologic features that cause the clinical manifestations of the disease (Compston and Coles, 2008). The exact

cause of MS is not known; however, in all cases demyelinated lesions are present throughout the CNS. MS lesions in the brain are typically located in the peri-ventricular WM, subcortical WM and the corpus callosum (Ludwin, 2006). However, lesions may also occur throughout the grey matter of the brain, brain stem and throughout the spinal cord (Chitnis, 2006). Demyelination occurs in a variety of ways, including the loss of oligodendrocytes (OL) or the destruction of the myelin with the OL body being preserved (Ludwin, 2006). The ability of the CNS to successfully remyelinate acute lesions has been well established (Johnson and Ludwin, 1981; Raine et al., 1988; Prineas et al., 1989; Prineas et al., 1993; Raine and Wu, 1993). However, failure of the CNS to continually repair chronic demyelinating lesions results in the formation of plaques and glial scarring associated with chronic MS lesions. These plaques lead to the severe irreversible neurological deficits that lead to permanent clinical disability in the later progression stages of the disease.

### ***MYELIN***

Myelination is critical for normal mammalian development. The myelin sheath is formed by OL and consists of multiple layers of a lipid-rich membrane, wrapped around the axon to prevent the loss of ions during membrane depolarization. Myelin covers the axon at intervals (internodes), leaving bare gaps- the node of Ranvier (Poliak and Peles, 2003). Although nodes in the PNS and CNS show similar structural characteristics, some differences are also observed (Poliak and Peles, 2003). In the PNS, nodes are encapsulated by microvilli emanating from the outer aspect of the Schwann cell membrane, whereas in the CNS nodes are encapsulated by perinodal extensions from astrocytes (Girault and Peles, 2002). The nodes contain  $\text{Na}^+/\text{K}^+$  ATPases,

$\text{Na}^+/\text{Ca}^{2+}$  exchangers and a high density of voltage-gated  $\text{Na}^+$  channels which allow the generation of the action potential during saltatory conduction (Waxman and Ritchie, 1993). The nodes of Ranvier in the adult CNS and PNS mostly consist of  $\alpha\text{Nav}1.6$  and  $\beta 1$  subunits (Caldwell et al., 2000; Ratcliffe et al., 2001). In addition to voltage gated sodium ion ( $\text{Na}^+$ ) channels, several other transmembrane and cytoskeletal protein as well as potassium ion ( $\text{K}^+$ ) channels have been identified (Poliak and Peles, 2003). The main function of nodes of Ranvier is to allow action potential signals jump along the axons, from node to node, with the help of voltage gated  $\text{Na}^+$  and  $\text{K}^+$  ion channels.

The importance of myelination to normal physiological functioning is evident from the clinical presentation of white matter disease pathology. Although the main function of a myelin sheath is to increase the propagation of nerve impulses along axons it also acts to maintain the ionic balance in the peri-axonal space, and acts as a water exchange pump maintaining the diameter of the axon (Dyer, 2002). The glial cells of the CNS responsible for forming the myelin sheaths are called OL while the myelinating glial cells of the PNS are called Schwann cells. It is interesting to note that a single OL interacts with up to 50 axons, compared to the Schwann cell that only interacts with one axon at a time. Myelin is composed of about 80% lipid fats and about 20% proteins compared to other cell types. Some of the predominant proteins that compose myelin are myelin basic protein (MBP), myelin oligodendrocytic glycoprotein (MOG), and proteolipid protein (PLP) (Jahn et al., 2009). The importance of these proteins is clearly demonstrated using transgenic knockout mice. Ablation of MBP and or PLP results in an almost total lack of myelin in the CNS (Campagnoni and Skoff, 2001). In contrast, ablation of MOG does not result in

any clinical abnormalities. Interestingly, MOG is commonly used as an antigen to induce demyelination in the mouse CNS (Delarasse et al., 2003).

### ***EPIDEMIOLOGY OF MS***

Epidemiological studies have been beneficial in the identification of a variety of factors that may be associated to the risk of developing MS. These factors include, but are not limited to, geography, genetics and infectious diseases. The world wide prevalence of MS identifies that approximately 1 000 000 people have been diagnosed between the ages of 17 and 65 years (Kantarci and Wingerchuk, 2006). Globally, the median estimated prevalence of MS is 30 per 100 000 (Duquette et al., 1987). The countries reporting the highest estimated prevalence of MS include Hungary (176 per 100 000), Slovenia (150), Germany (149), United States of America (135), Canada (132.5), Czech Republic (130), Norway (125), Denmark (122), Poland (120) and Cyprus (110) (Atlas of MS resources, 2008). According to the Atlas of MS report, Canada has the 5th highest prevalence of MS in the world. British Columbia, the Prairie region, Ontario, Quebec, and the Atlantic region have higher prevalence than among other provinces in Canada. The estimated range of MS cases in Canada is from 55,000 to 75,000. ([http://www.mssociety.ca/en/research/medmmo-prev-may\\_02.htm](http://www.mssociety.ca/en/research/medmmo-prev-may_02.htm)). The disease preferentially affects females, although males have a tendency for later disease onset with worse prognosis, supporting gender-dependent factors in the etiology and phenotypic variability (Kantarci and Wingerchuk, 2006). Globally, the median estimated male/female ratio is 0.5, which extrapolates to a value of 3 women for every 1 man. However these global values vary within Canada where women are more than three times more likely to

get MS compared to their male counterparts (<http://www.cbc.ca/health/story/2008/09/18/f-multiple-sclerosis.html>).

Although MS occurs most commonly in adults, it also diagnosed in children and adolescents (Banwell, 2004; McLaughlin et al., 2009). Research has identified that 2.7% to 10.5% of patients have reported to develop their first symptoms prior to their 18<sup>th</sup> birthday (Duquette et al., 1987; Simone et al., 2002). Diagnosis of MS in children is more challenging than in adults due to other childhood co-morbidities that may have similar symptoms and characteristics such as acute disseminating encephalomyelitis (Callen et al., 2008). The most common initial symptoms of pediatric MS are sensory deficits such as neuropathic pain, followed by optic neuritis (Boiko et al., 2002).

### ***CLINICAL PRESENTATION OF MS***

There are many different clinical manifestations of MS by which the disease can present. Its clinical presentation is highly individualized and rarely affects people in exactly the same way. During an attack, a person experiences a sudden worsening of normal physical activities that may range from mild to severe. Four main types MS are indentified which include i) Benign, ii) Relapsing Remitting, iii) Secondary chronic progressive, iv) Primary progressive. Relapsing remitting form (RRMS) is the most common type of MS. In general, children experience longer relapsing-remitting periods than adults, displaying longer mean times to sustained disability. Based on the natural history of disease, patients with pediatric MS tend to convert to the secondary progressive form of the disease course earlier in their lives than adult onset patients (Chitnis, 2006) The MRI of pediatric MS shares many similar features with those of adult MS. Lesion development can be significantly inhibited by the use of disease modifying medications e.g. interferon beta-1a

(Avonex), interferon beta-1b (Betaseron), glatiramer acetate (copaxone) and mitoxantrone (Novantrone) (Frohman et al., 2002; Wiendl and Kieseier, 2003). Children who receive treatment regimes early during the course of disease show benign disease progression compared to adult onset patients with similar relapse frequency. A high frequency of relapses and the onset of permanent disability at an early age has been the common end result of undiagnosed pediatric MS (Boiko et al., 2002).

### ***ETIOLOGY OF MS***

The exact cause of MS is still not known, however, research suggests that a combination of several factors may play a role. Genetic factors take part in the development of MS, although MS is not considered a hereditary disease. However, a number of genetic variations have been shown to increase the risk of developing the disease (Dyment et al., 2004). MS is 20–40 times more common in first-degree relatives, dropping off rapidly with the degree of relatedness, and lack of excess of MS in adopted relatives of patients with MS (Kantarci and Wingerchuk, 2006). Monozygotic twin studies suggest that up to 25–30% of MS risk is genetically determined and the risk rapidly drops to 3–5% with dizygotic twins, supporting the complex susceptibility to MS (Kantarci and Wingerchuk, 2006). There is more than one gene that increases the likelihood of an individual to get MS. The association between MS and class II alleles of major histocompatibility complex, particularly the DRB1\*1501-DQB1\*0602 haplotype, is well established (Hensiek et al., 2002; Barcellos et al., 2006). Some studies have also suggested that viral infections represent a potential risk factor for MS. For example, human herpes virus represents a plausible candidate that has been linked to MS (Christensen, 2007). There is also evidence suggesting the etiological participation of varicella-zoster virus in MS

(Sotelo, 2007) but the most reproduced finding is the reduced risk of in those patients never infected by the Epstein-Barr virus (Ascherio and Munger, 2007a; Lunemann et al., 2007). People in certain geographical regions are also known to be at higher risk for MS. This explains the added importance of the environmental effects in the pathogenesis of MS. In addition, other factors such as dietary fat, antioxidants, stress, trauma, nutrition, hormone, sunshine, vitamin D or latitude have also been associated with the development of MS (Niino et al., 2008). Recent research has focused on the importance of vitamin D in MS (Cantorna, 2008). Vitamin D is produced by the body when the skin is exposed to sunlight. In regions far from the equator, the atmosphere filters out more of the sun's rays which decrease vitamin D production in the body. As a result, reduced sun exposure and lack of vitamin D supplementation have been associated with an increase risk of MS (Kantarci and Wingerchuk, 2006). Smoking has also been implicated in this disease. For example, the risk of MS was 1.8-fold higher among tobacco smokers compared with those who had never smoked in one study (Kantarci and Wingerchuk, 2006). Results of ecological studies and one case control investigation have also suggested that diets high in animal/saturated fats and low in polyunsaturated fats may also increase the risk MS (Ascherio and Munger, 2007b). Sex hormones such as estrogen also appear to be implicated in the disease. For example, high levels of estrogen appear to shift the immune response from the proinflammatory type 1, dominant in MS, to the non-inflammatory type 2. This effect may explain the decrease in the number of MS relapses in pregnancy, when estrogen levels are high, and its rebound in the postnatal stage of child birth (Ascherio and Munger, 2007b). There are no direct relationships between dietary antioxidants and the risk of MS, but their effect on MS can not be excluded (Ascherio and Munger, 2007b).

## ***AUTOIMMUNITY AND MS***

The immune system is the body's defense against infectious organisms and other invaders. The major cellular components involved in the adaptive immune response are the T cells and B cells. These are the cells responsible for recognizing specific "non-self" antigens during the process of antigen presentation. These cells can develop memory after initial exposure to the antigen and allow the adaptive immune system to respond more quickly and strongly against the same antigen in the future. T cells originate from bone marrow derived stem cells and migrate to the thymus gland in the neck, where they mature and differentiate into several different subsets (Figure 5), each with distinctive functions. T cells express either CD4 or CD8 co-receptor on their surface. These co-receptors assist the T cell receptor in activating the T cells following an interaction with antigen presenting cell. CD4 is predominantly expressed on the surface of helper T cells whereas CD8 is predominantly expressed by cytotoxic T cells. CD4+ T helper cells play a critical role in MS (Chitnis, 2007). There are four predominant subtypes of helper T cells (Th1, Th2, Th3, and Th17), with each subtype secreting a different array of cytokines (Figure 5). B cells also originate from bone marrow and migrate to secondary lymphoid organs for maturation and differentiation. The principal functions of B cells are to make antibodies against antigens.

The normal immune repertoire also includes self reactive T and B cells which are likely to react with self antigens and may allow an immune response against the host's cells and tissues (Lassmann et al., 2007). In order to avoid the harmful consequences of this autoimmune response, the body develops self tolerance to self antigens (Rose, 1998). There are many ways in which self tolerance can be overcome. When this tolerance to a

particular self antigen is removed, the immune system reacts and damages the body's own tissue. These diseases are known as the autoimmune diseases.

MS is now considered as classical T cell mediated autoimmune disease (Chitnis, 2007; Greenstein, 2007; Melanson et al., 2009). According to the autoimmune theory, circulating Th1 cells in the blood become activated when exposed to specific CNS antigenic proteins including the myelin proteins MBP, PLP and/or MOG. Once activated in the blood, Th1 cells begin to secrete inflammatory cytokines such as interleukin-12 (IL-12), interferon gamma (IFN- $\gamma$ ) and TNF- $\alpha$ . These cytokines are known to orchestrate a pathogenic immune response directed against CNS myelin. Specifically, IL-12 facilitates the conversion of naïve T-cells to the Th1 lineage that drives inflammation (Nelson, 1993; Martino and Hartung, 1999; Ozenci et al., 2002) and induces cell-mediated cytotoxicity. In addition, IL-12 is a powerful inducer of IFN- $\gamma$  from T-cells and natural killer cells (Trinchieri, 1995). The increased production of IFN- $\gamma$  from activated T-cells induces the expression of major histocompatibility complex type II (MHC II) on antigen presenting cells (APCs). In addition, IFN- $\gamma$  stimulates further production of IL-12 thereby creating a positive feedback cycle that sustains the inflammatory immune response characteristic of MS (Martino et al., 1998).

### ***BLOOD BRAIN BARRIER (BBB)***

The BBB is a complex organization of cerebral endothelial cells (CEC), pericytes and their basal lamina, which are surrounded and supported by astrocytes and perivascular macrophages (Minagar and Alexander, 2003). In MS, immune cells are allowed to enter the CNS, implying that the BBB is damaged or compromised in some way. BBB disruption is one of the hallmarks of MS; however it is not known whether BBB

disruption is the cause or effect of cellular infiltration into the CNS (Waubant, 2006). The continued production of IFN- $\gamma$  and TNF- $\alpha$  from activated Th1-cells is essential for the up-regulation of adhesion molecules, such as vascular lectins e.g. intercellular adhesion molecule-1 (ICAM-1), vascular cell adhesion molecule-1 (VCAM-1), on the surface of the endothelial cells that form the BBB (Ozenci et al., 2002). These adhesion molecules facilitate the initial attachment of activated circulating Th1 cells to the endothelium. As more T-cells begin to dock on to the surface of the BBB, their continued release of chemoattractant cytokines promotes additional T-cell recruitment and aggregation. The continued aggregation of activated T-cells subsequently activates the induction of metalloproteinases 3 and 9 (MMP-3, MMP-9) which loosen the tight-junctions between endothelial cells. The compromised status of the BBB facilitates the passage of blood-borne antigenically activated Th1 cells directly into the CNS (Dhib-Jalbut et al., 1996). Th1 cells become reactivated following entry into the CNS and continue promoting inflammation by continued production of inflammatory cytokines. TNF- $\alpha$  and complement, in particular, are known to cause OL death resulting in demyelination (Kornek and Lassmann, 2003; Nakazawa et al., 2006). Demyelination interferes with nerve impulse transmission to effector targets. The reduction or total loss of nerve impulses to effector targets, manifests as a variety of disease-induced symptoms such as: weakness, fatigue, cognitive dysfunction and sensory abnormalities including neuropathic pain (Nakazawa et al., 2006).

### ***SYMPTOMS OF MS***

The signs and symptoms of MS are unpredictable and vary from person to person. Symptoms also depend on the underlying pathological changes that occur in the CNS,

type as well as location of lesions. MS lesions are characterized by inflammation, demyelination and axonal damage or loss. These pathological changes may result in either slowing or complete disruption of nerve impulse conduction and produce clinical features accordingly (Lublin, 2005). The most common symptoms of MS include optic neuritis (Soderstrom, 2001), pain (Chatel et al., 2001; Osterberg et al., 2005; Osterberg and Boivie, 2009), fatigue (Bakshi et al., 2000; Krupp, 2006), depression (Siegert and Abernethy, 2005), spasticity (Barnes et al., 2003), cognitive impairment (Amato et al., 2001), and bladder dysfunction (Crayton et al., 2004).

### ***MS ASSOCIATED PAIN***

Pain is a frequent and disabling symptom among MS patients but the scope, nature and impact of pain on lives of MS patients remain unknown. MS-related pain can be neuropathic or musculoskeletal in nature, and both acute and/or chronic (Ehde et al., 2003). Pain may originate in different body sites (Archibald et al., 1994; Rae-Grant et al., 1999) and may be either unrelated or secondary to MS disease processes. A recent report revealed that the most common site of pain is the legs (74% of adult MS patients), with 59% of patients reporting pain in the lower back, 52% the neck and 49% the shoulders (Ehde et al., 2006). Pain in the hands and feet are the next most common anatomical sites with 48% and 47% respectively (Ehde et al., 2006).

### ***NEUROPATHIC PAIN***

Neuropathic pain is a complex, chronic pain state that usually is produced by damage to or pathological changes in the peripheral or central nervous system. The damaged nerve fibers send incorrect signals to the pain centers and cause symptoms which include the feeling of pins and needles, burning, shooting, and/or stabbing pain with or without

throbbing and numbness. Although the etiology of neuropathic pain has been studied for many years, the exact mechanism underlying the pathogenesis is still unknown. However, drug, injury, and disease-induced destruction of the sensory afferent fibers of the DRG or nerve axons of the CNS are involved in the synaptic nociceptive procession (Namaka et al., 2004). In drug, disease and injury induced events, there is a degeneration and loss of A $\delta$  and C fibers projection in laminae II. Subsequently, the central projections of surviving A $\beta$  fibers in lamina III and IV may sprout into the territory vacated by the A $\delta$  and C-fiber terminals and make contact with second order pain transmission neurons in laminae II. Thus, non-noxious information, such as proprioceptive information or touch may be interpreted as being of noxious origin.

Various drugs have been associated with the development of neuropathic pain. These include antimicrobials such as isoniazid, ethambutol, ethionamide, nitrofurantoin, metronidazole, vinca alkaloids, oxaliplatin, cisplatin, epothilone; thalidomide, bortezomib, pyridoxine, perhexiline, hydralazine, methaqualone, gold, indomethacin, chloroquine, leflunomide, and statins (Argov and Mastaglia, 1979; Donaghy, 2002; Martin et al., 2005; Umapathi and Chaudhry, 2005).

Physical injury is one of the most common causes of injury to a nerve. Injury or trauma caused by automobile accidents, falls, or sport injuries can cause nerves to become partially or completely severed, crushed, compressed, or stretched. These types of injuries can cause chronic pain symptoms.

Certain diseases such as alcoholism, diabetic neuropathy, HIV infections or AIDS (Acquired Immune Deficiency Syndrome), Guillian Barre Syndrome, and MS have also

been reported to induction of chronic neuropathic pain (Katz, 2000; Raskin et al., 2006). Approximately 75 % of all MS patients suffer from neuropathic pain, placing it as the 2nd worst disease induced symptom (Nelson, 1993; Chatel et al., 2001).

Irrespective of its cause, activation of the DRG in the PNS have been recognized as a principle mediator in the development of chronic neuropathic pain (Miao et al., 2008).

### ***PAIN TRANSMISSION***

#### ***PAIN PROCESSING LOOP***

Pain generally starts with a drug, disease or injury induced event. The sensation of pain usually depends on the activation of a set of neurons that includes primary afferent nociceptors, interneurons in the spinal cord, cells of the ascending tracts, thalamic neurons and neurons of the cerebral cortex (Kitahata, 1993; Millan, 1999). Due to an injury, pain receptors in the periphery become stimulated and release various nociceptive mediators including histamine, substance P, serotonin, bradykinin and prostaglandins (Namaka et al., 2004). The pain signal is then transmitted via primary afferent sensory fibers (A $\delta$  and C fibres) to the DRG. The nociceptive impulses received by the DRG is then transmitted centrally via dorsal roots to the main pain processing areas of the spinal cord dorsal horn in the superficial laminae I-II (Millan, 1999). Following integration in the DH, nociceptive information is conducted to the higher centres in the brain via ascending pathways where noxious and non-noxious signals can be perceived. In the pain processing center (primary sensory cortex) the nociceptive information is processed and activates the descending control pathways originating in the brainstem or other cerebral structures, to release various neurotransmitters such as adrenalin, norepinephrine (NE),

serotonin (5-HT), endogenous opioids, such as endorphins and enkephalons, NPY, and gamma aminobutyric acid (GABA). These neurotransmitters subsequently elicit a complex cascade of interactions that ultimately inhibit the excitatory transmission that originated in the nociceptors at the spinal cord level (Millan, 1999). Overall, the net result is the formation of an entire pain processing loop driven by nociceptive afferent fiber input that is eventually suppressed by a descending antinociceptive output (Millan, 1999; Namaka et al., 2004) (Figure 6) (Millan, 1999).

### ***PATHOPHYSIOLOGY OF NEUROPATHIC PAIN***

The mechanisms involved in neuropathic pain are considered to be complex and multifactorial and involve both peripheral and central pathophysiologic events. Current research is rapidly expanding our understanding of the pathophysiology underlying neuropathic pain. A number of cellular changes occur in the peripheral and central nervous system resulting from altered ion channel expression and nociceptive mediators.

### ***IONIC MECHANISM***

Recent studies describes that changes of certain ionic channel activity can be a major contributor in the development and maintenance of neuropathic pain (Aurilio et al., 2008). Specifically, alterations in the ionic transport of ions such as sodium ( $\text{Na}^+$ ), potassium ( $\text{K}^+$ ), calcium ( $\text{Ca}^+$ ) and Hyperpolarization-activated cyclic nucleotide gated (HCN) channel across cell membranes subsequently result in the alteration of the membrane potential to a depolarized state that can lead to pathological neuronal excitation of dorsal horn neurons in the spinal cord.

### ***SODIUM CHANNEL***

Voltage gated Na<sup>+</sup> channels have an essential role in the initiation and propagation of action potentials in neurons and other excitable cells (Hargus and Patel, 2007; Kole et al., 2008). Following peripheral nerve injury, a HCN channel, also known as ectopic neuronal pacemaker channels, can develop in the proximal stump (e.g. neuroma), in the cell bodies of DRG, and in focal areas of demyelination along the nerve. Thus, the accumulation of Na<sup>+</sup> channels in both the neuroma and the DRG (Zimmermann, 2001) result in focal areas of hyperexcitability and ectopic action potential discharge in the axon and cell body of injured sensory neurons (Woolf and Mannion, 1999).

### ***POTASSIUM CHANNEL***

Voltage-gated K<sup>+</sup> channels play a crucial role during the action potential in returning the action potential to a resting state, but little is known about the molecular identity of voltage gated K (Kv) channel in sensory neurons (Rasband et al., 2001). Reduction in voltage-gated K<sup>+</sup> channel subunit expression leads to hyperexcitability of injured nerves (Rasband et al., 2001) representing the hallmark cellular characteristic of neuropathic pain (Jensen, 2002).

### ***HYPERPOLARIZATION-ACTIVATED CYCLIC NUCLEOTIDE GATED CHANNEL***

HCN channels, referred to as pacemaker channels, help to generate rhythmic activity within groups of heart and brain cells. HCN channels are encoded by four genes (HCN1-4), out of them HCN1 channel is abundant in rat primary sensory somata (Chaplan et al., 2003). Spontaneous firing of injured nerves is known to play a crucial role in the induction and maintenance of neuropathic pain. Several studies noted increased

pacemaker current in DRG neurons after injury which can enhance neuronal excitability (Chaplan et al., 2003; Yao et al., 2003). The role of HCN channel in the pain states initiated by nerve injury is supported by the observation that pharmacological blockade of HCN activity reverses abnormal hypersensitivity to light touches and decreases firing frequency of ectopic discharges originating in A $\beta$  and A $\delta$  fibers without conduction blockade (Chaplan et al., 2003).

### ***CALCIUM CHANNEL***

Voltage-dependent Ca<sup>+</sup> channels (VDCC) are found in the excitable cells (e.g. muscle, glial cells, neurons) which promote the entry of Ca<sup>+</sup> ions entry into the cells, resulting in muscle contraction, excitation of neurons, release of neurotransmitters, activation of second messenger signaling and gene transcription. Five major types of VDCCs have been identified (L, T, N, P/Q and R types), with a variety of properties (Bowersox et al., 1996). Several different studies have emphasized the contribution of these channels to neuropathic pain conditions (Bowersox et al., 1996; Dogrul et al., 2003; Snutch, 2005). Studies show that enhanced activity of Ca<sup>+</sup> current is associated with increased neuronal activity. Blockade of N and P/Q –type, but not L-type Ca<sup>+</sup> channels, does not block experimental neuropathic pain (Dogrul et al., 2003). However selective T- type Ca<sup>+</sup> channels may play a role in the expression of neuropathic state (Dogrul et al., 2003).

### ***NEUROTRANSMITTER MECHANISMS***

In combination with electrolyte changes, mediators released by inflammatory and immune cells play a key role in the development of neuronal hyperexcitability (Moalem and Tracey, 2006). These includes glutamate (GLU), substance P (SP), calcitonin gene related peptide (CGRP), adenosine triphosphate (ATP), nitric oxide (NO), prostaglandins

(PGs), neurotrophins (growth factors) and cytokines (Millan, 1999). During the resting state, a balance exists between excitatory and inhibitory neurotransmitters.

Glutamate, the major excitatory neurotransmitter, exerts its effects by binding with two major ionotropic receptors, alpha-amino-3-hydroxy-5-methyl-4-isoxasolepropionic acid (AMPA), and *N*-methyl-d-aspartate (NMDA). During a triggering event, released glutamate is able to bind both AMPA and NMDA receptors which are involved in the opening of Na<sup>+</sup> and Ca<sup>+</sup> channels (Namaka et al., 2004). The influx of these cations results in an excitatory depolarizing response of the neuronal cell (Martinez-Sanchez et al., 2004). Besides ionotropic receptors, there are metabotropic G protein-coupled glutamate receptors (mGluR), which modify neuronal and glial excitability through G protein subunits acting on membrane ion channels and second messengers such as diacylglycerol and cAMP. mGluRs are divided into three groups, with a total of eight subtypes. Each of the groups has a specific regional distribution in the brain and displays a distinct pharmacological profile (Muto et al., 2007).

In contrast, inhibitory neurotransmitters such as GABA attempt to restore the normal balance between excitation and inhibition (Namaka et al., 2004). GABA acts by binding with GABAA and GABAB receptors on the cellular surface. The binding of GABA to GABAA receptors produces fast synaptic inhibition through the opening of chloride (Cl<sup>-</sup>) channels resulting in the influx of anions into the cell suppressing cellular excitation (Namaka et al., 2004). GABA can also exert its inhibitory effect by binding with GABAB receptors. Failure of these inhibitory mechanisms can lead to pronounced neuronal hyperexcitability (Namaka et al., 2004).

In addition to GABA, adrenaline, norepinephrine, serotonin (5-HT), endorphins, enkephalins, dynorphins, and neuropeptide Y (NPY) are also known to be inhibitory neurotransmitters. Activation of descending pathways results in the release these inhibitory neurotransmitters that ultimately suppress excitatory transmission originated at the dorsal horn level of the spinal cord.

In addition to faulty ionic or neurotransmitter mechanisms, the enhanced production of pro-inflammatory cytokines has also been implicated in the facilitation of inflammation and hyperalgesic states of neuropathic pain (Sommer and Kress, 2004).

### ***CYTOKINES***

Cytokines are signaling peptides, released by many different types of cells and are important in innate and adaptive immune responses. They are generally produced in small quantities in response to local stimuli, such as the presence of antigens or endotoxins, or the transduction of signals provided by other cytokines (Ozenci et al., 2002). They bind to specific cell-surface receptors producing intracellular signaling cascades that can up- or down-regulate genes, transcription factors, and other cytokines and cytokine receptors. Some cytokines are involved in the amplification of inflammatory responses and are called pro-inflammatory cytokines, whereas others serve to reduce inflammation by inhibiting the production of pro-inflammatory cytokines and are thus called anti-inflammatory cytokines. Th1 and Th2 cells predominantly release pro-inflammatory and anti-inflammatory cytokines respectively (Figure 5). In order to maintain normal homeostasis, a balance must exist between pro- and anti-inflammatory cytokines (Ozenci et al., 2002). Inadequate concentrations of anti-inflammatory cytokines may result in a

prolonged inflammatory response that can result in pathological conditions such as pain or MS (Imitola et al., 2005).

The major pro-inflammatory cytokines thought to be involved in the pathogenesis of neuropathic pain include; interleukin-12 (IL-12), interferon- gamma (IFN- $\gamma$ ), and tumor necrosis factor-alpha (TNF- $\alpha$ ) (Leung and Cahill; Ozenci et al., 2002; Tsuda et al., 2009).

### ***TUMOR NECROSIS FACTOR ALPHA (TNF- $\alpha$ )***

TNF- $\alpha$  is a soluble 17-kDa protein composed of 3 identical subunits (Imitola et al., 2005). TNF- $\alpha$  predominantly mediates immune and inflammatory responses. It is produced mainly by activated mononuclear phagocytic cells, as well as by natural killer cells, B cells, activated T cells, astrocytes and microglia in the CNS (Imitola et al., 2005).

### ***TNF- $\alpha$ RECEPTORS***

TNF- $\alpha$  exerts its effects through two distinct cell surface receptors: TNF- $\alpha$  receptor 1 (TNFR1; p55) and TNF- $\alpha$  receptor 2 (TNFR2; p75) (MacEwan, 2002). The cytotoxic effects of TNF- $\alpha$  are mediated by TNFR1 which contains a death domain (Figiel and Dzwonek, 2007). The death domain is a critical structural element involved in signal transduction that leads to apoptosis (Hofmann and Tschopp, 1995). TNFR2 has been reported to promote neuronal survival (Takei and Laskey, 2008b). TNF- $\alpha$  signaling through TNFR2 depends on the nerve growth factor (NGF). Studies shown that in the presence of NGF, TNF- $\alpha$  activate TNFR2 and promote neuronal survival (Takei and Laskey, 2008a). However, TNFR2 can indirectly contribute to cytotoxicity through endogenous production of TNF- $\alpha$  and autocrine or paracrine activation of TNFR1 (Takei and Laskey, 2008b). Both TNF- $\alpha$  receptors have been reported as being present within rat

DRG, although the cellular distribution remains controversial (Pollock et al., 2002; Schafers et al., 2003b; Li et al., 2004). TNF- $\alpha$  receptors in the brain are scant but report suggests that both of them are expressed by all cell types, albeit at low levels (Kinouchi et al., 1991). Studies showed that microglia express both TNFR1 and TNFR2, whereas astrocytes and OL predominantly express TNFR1 (Dopp et al., 1997).

### ***THE FUNCTION OF TNF- $\alpha$***

TNF- $\alpha$ , has been shown to play an integral role in facilitating the development of neuropathic pain (Sommer et al., 1998a; Hermann et al., 2001; Naidu et al., 2001; Zimmermann, 2001). Several studies involving the use of cytokine inhibitors, knock-out mice, or direct application of cytokines with subsequent investigation of electrical activity and behavioral changes support the involvement of TNF- $\alpha$  in the development of chronic neuropathic pain (Sommer et al., 1998a; Zhang and Liu, 2002). However, specific increases in neuronal TNFR1 expression were reported following administration of intraperitoneal (i.p.) lipopolysaccharide (LPS), suggesting a direct effect for TNF- $\alpha$  on nociceptive pathways via TNFR1 (Sommer et al., 1998a; Li et al., 2004). In addition, the effects of TNF- $\alpha$  have also been linked to the intracellular signaling pathways that play a role in the pathogenic activation of DRG cells following inflammation or injury (Takahashi et al., 2006; Melanson et al., 2009).

Further, TNF- $\alpha$  has also been shown to directly induce neuronal production of neuropeptides and inflammatory agents such as Substance P and Calcitonin gene related peptide (CGRP) within the DRG and spinal cord (Ohtori et al., 2004). The documented effects of CGRP and SP on neuropathic pain are well known (Frisen et al., 1993; Ding et al., 1995). Alternatively, TNF- $\alpha$  has also been reported to sensitize nociceptive neurons

indirectly via induction of a pro-inflammatory cytokine cascade involving IL-1 $\beta$ , IL-6, and IL-8. This cytokine cascade results in the release of prostaglandins and other inflammatory mediators from immune cells (Cunha et al., 1991; Feiguin et al., 1994; Woolf et al., 1997). In addition, TNF- $\alpha$  is also capable of directly inducing pain, as evidenced by its role in producing a state of painful neuropathy when injected directly into the sciatic nerve (Myers et al., 2003). Electrophysiological studies confirm the effects of TNF- $\alpha$  in inducing pain. For example, subcutaneous injections of low dose TNF- $\alpha$  induce ectopic activity in nociceptive neurons within two minutes, with higher doses producing significant mechanical and thermal hyperalgesia by 15 minutes (Sorkin et al., 1997; Junger and Sorkin, 2000; Zelenka et al., 2005). Specifically, this ectopic activity was associated with enhanced influx of Ca<sup>2+</sup> and Na<sup>+</sup> ions which facilitated increased neuronal sensitivity to neurotoxins, such as capsaicin, in cultures of sensory neurons (Pollock et al., 2002). Further, studies have shown that the time course of TNF- $\alpha$  activity within the DRG and spinal cord have identified a transient period of elevated TNF- $\alpha$  expression which is much shorter than that required for injury evoked mechanical allodynia and thermal hyperalgesia (Chang et al., 2004; Xu et al., 2006). As a result, TNF- $\alpha$  is thought to be responsible for the “initiation” rather than the maintenance of neuropathic pain (Ji and Strichartz, 2004).

### ***NEUROTROPHINS***

The neurotrophins are a family of proteins that support neuronal survival and growth during development of the nervous system. They maintain the structural and functional integrity of the adult nervous system, and regulate plasticity of the injured or diseased adult nervous system (Sah et al., 2003). The family includes nerve growth factor (NGF),

BDNF, neurotrophin (NT)-3, and neurotrophin (NT)-4/5. Glial cell line-derived neurotrophic factor (GDNF) also essential for development of sensory neurons and critical for the survival of DRG cells (Wang et al., 2003).

### ***NEUROTROPHIN RECEPTORS***

Receptors for the neurotrophin family are found in adult sensory neurons. There are two classes of receptors, p75 (low affinity receptor capable of binding all neurotrophins) and “Trk” family of tyrosine kinase receptors, TrkA, TrkB, TrkC. Trk receptors are a family of tyrosine kinases that regulates synaptic strength and plasticity in the mammalian nervous system (Huang and Reichardt, 2003). TrkA selectively binds NGF, TrkC selectively binds NT-3 and TrkB binds both BDNF and NT- 4/5 (Banfield et al., 2001). It is now known that neurotrophins play a significant role in the pathophysiology of neuropathic pain. There is plenty of evidence regarding the upregulation of neurotrophins and their receptors in animal models of neuropathic pain (Lewin et al., 1993; Quintao et al., 2008; Wang et al., 2009).

### ***NERVE GROWTH FACTOR (NGF)***

NGF was the first neurotrophin identified in 1954 (Cohen et al., 1954). NGF is a major contributor to the development and maintenance of neuropathic pain. Systemic administration of NGF induces both thermal and mechanical hyperalgesia in rodents (Lewin et al., 1993). Furthermore, studies showed that in a model of acute inflammation endogenous NGF was also involved in the development of thermal hyperalgesia (Lewin et al., 1994) which can be blocked by administration of anti-NGF or an IgG fusion molecule for the NGF receptor TrkA (Lewin et al., 1994; McMahon et al., 1995). The hyperalgesic action of NGF is mediated via sensory neurons, inflammatory cells, or

sympathetic cells (Woolf et al., 1996). NGF not only induces inflammatory hyperalgesia but also plays an important role in nerve injury induced neuropathic pain (Ramer and Bisby, 1999; Theodosiou et al., 1999; Li et al., 2003).

### ***BRAIN DERIVED NEUROTROPHIC FACTOR (BDNF)***

BDNF is basic protein widely expressed in both the peripheral and central nervous systems. The BDNF functions are developmentally regulated by secretion of pro BDNF or mature BDNF and by local expression of p75 and TrkB (Yang et al., 2009). BDNF binds to TrkB receptors (Zhou and Rush, 1996), and is involved in the modulation of painful stimuli (Obata and Noguchi, 2006). Evidence suggests that following peripheral nerve injury or inflammation, sensory processing in the dorsal horn results in synaptic plasticity which leads to the development of neuropathic pain (Ji and Woolf, 2001). Interestingly, BDNF is thought to play a significant role both in spinal plasticity and in transmission of nociceptive information (Miletic and Miletic, 2002). In animal models of neuropathic pain, nerve injury increased the concentration of BDNF in the spinal dorsal horn (Miletic and Miletic, 2002; Yajima et al., 2005) and there is a correlation in the time line of development and disappearance of behavioural signs of neuropathic pain and changes of BDNF expression (Miletic and Miletic, 2002). The thermal hyperalgesia and tactile allodynia induced by sciatic nerve ligation were completely suppressed by intrathecal injection of a TrkB/Fc chimera protein, which sequesters endogenous BDNF (Yajima et al., 2005). In addition, BDNF heterozygous (+/-) knockout mice exhibited a significant suppression of nerve ligation-induced thermal hyperalgesia and tactile allodynia compared with wild-type mice, this further supports a role for BDNF in the development of neuropathic pain (Yajima et al., 2005).

### ***GLIAL CELL LINE-DERIVED NEUROTROPHIC FACTOR (GDNF)***

GDNF is a member of the transforming growth factor  $\beta$  cytokine superfamily. It is the first identified member of the GDNF family of neurotrophins which also includes artemin, neurturin and persephin (Baloh et al., 2000). GDNF has also been studied in the context of neuropathic pain. GDNF is necessary for the development of sensory neurons and appears to be critical for the survival of DRG cells that bind the lectin IB4 (Wang et al., 2003). In spinal nerve ligation (SNL) and partial ligation of one sciatic nerve injury models, GDNF has been shown to both prevent and reverse sensory abnormalities (Boucher et al., 2000; Wang et al., 2003). A potential role of NT3 in neuropathic pain has also been studied. The contribution of NT3 in development of neuropathic pain is less well understood in comparison to that of the other neurotrophins (Sah et al., 2003).

### ***EFFECTS OF NEUROTROPHINS AND CYTOKINES ON OLIGODENDROCYTES***

As both cytokines and neurotrophins are known to be involved in neuropathic pain and MS an interactive connection between these two classes of proteins could be possible. This cytokine/neurotrophin interaction is also supported by the fact that immune mediated cellular mechanisms responsible for pain induction also share a similar pathology involved in the subsequent immune mediated attack on OLs in MS. Specifically, TNF- $\alpha$  is also known to induce the intracellular NF-kappa B pathway resulting in OL death (Kim et al., 2001). In addition, TNF- $\alpha$  is also known to decrease OL proliferation (Arnett et al., 2001) and increase astrocyte formation (Dopp et al., 1997) via TNFR1 leading to scar tissue formation thereby preventing proper myelin repair. Other factors BDNF and NGF have been shown to have similar roles to TNF- $\alpha$  with regards to pain (Ugolini et al., 2007; Ulmann et al., 2008; Wilson-Gerwing et al., 2008; Lu et al., 2009) but they differ in

their effects on OL's. For example, BDNF has an important role in OL differentiation and proliferation (Van't Veer et al., 2009), thereby promoting myelin formation and repair. As a result, cytokines and neurotrophins are thought to be involved in an interconnected network that ultimately determines the final cellular response to TNF- $\alpha$  signaling (Takei and Laskey, 2008a, b).

### ***NEUROTROPHIN INTERACTIONS***

BDNF is thought to act as a chemo-attractant directional cue for NGF (Dasari et al., 2007; Lykissas et al., 2007) which subsequently promotes preferential TNF- $\alpha$  signaling via TNFR2. In this manner, the signalling effects of TNF- $\alpha$  can be protective rather than pathogenic. Support for the TNF  $\alpha$ , BDNF, NGF interactive triad becomes evident from transgenic mouse studies where TNF- $\alpha$  over expressing mice induce elevations in BDNF protein in cortical neurons (Aloe et al., 1999) . Furthermore, the addition of TNF- $\alpha$  to astrocyte cultures also results in the induction of BDNF protein (Saha et al., 2006). Elevated BDNF levels could also function as a directional cue for the up-regulation of NGF. As a result, it is plausible that during normal myelin repair in MS the transport of DRG derived transport of BDNF and NGF into the areas of inflammation of the spinal cord prevents the pathogenic TNF- $\alpha$  signaling via TNFR1(Takei and Laskey, 2008a, b) . Failure to achieve adequate levels of these key neurotrophins to the spinal cord would therefore result in permanent lesion formation or MS plaques mediated via TNF- $\alpha$ /TNFR1 pathway.

Based on the above information, DRG are known to have a critical role in the development of neuropathic pain which often precedes the diagnosis of MS (Nelson, 1993; Chatel et al., 2001). The main function of the DRG is to regulate and maintain

sensory homeostasis. During the period(s) of immune activation known to occur in MS, rapid and sustainable bursts of inflammatory cytokine activity in the DRG (e.g. TNF- $\alpha$ , IL-12, IFN  $\gamma$ ) may serve as the abnormal stimulus that eventually disrupts this sensory equilibrium (Ferreira et al., 1993; Groves et al., 1997; Hermann et al., 2001; Gabay and Tal, 2004; George et al., 2004; Fernyhough et al., 2005). The highly permeable endothelial vasculature that surrounds DRG may facilitate the bi-directional transport of cytokines between the DRG and peripheral blood. As a result, DRG could function as a pivotal reservoir for MS-induced inflammatory cytokines accounting for direct effects on sensory neurons (Portenoy et al., 1988; Won et al., 2000).

#### ***DRG/SPINAL CORD MODEL OF MS INDUCED NEUROPATHIC PAIN***

According to the known cellular pathogenesis of MS, antigen induced activation of Th1 cells in the peripheral blood represents a pivotal step that leads to elevated production of inflammatory cytokines such as TNF- $\alpha$  that have been directly linked to disease induction. In addition to its key role in the cellular pathogenesis of MS, TNF- $\alpha$  is also known to play a vital role in facilitating the development of neuropathic pain that often precedes the diagnosis of MS. Following the antigenic induction of inflammatory cytokines TNF- $\alpha$ , research suggests that these blood borne inflammatory cytokines gain access to the spinal cord via the peripheral nervous system DRG and facilitates key cellular interactions with sensory neurons housed within the DRG that subsequently trigger the release of neurotrophins such as BDNF and NGF. As a result, TNF- $\alpha$ , BDNF and NGF produced within the DRG can undergo axoplasmic transport directly into the CNS via the dorsal root port of entry to the spinal cord and participate in direct cellular interaction with dorsal horn neurons. Therefore, we developed a DRG/Spinal cord model

of MS-induced neuropathic pain (Figure 7) (Melanson et al., 2009). The resultant cytokine-neurotrophin interaction in the DRG followed by transport to the dorsal horn represents a plausible mechanism for MS-induced neuropathic pain involving the pathological activation of dorsal horn neurons.

## ***HYPOTHESIS AND AIMS***

### ***HYPOTHESIS***

The elevated production of TNF- $\alpha$  in the early stage of MS is responsible for the initial activation of DRG and/or spinal cord that facilitate the downstream cellular cascade of events involved in the underlying pathogenesis of MS-induced neuropathic pain.

### ***SPECIFIC AIMS***

- i. To determine if the protein and gene expression levels of TNF- $\alpha$  is up-regulated within the DRG and spinal cord of rodents induced to a state of MS.
- ii. To correlate the relative temporal changes in production of TNF- $\alpha$  within the DRG and spinal cord to the global neurological disability scoring used to confirm disease development.
- iii. To correlate the relative temporal changes in production of TNF- $\alpha$  within the DRG and spinal cord to specific behavioral assessments used to confirm the early onset of MS induced neuropathic pain.
- iv. To identify a cell specific source of TNF- $\alpha$  via immunohistochemistry (IHC).

## **CHAPTER 2: MATERIALS AND METHODS**

### ***ANIMAL MODEL***

A variety of animal models of MS have been developed in different species: models induced by immunization against CNS proteins or by infection with neurotrophic virus or spontaneous transgenic or humanized models (Madsen et al., 1999; Lassmann, 2008). No single animal model exist that represents all the features of human MS, rather the available models reflect specific facets of the disease (Gold et al., 2000). The classic and most common model of MS is actively induced experimental autoimmune encephalomyelitis (EAE) (Furlan et al., 2009). EAE can be induced in a number of different animal species including mice, rats, guinea pigs and rabbits using several protein or parts of protein including MBP, PLP, MOG. For various reasons, including the number of immunological tools, the availability, lifespan and the resemblance of the induced disease to MS, mice and rats are the most commonly used species. As with humans and MS, not all the strains of mice or rat are equally susceptible to EAE induction. The mode of sensitization, nature of immunogen and genetic make-up of the recipient animal determine the clinical, pathological and immunological picture of autoimmune models (Furlan et al., 2009). EAE may have a monophasic disease course, acute relapsing, or primary progressive course depending on species and immunogen used (Furlan et al., 2009).

In MS patients, neuropathic pain is known to occur prior to the diagnosis of MS (at the inflammatory stage prior to de-myelination), therefore, our study utilized a model of EAE that is characterized by a strong inflammatory response with associated neurological

disability characteristic of the early inflammatory stage of human MS. Specifically, we used the Lewis rat MBP EAE model (Melanson et al., 2009) to correlate surges of immune activation during the disease induction with changes in cytokine expression within the DRG and spinal cord. In MBP induced EAE in Lewis rats, neurological deficits build up and resolve spontaneously within 15 days, without having any demyelinating lesions, and this model is often used to evaluate the effects of antigen induced inflammation prior to de-myelination (Gold et al., 2000). In addition, based on the inherent pre-disposition of the disease in humans to occur in young adult females compared to males, adolescent Lewis *female* rats were specifically chosen.

### ***EXPERIMENTAL ANIMALS***

Adolescent female Lewis rats (7.2 weeks of age) were purchased from Charles River Laboratories, Montreal, QC. Animals were housed in the central animal care facility at the University of Manitoba. Animals were given food and water ad libitum. In conducting the research described in this study, all animals received humane care in compliance with the guidelines of the animal care and use committee of the University of Manitoba (Animal protocol number: F07-027), which is in accordance to the Canadian Council on Animal Care criteria.

### ***INDUCTION OF EAE***

A total of 66 rats were randomly divided into three experimental groups: naïve control (n=6), active control (n=30) and active EAE (n=30) (Table 2). Each active EAE rat received Freund's incomplete adjuvant (Sigma, Cat# F-5506) + 500µg Mycobacterium tuberculosis (DIFCO LABORATORIES) + 100µg guinea pig MBP (Cedarlane, Cat#

GP68-84). Each active control rat received Freund's incomplete adjuvant + 500 µg Mycobacterium tuberculosis + equal volume of Phosphate buffered saline (PBS) replaces MBP. Pertussis toxin (LIST BIOLOGICAL Laboratories, INC.) was given to all active EAE (aEAE) and active control (AC) animals by intraperitoneal injection (Rt. Side) on Day 0 and repeated on Day 2 in order to prime the immune system. Naïve control (NC) animals did not receive any injections.

In preparation for antigenic induction, the anesthetized (Isoflurane, PPC, DIN #02231929) animal was shaved over the hip area and the skin aseptically prepared using a three-stage surgical preparation involving surgical soap, alcohol rinse and surgical preparation solution. An injection of 0.3 µg of pertussis toxin in 200 µl of sterile phosphate buffered saline (PBS) was administered by intraperitoneal injection to prime the immune system. 100 µl of the immunogen (MBP) /adjuvant mixture (Active EAE animal) or adjuvant/saline mixture (Active Control animal) was drawn from the glass syringe into a 1.0 ml syringe which was then fitted with a 25 gauge hypodermic needle. Two 50 µl injections were given subcutaneously over each hip (total volume 100 µl per rat) at the base of the tail with no adjuvant leakage occurring along the needle track when entering or leaving the subcutaneous space. After the injection, the rat was removed from the inhaled anesthesia and placed in the recovery cage equipped with paper towels on the bottom of the cage with a dark towel surrounding the cage to keep the animal warm. When recovery to the point of purposeful movement was confirmed the animal was then returned to its individual cage. All rats were examined for clinical signs of EAE every day beginning the day after immunization and were assessed according to the EAE score described below.

### ***CLINICAL ASSESSMENT***

Following induction each rat was assessed daily for clinical signs of EAE. Six specified domains tail, bladder, right and left hind limb, right and left fore limb were monitored and scored on the following scale 0, 1, 2 according to their disability (Table 3). Animals with minimal disability in any of the assessed domains displayed a score of 0 with severe disabilities warranting a score of 2. Active EAE animals that began to show clinical symptoms were assessed several times a day and an average score was calculated. Body weight was also measured daily to assess general health and well being of the animal.

### ***BEHAVIORAL ASSESSMENTS***

#### ***THERMAL SENSORY TESTING***

Thermal sensory was tested in collaboration with Dr. Brian MacNeil to find out the changes of the sensitivity to noxious heat stimulus. Withdrawal latency to radiant heat stimulus for each rat were assessed according to previously described methods (Aicher et al., 2004) using a Model 336G Plantar/Tail Stimulator Analgesia Meter (IITC Life Sciences, Woodland Hills, CA). The rats were placed on a glass surface kept at a constant room temperature at the animal care facility and a light beam (50% intensity) was focused on a 4 X 6 mm region of the skin. The light beam was projected on the tip of the tail and plantar surface of the hind and fore paws. The time taken to move the tail and paw from heat source was recorded as withdrawal latency. Region specific withdrawal responses consisted of licking the paws and flicking the tail in response to the heat stimulus. A maximum of 10 s cut off point was programmed into the timer to prevent tissue damage. Withdrawal latency was recorded at three separate times for each paw and tail and average withdrawal latency was calculated.

Rats were habituated to the testing apparatus for 30 min 4 days prior to any testing and for 10 min prior to testing on each test day. After the habituation period, baseline withdrawal latencies were measured for each animal on four separate days prior to immunization. Each experimental group was tested daily for a specified time period on day 3, 6, 9, 12 and 15 after immunization.

### ***MECHANICAL ALLODYNIA***

Mechanical allodynia is the painful sensation due to a non-painful stimulus. To quantify mechanical allodynia, rats were placed in lucite cubicles over top of a metal mesh floor and mechanical stimuli will be applied to each hind paw with a 1.0 mm von Frey filament attached to a digitized strain gauge (Moller et al., 1998). The maximum force generated before withdrawal is recorded for each hind paw over three trials and averaged. Baseline measurements were obtained for four days prior to EAE-induction.

### ***TISSUE COLLECTION***

At pre-defined specific time points (3, 6, 9, 12, 15 days of post disease induction) during onset, progression and remission of the inflammatory state tissues from 66 animals were harvested for analysis (Table 4). A total of 33 animals underwent full body intra-cardiac perfusion fixation and tissues were harvested for IHC and in situ hybridization (ISH) analysis. Tissues from the remaining 33 animals were harvested for subsequent quantitative qRT-PCR analysis.

### ***ANIMAL PERFUSION***

Animals were deeply anaesthetized using an I.P. injection of ketamine (30mg/100g body weight, Biospecific CN: A52310) and Xylazine (3mg/100g body weight, Bayer Health

Care, DIN: 02169592) diluted in saline. When there was no pedal reflex, using scissors the skin and muscle layers of the abdomen and chest were cut to expose the heart. A 21G needle was inserted into the left ventricle of the heart and clamped in place, and the superior vena cava cut to allow the fluid to escape. Following this, the perfusion pump (VWR, variable flow pump catalog number: 54856-075) was turned on at a fixed speed (11-14 ml/min) and the animal was perfused with a pre-fixative solution containing 1U/ml heparin (LEO Pharma Inc. DIN: 00453811) and 0.1% sodium nitrate (ThermoFisher Scientific, Cat: S343) in 0.9% sodium chloride (Sigma Aldrich, Cat: S9625) at a volume equal to 1/3 of the animals body weight for calculated time (ie. animal body weight=200 g, prefix volume=1/3 of the body weight. Therefore,  $200 \text{ g} \div 3 \div 10 \text{ ml/minute} = 6.6 \text{ minutes}$ ). Next a 4% paraformaldehyde (Sigma Aldrich: cat. # 158127) fixative in 0.1% phosphate ( $\text{PO}_4$ ) buffer (final concentration) was perfused into the animal at a volume equal to 2x the body weight of the animal for calculated time (ie. animal body weight= 200 g, fixative= 2x of the body weight, pump speed=10 ml/min. Therefore,  $200 \text{ g} \times 2 \div 10 \text{ ml/minute} = 40 \text{ minutes}$ ). After fixation, the animal was decapitated as close as possible to the first cervical vertebra. The cranium was removed and the entire intact brain was collected and placed into the appropriately labeled vial of post-fixative (4% paraformaldehyde).

Through the existing abdominal incision, the entire intestine was removed. The spleen and the liver were collected for control tissue samples, and placed into two vials with post-fixative. The whole spinal column was removed, dissected free of soft tissue and placed into glass cylinders for post-fixation. All specimens were then post-fixed in 4% paraformaldehyde at 4°C for 24 hrs. After post-fixation all specimens except the spinal

column were stored in 30% sucrose solution at 4°C and storage solution was changed every two weeks until cryosectioned. Spinal columns were further processed for decalcification (Begum et al., 2010).

### ***DECALCIFICATION OF SPINAL COLUMN***

Analysis of protein and gene expression is critical for the success of the project and, as we hypothesized that there is transport between the peripheral DRG and central spinal cord, it is essential to our experiments that we can section the spinal column maintaining the peripheral/central connectivity from the DRG via the nerve roots to the dorsal horn of the spinal cord (Figure 8). Therefore, we have developed a novel technique to decalcify the bone of the spinal column, this allows us to accurately assess protein and gene expression without disrupting the integrity of the myelin sheaths of either the peripheral or central nerves (Begum et al., 2010). We compared the effect of four different decalcification reagents (RDO Gold, Krajian's Solution, EDTA Glycerol and 6% TCA) on the quality of myelin structure as assessed by MBP immunoreactivity. The results of our study (Begum et al., 2010), clearly show that 6% TCA decalcification is superior to the other treatments when investigating the fine structure of myelin sheaths in the grey and white matter of the spinal column (Figure 9).

Therefore, the whole spinal column was decalcified in 6% Trichloroacetic acid (TCA) using our published in-house technique (Begum et al., 2010). After fixation, the specimen was washed in PBS for 18-20 min. The whole vertebral column was then decalcified in 6% TCA (Sigma–Aldrich: cat. # T6399) in distilled water, for 5 days at 4° C. Incubation time was assessed at several time points using insertion of a sharp needle into the bone

and chemical testing to determine the end-point of decalcification. After decalcification in 6% TCA, the vertebral column was washed in PBS for 20min.

### ***TISSUE PREPARATION AND FROZEN SECTIONS***

After decalcification, the specimens were cryopreserved in 20% sucrose (MP Biomedicals, LLC, Solon, OH: cat. # 904713) in PBS for 24 h and 30% sucrose in PBS for another 24 h at 4°C. Vertebral columns were divided into segments (<1 cm), then placed in Tissue-Tek O.C.T. (Sakura Finetek, Torrance, CA: cat. # 4583) overnight at 4°C. The pieces were then embedded in OCT and stored at -80°C until cryosectioned.

Serial sections were cut at 10µm thickness using a Thermo Shandon CME cryostat, air dried onto SuperFrost microscope slides (Thermo Fisher) and stored at -80°C.

### ***TISSUE COLLECTION FOR QUANTITATIVE REAL-TIME PCR (qRT PCR)***

The other half of the experimental animals was designated for qRT-PCR analysis. These animals were sacrificed with a lethal dose of ketamine (30mg/100g body weight, Biospacific CN: A52310) and xylazine (3mg/100g body weight, Bayer Health Care, DIN: 02169592) diluted in saline, followed by decapitation according to approved animal use protocols. Once the animal was dead (assessed by no breathing and no response to any painful stimuli) the animal was decapitated as close as possible to the first cervical vertebrae. The cranium was removed and frozen in dry ice. Through the abdominal incision all intestines were removed. Then spleen and the liver were collected and frozen in dry ice. Dorsal lamina of the spinal column was removed working from the cervical to the sacral end of the spinal column. Using fine spring scissors, the membrane covering the spinal cord was split down the center of the entire length of the spinal cord being

extremely careful not to nick the cord. After that the spinal cord was collected and frozen in dry ice. After removing the spinal cord, DRGs from cervical, thoracic and lumbar regions were collected and frozen. Tissues were then moved to -80°C and stored until used. The whole procedure was done within 45 minutes of the time of death of animal.

### ***IMMUNOHISTOCHEMICAL (IHC) CYTOKINE ANALYSIS***

Qualitative IHC analysis of lumbar spinal cord attached to the DRG via dorsal roots was conducted to detect the protein expression of TNF- $\alpha$ . Tissue from one animal per group (active EAE, active control and naïve control), 9 sections per animal, 3 fields of view per section were analyzed. In order to determine the cellular source(s) of cytokine production and signaling pathways, double label immunofluorescent staining using monoclonal antibody against the neuronal marker NeuN (Millipore Cat# MAB 377) was conducted in conjunction with the polyclonal antibody for TNF- $\alpha$  (R & D Systems, Cat# AF-510-NA). The slides were washed with PBS-T (PBS (Sigma, Cat# P-5368) and 0.1% triton X-100 (Sigma, X-100)) for three times for 5 minute intervals and blocked with 20% normal donkey serum (NDS) (Sigma, Cat# D9663), 20% normal goat serum (NGS) (Sigma, Cat#G9023) in PBS-T for 20 min at room temperature (RT). The primary antibodies against TNF- $\alpha$  (1:100) and NeuN (1:100) were diluted in PBS-T containing 20% NDS, and 20% NGS were applied to the sections and incubate overnight at 4°C. Following incubation with the primary antibodies the slides were then washed with PBS-T and incubated with the mixture of secondary antibodies (alexa 568 donkey anti goat, Invitrogen, Cat# A11057; Goat anti mouse IgG, (Jackson Immuno Research, Cat# 115-095-003) diluted in PBS-T containing 20% NDS and 20% NGS for 30 min at RT. The slides were then washed with PBS-T twice. In order to eliminate autofluorescence artifact

from the spinal cord sections, the cupric sulphate technique was used according to previously described methods (Tsai et al., 2004). Following washes with PBS-T, the slides were dipped in distilled water and treated with 4mM copper sulphate (Fisher Scientific, Cat# C-493) in ammonium acetate buffer (50mM, pH 5.0, MP Biomedicals LLC, Cat# 194000) for 20 min, dipped in distilled water and PBS-T once in each of them. Following washing, one drop of aqueous mounting medium (R&D Systems, Burlington, Ontario: Cat. #CTS011) was added to the tissue and mounted with a no.1 coverslip (Marienfeld, Ref# 0101242) and stored at 4°C. Spleen tissue was used as a positive control for TNF- $\alpha$  IHC staining. Omission of the primary and secondary antibodies during staining of the selected slides from each treatment group was conducted and used as omission controls to assess autofluorescence.

### ***QUANTIFICATION OF IMMUNOHISTOCHEMISTRY***

Imaging was performed using an Olympus IX81 scanning laser confocal microscope. Images were captured in Fluoview FV500 software. The picture processing and cell diameter measurements were performed using the software Image Pro Express (Media Cybernetics). The number of TNF- $\alpha$  positive neurons within the DRG of each animal group was counted. Cell diameters were only measured where the nucleus was visible. The image analysis program employed stereology for the total cell counting.

### ***IN SITU HYBRIDIZATION (ISH)***

ISH was performed using a modification of a method described in the Roche Applied Science Nonradioactive In situ hybridization Application Manual. In the pre-hybridization and hybridization step, all reagents were made with Diethylpyrocarbonate (DEPC) treated water. Briefly, 10  $\mu$ m serial sections of spinal column were warmed to

room temperature and dried in an oven at 40°C for 2 hr. In the pre-hybridization step, sections were incubated in PBS for 2 x 5 min, DEPC (Sigma, cat # D5758) treated PBS containing 100mM glycine (Sigma, cat# G8898) for 2 x 5 min, DEPC treated PBS containing 0.3% Triton X-100 for 15 min and washed in DEPC treated PBS for 2 X 5 min and permeabilized with 1µg/ml proteinase k (Sigma, Cat.#P2308) in TE buffer at 37°C for 30 min. Sections were post-fixed with 4% paraformaldehyde (Fisher, cat# 04042) at 4°C for 5 min and washed in PBS for 2 x 5 min and acetylated with 0.25% freshly prepared acetic anhydride (Mallinckrodt, Cat#UN1715) in 0.1M triethanolamine (TEA; (Sigma cat# T58300) for 2 x 5 min. Sections were incubated with pre-hybridization buffer containing 2x SSC, 1x Denhardt's solution (Sigma, Cat#D2532), 10% dextran sulphate (Sigma, Cat#8906), 50mM Phosphate Buffer, 50mM DTT (Sigma, Cat#D0632), 250µg/ml yeast t-RNA (Sigma Cat#R5636), 100 µg/ml polyadenylic acid potassium salt: (Sigma# P9403), 500 µg/ml salmon sperm DNA (Sigma, Cat#D7656). Each slide was overlaid with 100 µl of prehybridization buffer at 49.2°C for 2 hr covering with parafilm. The parafilm was removed by immersing slides in 2x SSC for 5 min. Each slide was overlaid with 100µl of hybridization buffer containing 1ng/ml of custom made digoxigenin (DIG)-labeled TNF- $\alpha$  antisense oligonucleotide probe (Eurofins MWG Operon). The sequence of the probe was 5'[AminoC6+DIG]-GTCCCCCTTCTCCAGCTGGAAGACTCCTCC-3, HPLCPURE). The sections were covered with parafilm and incubated at 49.2°C overnight in a humid chamber containing 5xSSC: formamide: 1:1. After hybridization coverslips were removed by immersing slides in 2x SSC for 5 min and washed at 37°C in for 2 x 15 min in 2x SSC, followed by 1x SSC, and finally in 0.25x SSC using a shaking water bath. Sections were washed again in buffer 1 (100mM Tris-HCl, 150 mM NaCl in DEPC water) and

covered with blocking solution (buffer 1 containing 0.1% Triton X-100 and 2 % normal sheep serum (Sigma, cat# S3772) for 30 min. Following the removal of the blocking solution, sections were incubated with buffer 1 containing 0.1% Triton X-100, 1% sheep serum and 1:500 dilution of sheep anti-DIG-alkaline phosphatase (Roche, Cat# 11093274910) for 2 hr in a humid chamber. Sections were then washed in buffer 1 for 2 x10 min and incubated for 10 mins with buffer 2 (100mM Tris- HCl, 100mM NaCl, 50 mM MgCl<sub>2</sub> in DEPC water). Buffer 2 was removed and each section covered with 100 µl of BCIP/NBT (Dako, Cat# k0598) solution plus levamisole (Dako, Cat# X3021) (1drop per 1 ml of BCIP/NBT) and incubated in a humid chamber in the dark at 4°C for overnight. When color development was optimal (assessed by eye), the reaction was stopped by incubating in buffer 3[10mM Tris –HCl (pH 8.1), 1 mM EDTA] and washed in distilled water for 10 min and sections were mounted using an aqueous mounting medium. Appropriate TNF- $\alpha$  sense probe was not found to use as control.

### ***IMAGE ANALYSIS***

Imaging was performed under bright field conditions using an Olympus DP70 digital camera attached with Olympus BX51 microscope. Images were captured with DP controller software.

### ***QUANTITATIVE REAL- TIME POLYMERASE CHAIN REACTION (qRT-PCR)***

The real-time quantitative polymerase chain reaction (qRT-PCR) analysis was conducted according to previously established in-house methods (Miao et al., 2008). In order to fully quantify TNF- $\alpha$  expression within the DRG and spinal cord, qRT-PCR was performed using a Lightcycler real-time PCR thermal cycler (Roche diagnostics, Mannheim, Germany), with QIAquick PCR purification kit (Qiagen, Hilden, Germany) and

Lightcycler FastStart DNA Master SYBR Green I kit (Roche diagnostics, Mannheim, Germany).

### ***TOTAL RNA ISOLATION***

Using a power homogenizer (Brinkmann, Switzerland) tissue samples were homogenized in 1 ml Trizol Reagent (Invitrogen, Carlsbad, CA). The homogenized samples were then incubated for 5 minutes at room temperature to permit the complete dissociation of nucleoprotein complexes followed by the addition of 0.2 ml of chloroform. The sample tube caps were securely fastened to prevent leakage and sample loss. The sample tubes were then shaken vigorously by hand for 15 seconds and incubated for 2 to 3 minutes at room temperature. The samples were then centrifuged at 12,000g for 15 minutes at 4°C by using microcentrifuge (International Equipment, Needham heights, MA). Following centrifugation, the mixture separates into a clear, phenol-chloroform phase, and interphase, and an upper aqueous phase. RNA remains exclusively in the aqueous phase which is about 60% of the volume. The aqueous phase was extracted and transferred to a fresh tube where the total RNA was precipitated by mixing with 0.5 ml isopropyl alcohol (Sigma, St. Louis, MO). The samples were then incubated for 10 minutes at room temperature and centrifuged at 12,000g for 10 minutes at 4°C. The RNA precipitate, which was invisible before centrifugation, forms a gel-like pellet on the side and bottom of the tube. The supernatant was removed, and the RNA pellet was washed once with 1 ml of 75% ethanol (Fisher, Fair Lawn, NJ). The sample was mixed by vortexing, and centrifuged at 7,500g for 5 minutes at 4°C. The resultant RNA pellet was then air-dried for 10 minutes. Following this, the RNA was dissolved in RNase-free water by passing the solution a few times through a pipette tip, and incubating for 10 minutes at 60°C. At

the end of the procedure, the concentration of the total RNA was determined using ultraviolet (UV) spectrometry (Smart spectrum 3000, Bio-red, Hercules, CA). The RNA was then quantitatively diluted to a concentration of 1 µg/µl with RNase-free water and subsequently stored in -70°C.

### ***REVERSE TRANSCRIPTASE (RT)***

Total RNA stock solution was thawed on ice. To each of 1 µg RNA (1µl), 1 µl oligo (dT)<sub>12-18</sub> primers (Beckdon Dickinson, Palo Alto, CA), 1 µl 10mM deoxynucleoside triphosphate (dNTP) mix (Invitrogen, Carlsbad, CA) and RNase-free water to 12 µl was added. The resultant mixture was then heated for 5 minutes at 65°C and quickly chilled on ice. The contents of the tube were then collected by brief centrifugation. After that, 4 µl 5× First-strand buffer (Invitrogen, Carlsbad, CA), 2 µl 0.1M dithiothreitol (DDT, Invitrogen, Carlsbad, CA) and 1 µl RNaseOUT recombinant ribonuclease inhibitor (40 units/µl, Invitrogen, Carlsbad, CA) was added into the tube and then mixed the content gently by pipette tip and incubated for 2 minutes at 37°C. Next 1 µl moloney-murine leukemia virus reverse transcriptase (M-MLV RT, Invitrogen, Carlsbad, CA) was added and mixed by pipette tip. Incubated the samples for 50 minutes at 37°C and then inactivated the reaction by heating at 70°C for 15 minutes. Then 80 µl of RNase-free water was added into the tube to make the total volume 100 µl. The cDNA was then ready to be used as a template for polymerase chain reaction (PCR) amplification.

### ***AMPLIFICATION***

The expression of glyceraldehydes-3-phosphate dehydrogenase (GAPDH), a housekeeping gene found in all tissues at high level was detected prior to analyzing the expression of TNF-α in order to ensure that the tissues were processed correctly. The

following reagents were added into a PCR reaction tube for a final reaction volume of 50  $\mu$ l, using water as negative control and rat spleen as positive control:

0.5  $\mu$ l *Taq* DNA polymerase (Qiagen, Hilden, Germany)

10  $\mu$ l Q buffer (Qiagen, Hilden, Germany)

5  $\mu$ l PCR 10 $\times$  buffer (Qiagen, Hilden, Germany)

4  $\mu$ l 50mM MgCl<sub>2</sub> (Qiagen, Hilden, Germany)

1  $\mu$ l 10mM dNTP (Invitrogen, Carlsbad, CA)

1  $\mu$ l upper primer for GAPDH (**Table 1**, Invitrogen, Carlsbad, CA)

1  $\mu$ l lower primer for GAPDH (**Table 1**, Invitrogen, Carlsbad, CA)

22.5  $\mu$ l RNase-free water

5  $\mu$ l cDNA (from the RT reaction)

**Table 1:** sequence of GAPDH primers (Genbank number: NM017008)

	Sequence	Temperature	Length
upper	5'TTC TTG TGC AGT GCC AGC CTC GTC 3'		
lower	5' GCC GTT GAA CTT GCC GTG GGT AGA 3'	60 <sup>0</sup> C	203bp

After adding the reagents into tubes gently mixed them and mount the tubes to PCR thermal cycler (Mastercycler, Eppendorf, Westbury, NY) for amplification. As 38 cycles were required for the amplification, the temperature program was set as following:

1. 95<sup>0</sup>C 5 minutes
2. 95<sup>0</sup>C 1 minutes
3. 60<sup>0</sup>C 0.5 minutes
4. 72<sup>0</sup>C 1.5 minutes

Repeated the step-2 to step-4 for another 37 cycles

5. 72°C 8 minutes
6. Hold at 4°C

Following the amplification, the tubes were briefly centrifuged. 10 µl PCR products (double stranded DNA) and 2 µl loading buffer were gently mixed on parafilm and loaded onto 1% agarose gel containing 0.5µg/ml ethidium bromide. Electrophoresis was run in TBE buffer for 15 minutes. The agarose gel was viewed under UV light. When the luminosity of the GAPDH bands looked very similar, the TNF-α assay was started.

In order to determine the expression of TNF-α, the same procedure was followed but the primers for GAPDH was replaced by primers for TNF-α (**Table 2**, Invitrogen, Carlsbad, CA). As 32 cycles of the PCR amplification were required, the temperature program was set as following:

1. 95°C 5 minutes
2. 95°C 1 minutes
3. 59°C 0.5 minutes
4. 72°C 1.5 minutes

Repeated the step-2 to step-4 for another 31 cycles

5. 72°C 8 minutes
6. Hold at 4°C

**Table 2:** sequence of TNF-α primers (Genbank number: AF329982)

	Sequence	Temperature	Length
upper	5' AGC CGA TTT GCC ATT TCA TAC CAG 3'		
lower	5' CAC GCC AGT CGC TTC ACA GAG 3'	59°C	247bp

The photographs were taken with an instant camera (DS34, Polaroid), then scanned and electronically saved. The luminosity of the electrophoresis bands was analyzed by *ImageJ1.34* (Shareware, can be downloaded at <http://rsb.info.nih.gov/ij/download.html>).

### ***PURIFICATION OF DOUBLE-STRANDED DNA***

DNA purification was done according to QIAquick PCR purification kit (Qiagen, Hilden, Germany) manufacturer's procedure. In brief, 5 volumes of Qiagen PB buffer were added to 1 volume of the TNF- $\alpha$  PCR product. A QIAquick spin column was placed in a 2 ml collection tube. The sample was then applied to the QIAquick column and centrifuged for 30 seconds. The flow-through was discarded. The QIAquick column was then placed back into the same collection tube. Next 0.75ml Qiagen PE buffer was added to the QIAquick column and centrifuged for 30 seconds. The flow-through was discarded again. The QIAquick column was placed back into the same collection tube. The column was centrifuged for an additional 1 minute. The QIAquick column was then placed in a clean 1.5 ml microcentrifuge tube. To elute DNA, 25  $\mu$ l Qiagen EB buffer was added to the centre of the QIAquick membrane and the column was centrifuged for 1 minute. This step was done twice to ensure complete elution of bound DNA. The purified double-stranded DNA was then collected in the 1.5 ml microcentrifuge tube.

### ***STANDARD CURVES FOR QUANTIFICATION OF DNA***

The real-time PCR thermal cycler was programmed to determine the fluorescence of the reaction at each cycle of the amplification, and able to fully quantify the double-stranded DNA concentrations by making cycle dependent curves. The purpose of the standard curve was to have a reference standard for extrapolating quantitative information for DNA of unknown concentration. In detail, the concentration of purified double-stranded DNA was measured three times using UV spectrometer, and the average was calculated. The following equations were applied to obtain different concentrations of double-stranded DNA:

Known molecular weight of 1 base pair (bp) of double-stranded DNA=660Da (Roche Applied Science Lab FAQs, 2<sup>nd</sup> edition, Roche Diagnostics, Penzberg, Germany, 2002).

Known Avogadro's number:  $1\text{g} = 6.023 \times 10^{23}\text{Da}$ ,  $1\text{Da} = 1.660 \times 10^{-24}\text{g}$

Therefore,  $1\text{bp} = 660\text{Da} \times 1.660 \times 10^{-24}\text{g/Da} = 1.096 \times 10^{-21}\text{g}$

Hence,  $1\text{ copy of double-stranded DNA} = \text{length} \times 1.096 \times 10^{-21}\text{g/bp}$

$1\text{ copy of TNF-}\alpha\text{ double-stranded DNA} = 247\text{ bp} \times 1.096 \times 10^{-21}\text{g/bp} = 2.707 \times 10^{-19}\text{g}$

Since the average concentration obtained from UV spectrum of double-stranded DNA is  $112.79\mu\text{g/ml} = 112.79 \times 10^{-9}\text{g}/\mu\text{l}$ .

Therefore, the concentration of TNF- $\alpha$  double-stranded DNA in copies was:

$$\frac{112.79 \times 10^{-9}\text{g}/\mu\text{l}}{2.707 \times 10^{-19}\text{g/copy}} = 4.17 \times 10^{11}\text{copies}/\mu\text{l}$$

$2.40\mu\text{l}$  ( $10^{12}$  copies) of above solution was taken and  $97.60\mu\text{l}$  PCR grade water was added and mixed to make  $10^{10}$  copies/ $\mu\text{l}$  stock.

$1\mu\text{l}$  ( $10^{10}$  copies/ $\mu\text{l}$ ) of solution was taken and  $99\mu\text{l}$  PCR grade water was added to it and mixed to make  $10^8$  copies/ $\mu\text{l}$ .

$1\mu\text{l}$  ( $10^8$  copies/ $\mu\text{l}$ ) of solution was taken and  $99\mu\text{l}$  PCR grade water was added and mixed to make  $10^6$  copies/ $\mu\text{l}$ .

$1\mu\text{l}$  ( $10^6$  copies/ $\mu\text{l}$ ) of solution was taken and  $99\mu\text{l}$  PCR grade water was added and mixed to make  $10^4$  copies/ $\mu\text{l}$ .

PCR grade water was used as 0 copy/ $\mu\text{l}$ .

According to manufacturer's instruction of Light cycler FastStart DNA Master SYBR Green I kit (Roche diagnostics, Mannheim, Germany), the "Hot Start" reaction mix was prepared. One vial 1a containing the Lightcycler FastStart Enzyme and one vial 1b containing Lightcycler FastStart Reaction Mix SYBR Green I were briefly centrifuged. A total volume of 10  $\mu$ l was transferred from vial 1a to vial 1b. The resultant solution was then gently mixed by pipette tip. Vial 1b was relabeled with the new labels provided with the kit (vial 1: Lightcycler FastStart DNA Master SYBR Green I). The vial was protected from light with aluminum foil.

In order to obtain TNF- $\alpha$  standard curve of Real-Time PCR, the following reagents were added to a microcentrifuge tube for a final reaction volume of 20  $\mu$ l:

9.4  $\mu$ l PCR grade water

1.6  $\mu$ l MgCl<sub>2</sub>

1  $\mu$ l forward primer for TNF- $\alpha$

1  $\mu$ l reverse primer for TNF- $\alpha$

2  $\mu$ l SYBR mix (vial 1)

5  $\mu$ l double-stranded DNA ( $10^8$ ,  $10^6$ ,  $10^4$ , 0 copies/ $\mu$ l, respectively)

The contents of each tube were mixed gently by pipette and transferred to a Lightcycler capillary (Roche diagnostics, Mannheim, Germany). The Lightcycler capillaries were briefly centrifuged to ensure the contents stay at the bottom end of the capillaries without any air bubbles. The capillaries were then mounted into the Real-Time PCR thermal cycler. The temperature parameters on the computer that connects to the thermal cycler

were set according to manufacturer's instruction. The Real-Time PCR thermal cycler was then left to run overnight. The data of standard curves was saved in the computer connecting to the cycler. The black, red, green, and blue curves represent  $10^8$ ,  $10^6$ ,  $10^4$ , and 0 copies/ $\mu$ l double-stranded DNA, respectively.

### ***AMPLIFICATION OF SAMPLES***

The following reagents were added to a microcentrifuge tube for a final reaction volume of 20 $\mu$ l:

9.4  $\mu$ l PCR grade water

1.6  $\mu$ l MgCl<sub>2</sub>

1  $\mu$ l forward primer for TNF- $\alpha$

1  $\mu$ l reverse primer for TNF- $\alpha$

2  $\mu$ l SYBR mix (vial 1)

5  $\mu$ l cDNA (RT products) of the samples

The contents of each tube were mixed, and transferred carefully to a Lightcycler capillary. The capillaries were then briefly centrifuged, and mounted into Real-Time PCT thermal cycler with  $10^8$ ,  $10^6$ ,  $10^4$ , and 0 copies/ $\mu$ l standard curve stocks. The temperature parameters were set as the same as those of standard curve. The Real-Time PCR thermal cycler was then left to run overnight. The data of tested samples was saved on the computer.

## ***STATISTICAL ANALYSIS***

The data from thermal sensory testing was statistically analyzed using Statistica 5.1 (Stat Soft, Inc., Tulsa, OK). Repeated measures ANOVA was used to test for the effect of time for each of the five test sites. Significant main effects were further investigated using Tukey's honest significant difference test.

The data from cell percentages and qRT-PCR were analyzed statistically by SPSS 16.0 software in order to interpret the data relating to our experimental groups. All the data were tested using one way analysis of variance (ANOVA) with Tukey's post hoc comparisons. Significance was set at  $P < 0.05$ . Specifically for qRT-PCR data analysis, normality and homogeneity of error variance of dependent variable was tested by using Kolmogorov-Smirnov and Levene's test. The cell sizes were statistically analyzed using Graph Pad Prism-4 software. Cell sizes data were tested using one way analysis of variance (ANOVA) with Bartlett's test (for equal variances) and Dunnett's Multiple Comparison Test, significance was set at  $P < 0.05$ . Also, the process design was to detect the significant differences between means of different observational groups and scatter-plot was used to display those differences graphically. Statistical analysis of the cell percentages and cell sizes was done by an analyst blinded to each experimental group.

## **CHAPTER 3: RESULT**

### ***IMMUNOHISTOCHEMICAL (IHC) ANALYSIS OF TNF- $\alpha$ EXPRESSION***

IHC analysis was conducted to analyze TNF- $\alpha$  protein expression within the DRG and spinal cord. Double label immunostaining was conducted to detect TNF- $\alpha$  positive neurons in the DRG (Figure 10). Comparative IHC analysis of active EAE versus control groups euthanized at day 3, 6, 9, 12, 15 revealed pronounced TNF- $\alpha$  immunoreactivity in the DRG of active EAE day 12 relative to all other groups (Figure 11). IHC analysis of spinal cord tissue also showed pronounced TNF- $\alpha$  immunoreactivity in the spinal cord of active EAE day 12 compared to other groups (Figure 12).

### ***IN SITU HYBRIDIZATION (ISH)***

In situ hybridization was conducted to detect TNF- $\alpha$  mRNA expression within DRG and spinal cord. Our results reveal TNF- $\alpha$  mRNA expression in the DRG, dorsal roots and spinal cord (Figure 13). In addition, results also demonstrate increased TNF- $\alpha$  mRNA expression in the active group compared to control groups (Figure 14). These findings provide strong evidence to support the initial findings presented in the IHC analysis (Figure 11 and 12).

### ***QUANTITATIVE REAL-TIME PCR (qRT-PCR)***

Quantitative Real Time PCR (qRT-PCR) was conducted to detect TNF- $\alpha$  expression in the DRG as well as spinal cord tissue (lumbar segments). Our qRT-PCR results demonstrate that the TNF- $\alpha$  expression in DRG for animals of the active EAE group, euthanized at day 12, is significantly higher than other groups (naive control and active

control) ( $p < 0.05$ , Anova) (Figure 15). The qRT-PCR data for the spinal cord obtained from the same animals from each respective group also showed that TNF- $\alpha$  expression of the active EAE group, euthanized at day 15 was significantly higher than active EAE day 3 and active control day 15 group ( $p < 0.05$ , Anova) (Figure 16).

### ***NEUROLOGICAL DISABILITY ASSESSMENTS***

After MBP immunization, all animals in the active EAE groups were assessed for clinical deficits. The onset of clinical signs of neurological disability began at day 6 post disease induction (dpi) that progressively worsened upon daily assessment. Disability peaked at day 12 dpi and subsequently diminished by day 15 dpi when the animal entered remission phase of the disease, characteristic of the relapsing remission phase of disease (Figure 17). The results also showed symptoms began in the tail followed by hind limbs and fore limbs (Figure 18A-18G)). The control group did not show any clinical signs of disability, data not shown.

### ***BEHAVIORAL ASSESSMENTS***

#### ***ASSESSMENT OF SENSITIVITY TO NOXIOUS HEAT (THERMAL HYPOALGESIA/THERMAL HYPERALGESIA)***

For behavioral assessments, data were aligned to day of onset of clinical disease; ie, Day 0 was the first day of clinical symptoms/signs for each individual animal. Values were normalized to the average response seen over the 4 days prior to clinical onset (D-4 to D-1). Data from five specific sites tail, right and left hind paws, right and left fore paws were measured. Active EAE animals showed statistically significant increased tail withdrawal latency at day “0” compared to their baseline responses (Tukey,  $P = 0.002$ )

(Figure 19). Similarly, statistically significant increase of the withdrawal latency was observed for both fore paws and left rear paw (repeated measures Anova, Site X Day) (Figure 20).

#### ***ASSESSMENT OF SENSITIVITY TO TOUCH (MECHANICAL ALLODYNIA)***

For mechanical allodynia, data were recorded from both hind paws. Values were also normalized to baseline responses (average of Day -4 to Day -1). Data are aligned to day of onset of clinical disease; i.e., Day 0 is the first day of clinical symptoms/signs for each individual animal. No significant effects were shown using repeated measures ANOVA for SITE x DAY, (Figure 21).

#### ***CELLULAR SOURCE OF TNF- $\alpha$***

Analysis of TNF- $\alpha$  neurons in the DRG also showed a significantly increased percentage of TNF- $\alpha$  positive neurons in active EAE group compared to control groups ( $P < 0.05$ , Anova) ( Figure 22), with values peaking at day 12, and levels reduced by 15 dpi. Furthermore, a sub analysis of of the TNF- $\alpha$  positive neurons identified in the active EAE group revealed a cell size distribution that suggests small to medium diameter ( $< 25\mu$ , average =  $22.30\mu$ ,  $SD \pm 4.47\mu$ ) ( $P < 0.05$ ) sensory neurons which corresponds to C and A $\delta$  fibers respectively (Figure 23 ).

## CHAPTER 4: FIGURES AND TABLES

**Figure 1: Classification of spinal cord neurons involved in afferent pain transmission.**

The major type of neuron is the dorsal horn neuron. Dorsal horn neurons are subdivided into 4 predominant types: i) Nociceptive Specific (NS) ii) Wide Dynamic Range (WDR) iii) Non-nociceptive (NON-N) neuron iv) Interneuron (IN). Interneurons were subsequently subdivided into 3 types: i) Excitatory IN ii) Inhibitory IN iii) Both Excitator and Inhibitory IN (Based on facts from Millan, 1999).

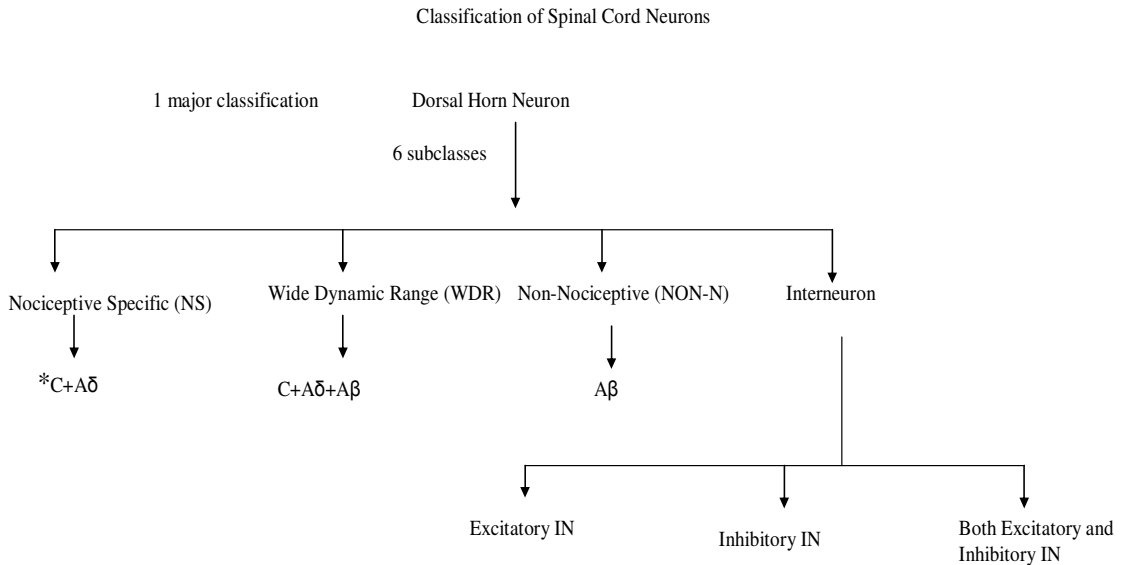


**Figure 2: Classification of Interneuron.**

3 subdivisions: i) Excitatory Interneuron release excitatory neurotransmitters ii) Inhibitory Interneuron release inhibitory neurotransmitters iii) Mixed Interneuron (Excitatory and Inhibitory) (Based on facts from Millan, 1999).

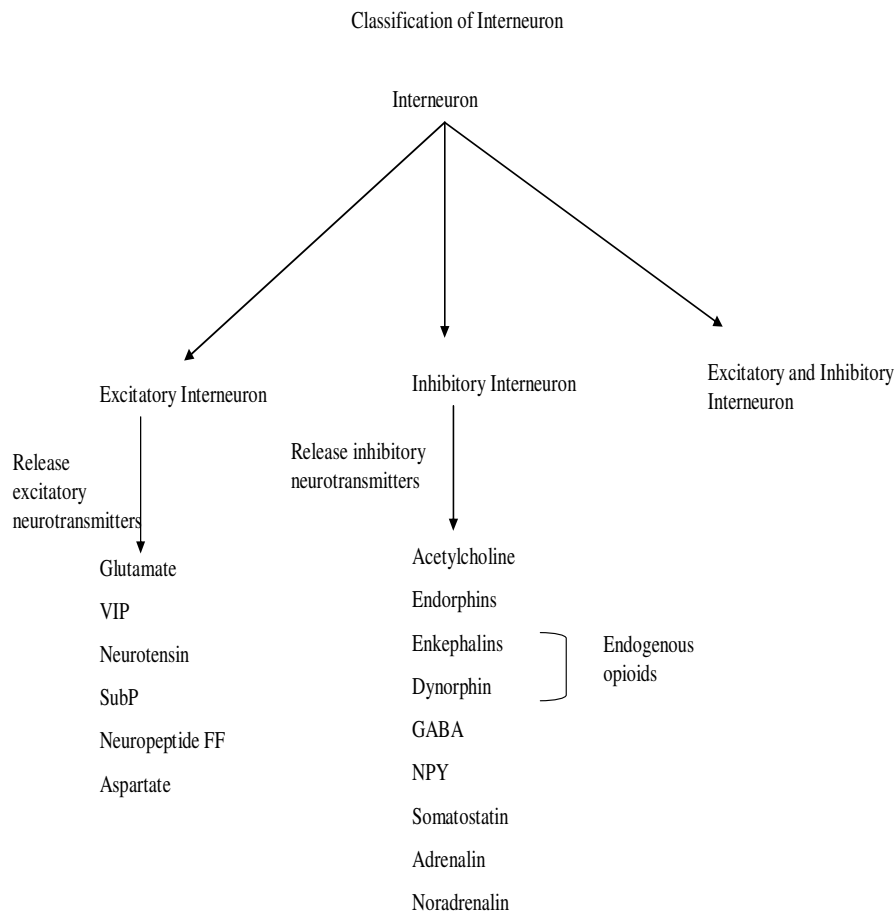
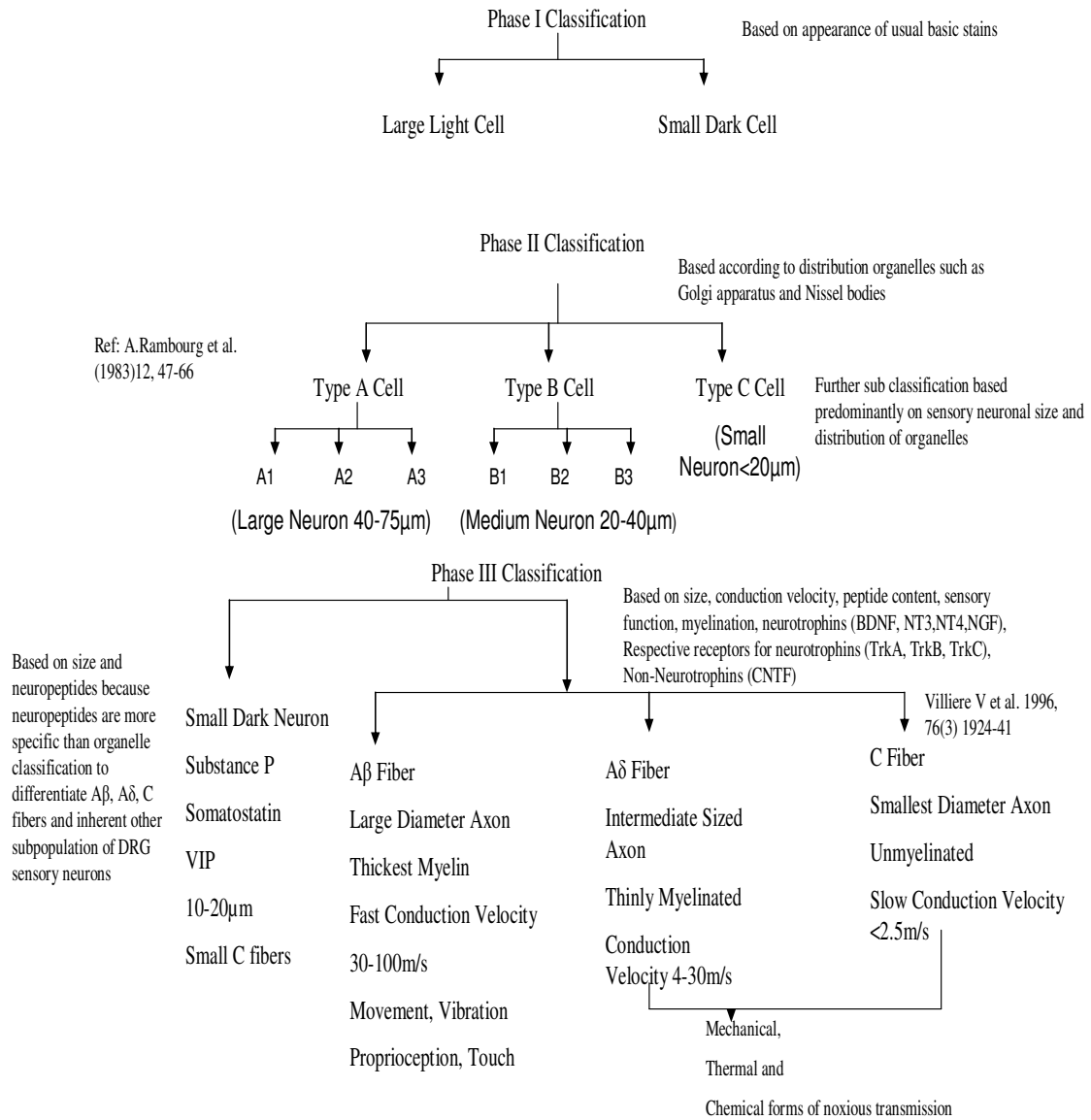


***Figure 3: Evolutionary Classification of Dorsal Root Ganglia (DRG).***

DRG classification is divided into 3 phases: i) Phase I classification –based on appearance of usual basic stains ii) Phase II classification –based on distribution of organelles such as Golgi apparatus and Nissel bodies iii) Phase III classification -Based on size, conduction velocity, peptide content, sensory function, myelination, neurotrophins (BDNF, NT3, NT4, NGF), Respective receptors for neurotrophins (TrkA, TrkB, TrkC), Non-Neurotrophins (CNTF) (Based on facts from Kai Kai, 1989; Rambourg et al., 1983; Villiere and McLachlan, 1996).

## Evolutionary Classification of Dorsal Root Ganglia (DRG)



Ref: A.Rambourg et al. (1983)12, 47-66

Based on size and neuropeptides because neuropeptides are more specific than organelle classification to differentiate Aβ, Aδ, C fibers and inherent other subpopulation of DRG sensory neurons

**Figure 4: Classification of sensory afferent fibers involved in pain transmission.**

Four subdivisions of sensory afferent fibers includes: i) Cutaneous afferents ii) Muscle afferents iii) Visceral afferents iv) Silent afferents (Based on facts from Millan, 1999).

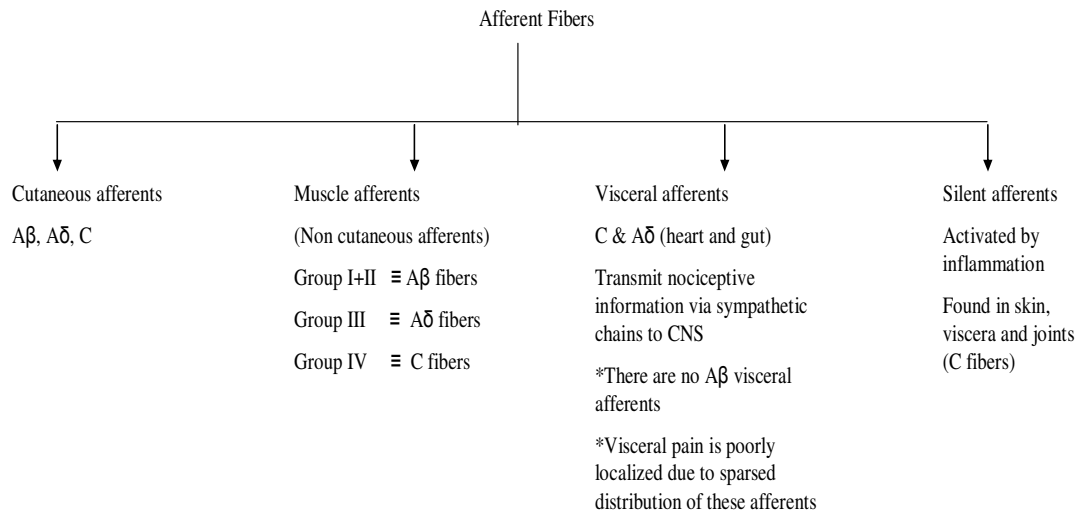


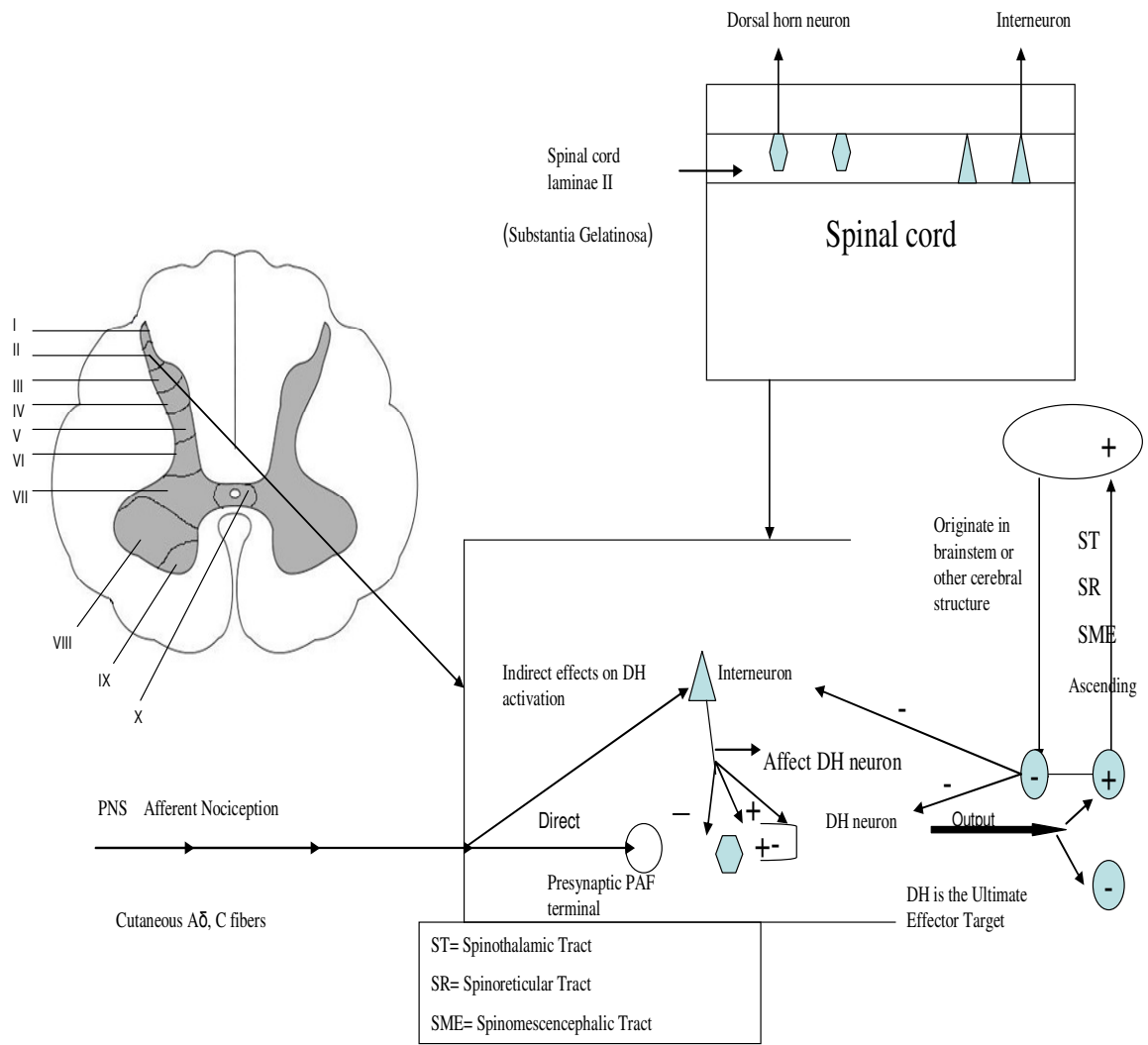
***Figure 5: Development of lymphocytes and subtypes of T cells.***

T and B cells originate from the bone marrow stem cells. T cells migrate to the thymus for maturation and differentiation. Six subtypes of T cell include: 1. Helper T cell, 2. Cytotoxic T cell, 3. Regulatory T cell, 4. Memory T cell, 5. Natural killer T cell 6. Gamma delta T cell. Helper T cell has 4 subtypes: Th1, Th2, Th3, Th17. B cell matured in the bone marrow and migrates in to the blood and hides into the secondary lymphoid organ for activation by T cell and antigen interaction. There are two subtypes of B cells: 1. Plasma cells and 2. Memory B cells. Plasma cells produce antibodies against antigens (Based on facts from [http://en.wikipedia.org/wiki/T\\_cell](http://en.wikipedia.org/wiki/T_cell), Kuby, J. Immunology. 3rd ed. P: 196).



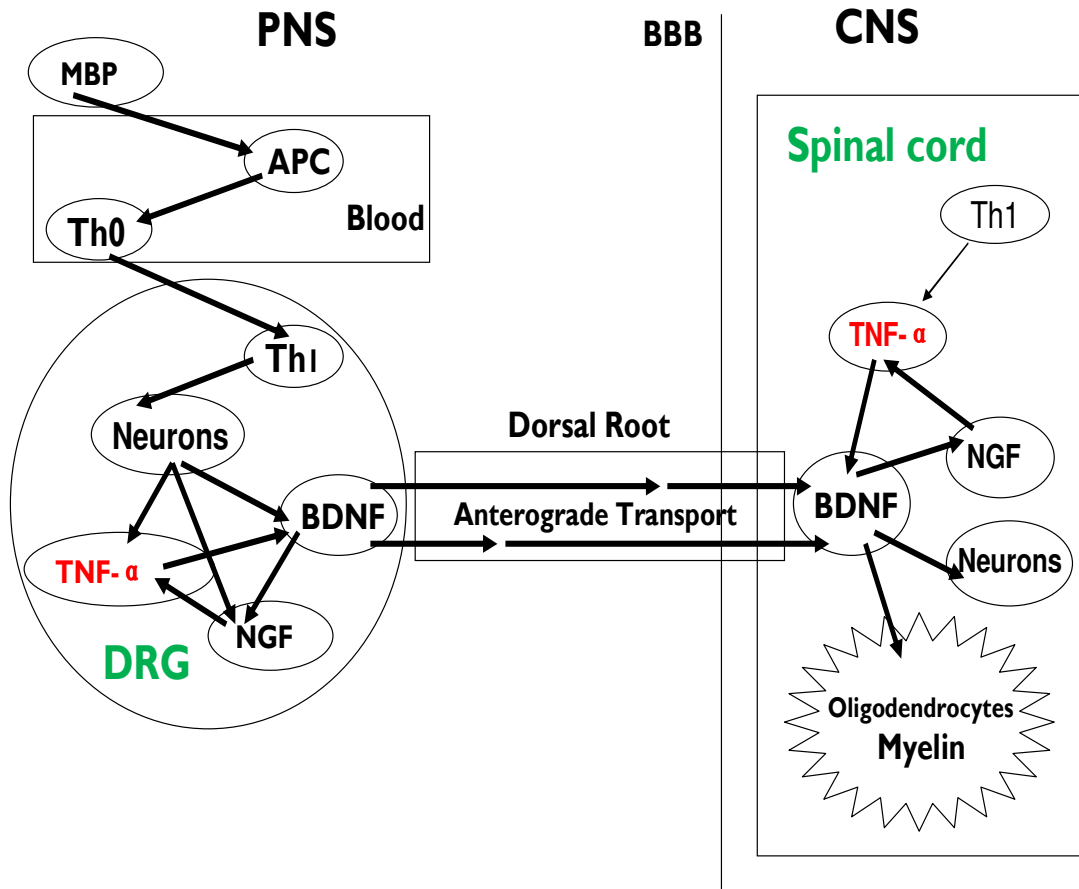
***Figure 6: Pathway of pain impulse transmission (PNS to CNS).***

Afferent nociceptive impulse from peripheral nervous system passes along the cutaneous A $\delta$  and C fibers. These afferent inputs can activate the dorsal horn (DH) neurons directly and indirectly via the activation of interneurons. Based on which type of interneuron involved in the activation of DH neurons, the output of the DH neuron can be excitatory or inhibitory. If it is inhibitory, the pain signal will not be transmitted. If the output is excitatory it then synchronously excites other DH neurons and the nociceptive information is subsequently relayed to the higher brain centres via the spinothalamic, spinoreticular or spinomesencephalic tract. In the brain the nociceptive information is processed and subsequently activates the descending inhibitory pathways originating in the brainstem or other cerebral structures. The activation of descending pathways inhibits nociceptive DH neuron both directly, and indirectly, via the inhibition of excitatory interneurons, the excitation of inhibitory interneurons. The inhibitory effects of DH neurons then synchronously inhibit other DH neurons. Ultimately no pain signal will be transmitted to the periphery (Based on facts from Millan, 1999).



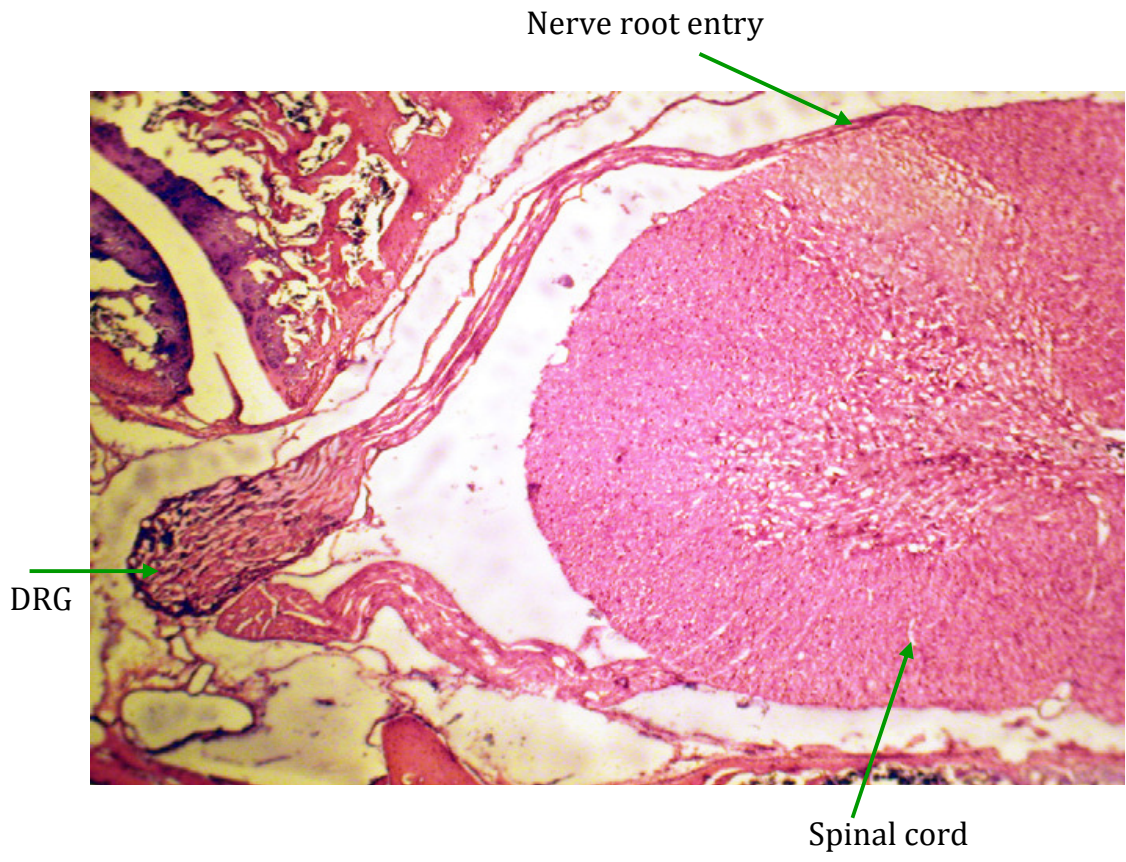
***Figure 7: Model of MS associated neuropathic pain & demyelination.***

DRG/Spinal cord interactions. i) Due to antigenic induction Th0 cells become activated and converted to Th1 cell in the peripheral blood. ii) Th1 cells transport to the DRG via the highly permeable capillaries that vascularize the DRG, where they cross the BBB and activate neurons iii) Neurons then produce the inflammatory cytokine TNF- $\alpha$  and neurotrophins such as BDNF and NGF. iv) TNF-  $\alpha$  can also induce BDNF and NGF production from neurons. v) From DRG; Th1 cells, cytokines, and neurotrophins are thought to undergo anterograde transport to the spinal cord via the dorsal roots vi) Inside the spinal cord Th1 become reactivated in presence of local CNS protein and produce TNF- $\alpha$ . vii) TNF- $\alpha$  will induce BDNF and NGF which ultimately affects OL (Based on facts from Melanson et al., 2009).



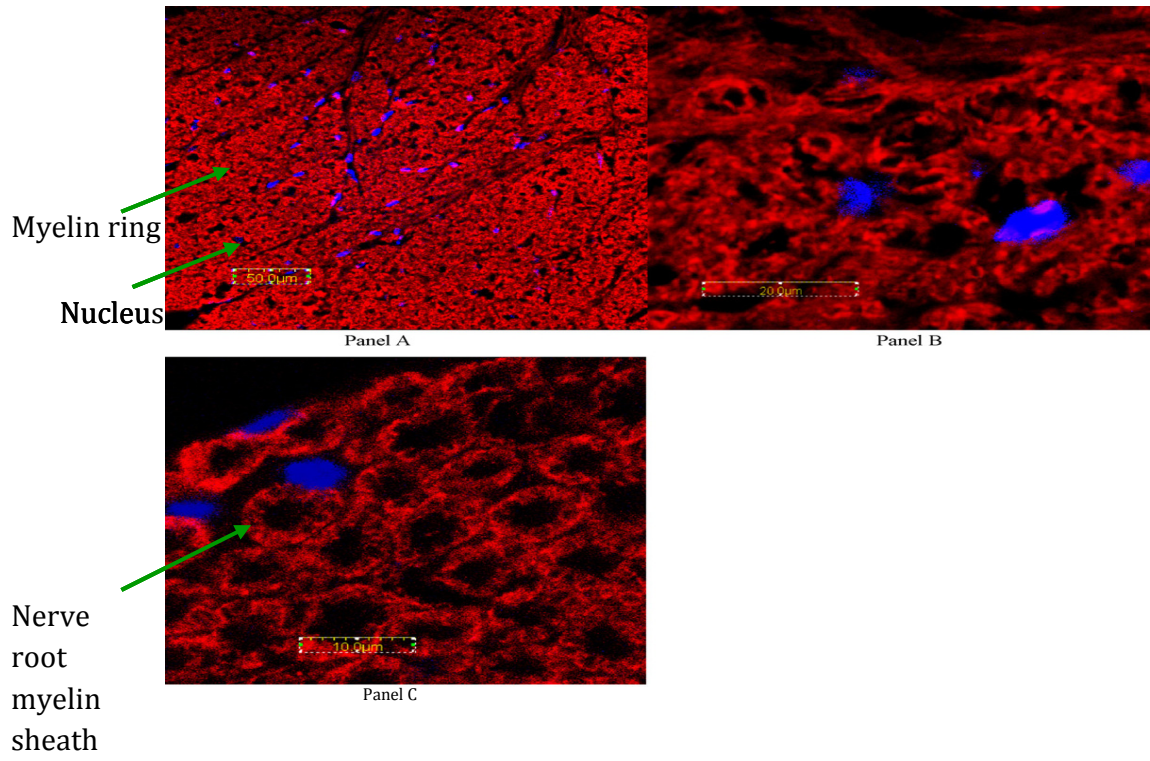
***Figure 8: Cross section of the 6% TCA decalcified spinal cord stained with hematoxylin and eosin (H&E) stain.***

Gross tissue morphology is unaffected by the decalcification process. The peripheral–central nervous system connections are shown, with the dorsal root connecting the spinal cord to the dorsal root ganglion (DRG). The ventral root is shown connected to the ventral horn and runs adjacent to the DRG towards the point of connection with the sensory root distal to the DRG. Bright field image at 4× magnification. (© Begum et al., (2010) A novel decalcification method for adult rodent bone for histological analysis of peripheral-central nervous system connections. *Journal of Neuroscience Methods* 187:59-66. Used with permission from Rightslink on July 8, 2010).



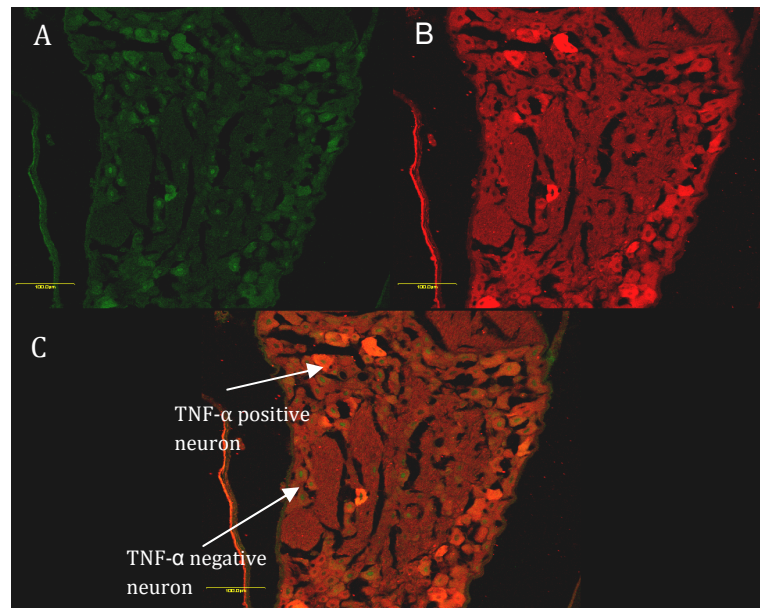
***Figure 9: Rat spinal cord myelin structure after 6% TCA solution decalcification of the vertebral column.***

10µm sections of spinal cord were immunostained for myelin basic protein (MBP). Nuclei were counterstained with DAPI (blue). Panel A—low power (40×) MBP immunoreactivity (red) shows clean and distinct myelin ring structures in the white matter of the spinal cord. Total magnification was 400×. Panel B—high magnification (100×) shows distinct myelin ring structure as well as nodes of Ranvier in the grey matter of the spinal cord. Total magnification was 1000×. Panel C—high magnification (100×) MBP immunoreactivity (red) shows distinct morphology of the nerve root myelin sheaths in a transverse section of sensory nerve root. (© Begum et al., (2010) A novel decalcification method for adult rodent bone for histological analysis of peripheral-central nervous system connections. *Journal of Neuroscience Methods* 187:59-66. Used with permission from Rightslink on July 8, 2010).



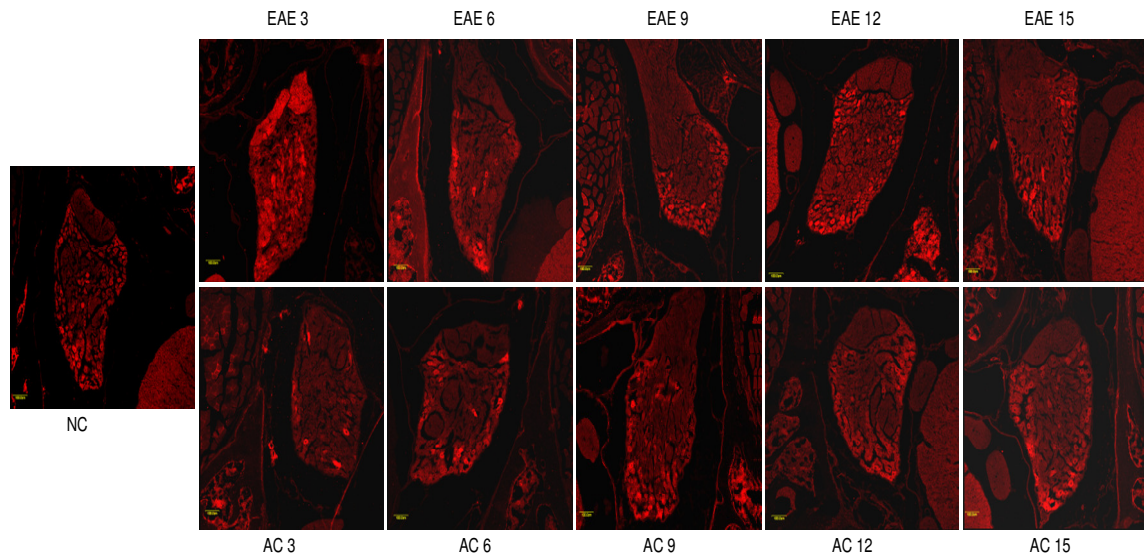
**Figure 10: TNF- $\alpha$  double immunohistochemistry.**

Confocal images of DRG neurons stained for TNF- $\alpha$  and neuronal nuclei. Serial sections were cut at 10  $\mu\text{m}$  thickness and DRG stained with TNF- $\alpha$  primary polyclonal antibody (R&D, goat anti rat, cat. # AF-510-NA: 1:100) and secondary (Invitrogen, donkey anti goat “Alexa 568” cat# A-11057: 1:500). Neuronal Nuclei were stained with NeuN primary antibody (Millipore, mouse anti-NeuN, cat. # MAB377:1:100) and secondary (Jackson ImmunoResearch, FITC conjugated goat anti mouse IgG, cat. # 115-095-003: 1:100). Panel A. Green shows neuronal nuclei immunoreactivity Panel B. Red shows TNF- $\alpha$  immunoreactivity in the neurons of DRG and. C. Composite picture. Total magnification 200x.



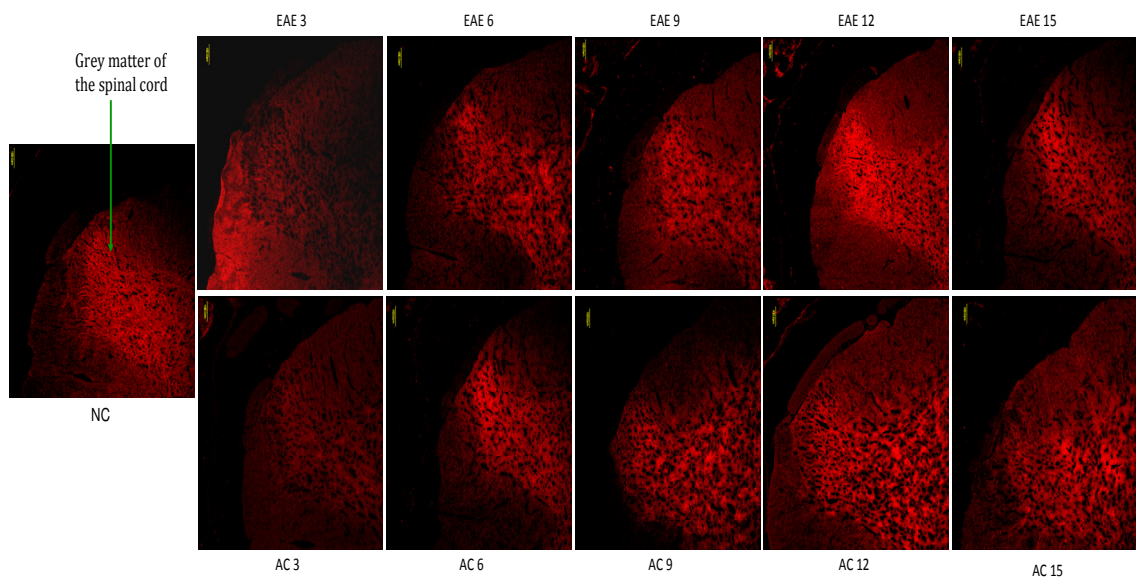
**Figure 11: TNF- $\alpha$  immunoreactivity in the DRG.**

Confocal images of DRG neurons. Serial sections were cut at 10  $\mu\text{m}$  thickness and DRG stained with TNF- $\alpha$  primary polyclonal antibody (R&D, goat anti rat, cat. # AF-510-NA: 1:100) and secondary (Invitrogen, donkey anti goat “Alexa 568” cat# A-11057: 1:500). Red shows TNF- $\alpha$  immunoreactivity in the neurons of DRG. Comparative IHC analysis showed increased TNF- $\alpha$  labeling at day 12 of EAE active relative to other groups. Total magnification 100x. Scale bar 100  $\mu\text{m}$ . NC= Naïve control, AC= Active control, EAE=Active EAE.



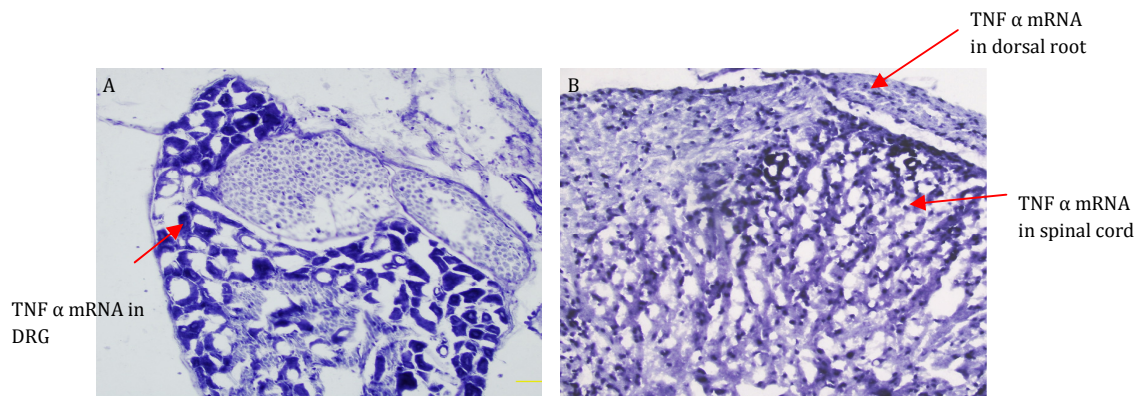
**Figure 12: TNF- $\alpha$  immunoreactivity in the spinal cord.**

Confocal images of spinal cord sections. Serial sections were cut at 10  $\mu$ m thickness. Spinal cord stained with TNF- $\alpha$  primary polyclonal antibody (R&D, goat anti rat, cat. # AF-510-NA: 1:100) and secondary (Invitrogen, donkey anti goat “Alexa 568” cat# A-11057: 1:500). Red shows TNF- $\alpha$  immunoreactivity. Comparative IHC analysis of spinal cord shows increased TNF- $\alpha$  immunoreactivity in the grey matter at day 12 active EAE relative to other groups. Total magnification 100x. Scale bar 100  $\mu$ m. NC= Naïve control, AC= Active control, EAE=Active EAE.



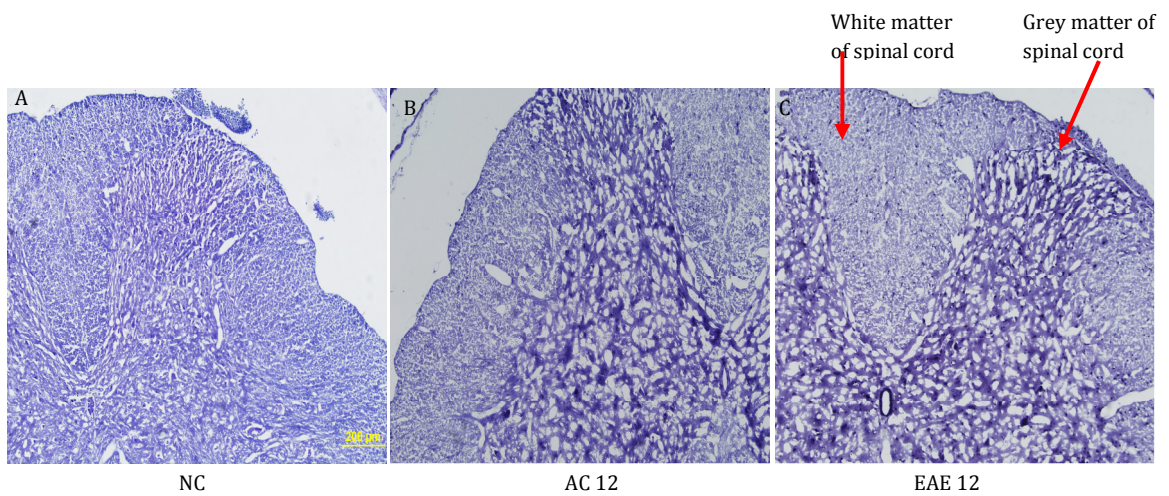
**Figure 13: In situ hybridization for detection of TNF- $\alpha$  mRNA.**

TNF- $\alpha$  mRNA was visualized in 10 $\mu$ m cryosections of frozen fixed tissue of spinal cord attached to the DRG of active EAE group using a digoxigenin labeled antisense oligonucleotide probe. Arrow shows TNF- $\alpha$  mRNA expression. Panel A. TNF- $\alpha$  mRNA in the DRG. Panel B: TNF- $\alpha$  mRNA in dorsal root and in the spinal cord. Total magnification 200x.



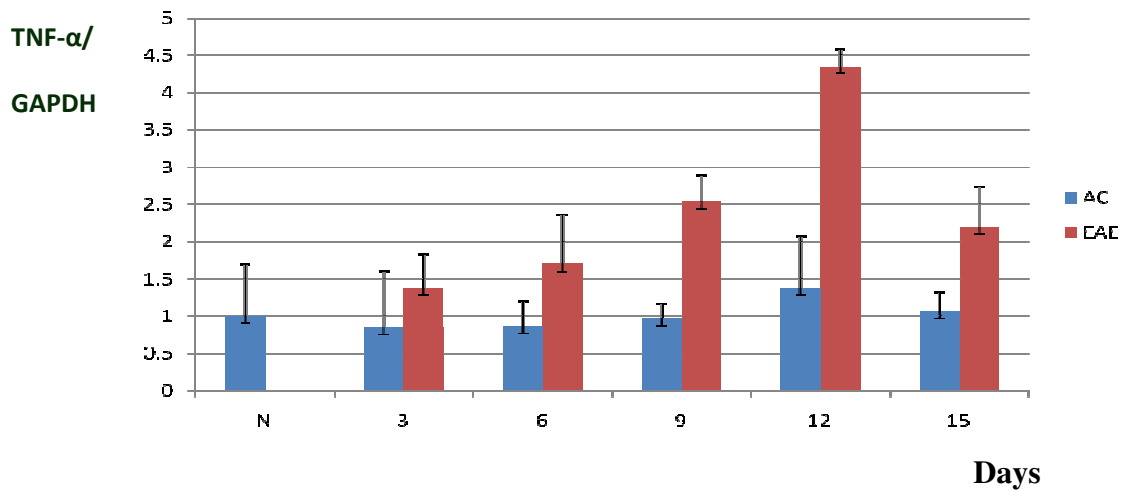
**Figure 14: In situ hybridization for detection of TNF- $\alpha$  mRNA within the spinal cord.**

Tissue from control rats Panel A. NC= Naïve control, Panel B. AC 12= Active control day 12, reveals decrease TNF- $\alpha$  mRNA expression in the spinal cord. Panel C. Active EAE day 12 reveals increase TNF- $\alpha$  mRNA expression compared with control rats. Total magnification 100x. Scale bar 200 $\mu$ m. NC= Naïve control, AC= Active control, EAE=Active EAE.



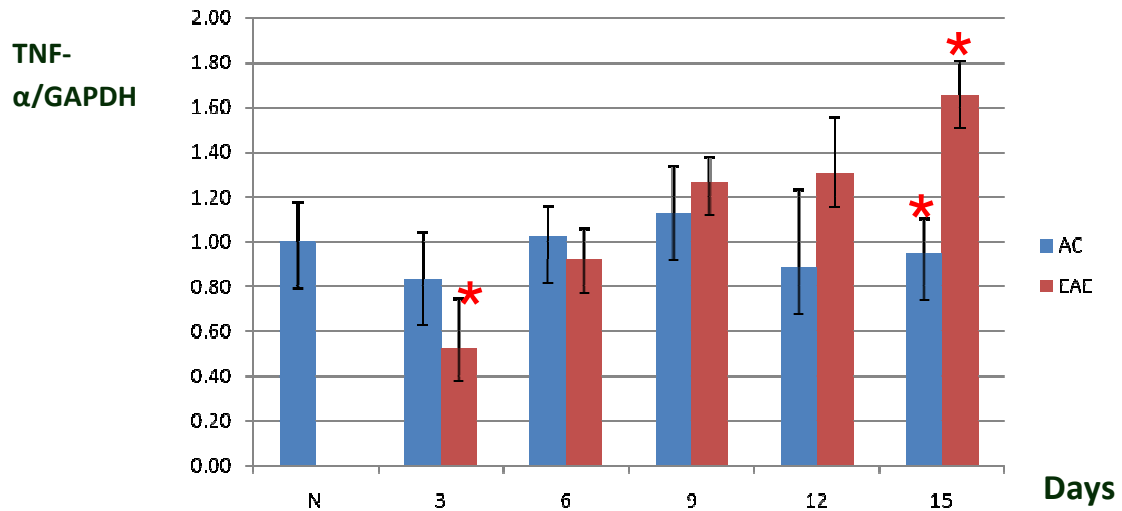
**Figure 15: Real-time PCR results of TNF- $\alpha$  expression within DRG.**

The TNF- $\alpha$  expression of DRG for animals of the active EAE group, euthanized at day 12 is significantly higher than other groups (naive control and active control (AC) ( $p < 0.05$ , Anova).



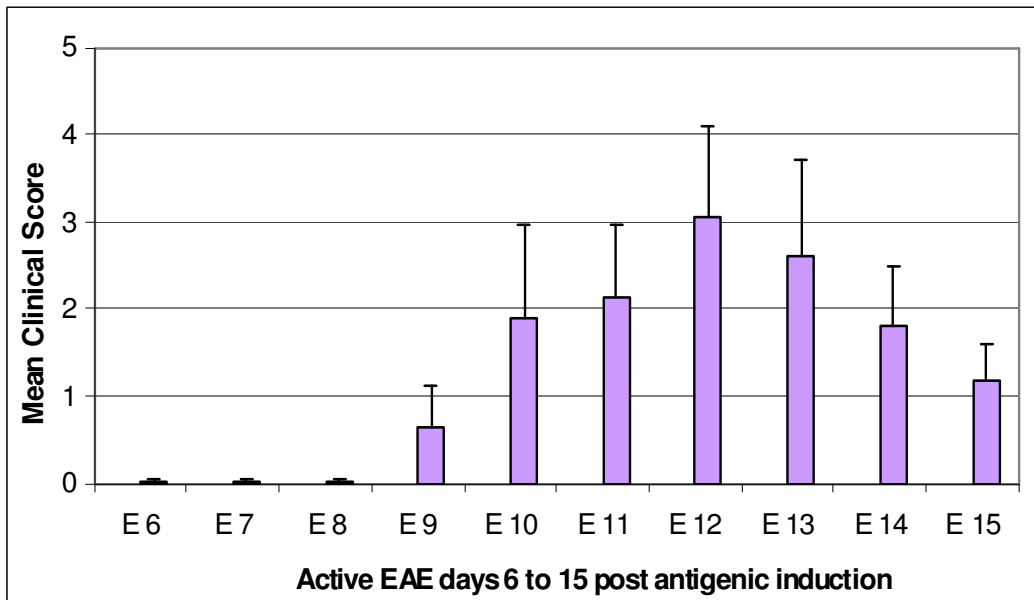
**Figure 16: Normalized Real-time PCR results of TNF- $\alpha$  expression within spinal cord.**

The TNF- $\alpha$  expression of spinal cord for animals of the active EAE group, euthanized at day 15 is significantly higher than EAE day 3 group and active control day 15 group ( $p < 0.05$ , Anova). NC= Naïve control, AC= Active control, EAE=Active EAE.



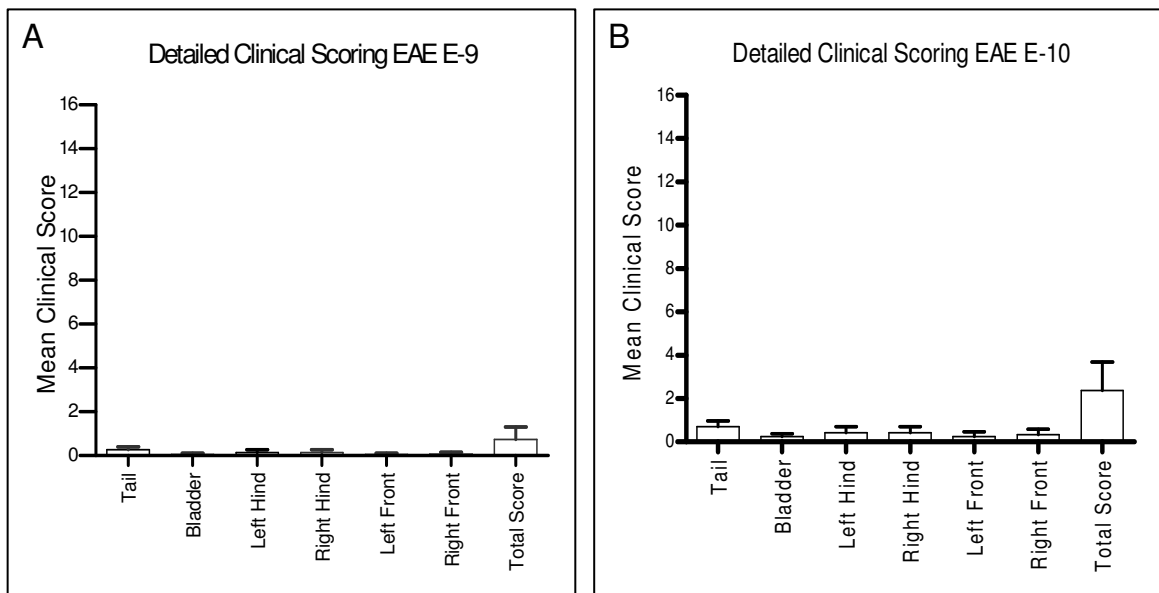
**Figure 17: Global Neurological Disability Score for animals induced to a state of EAE.**

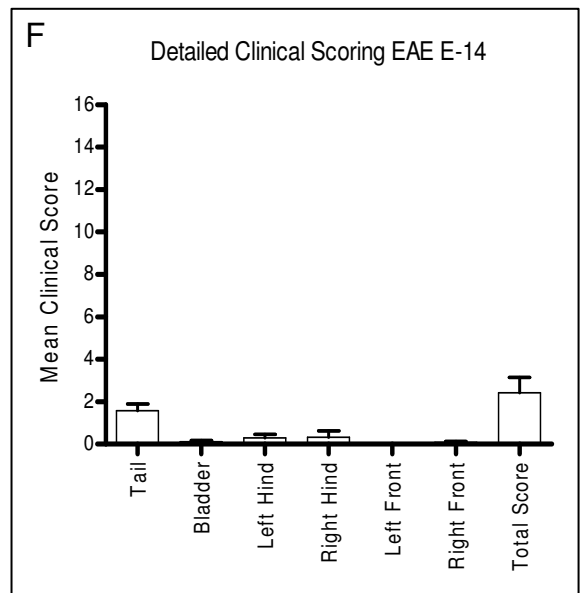
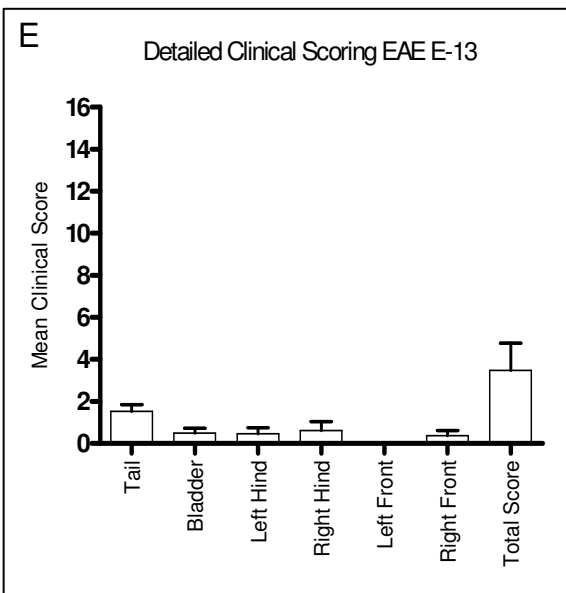
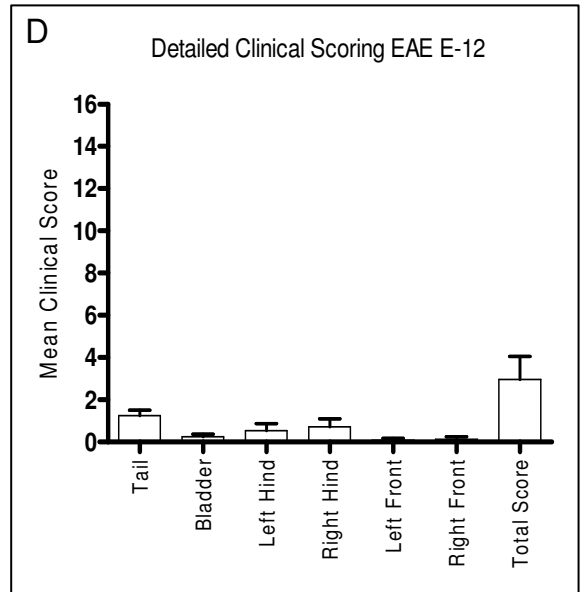
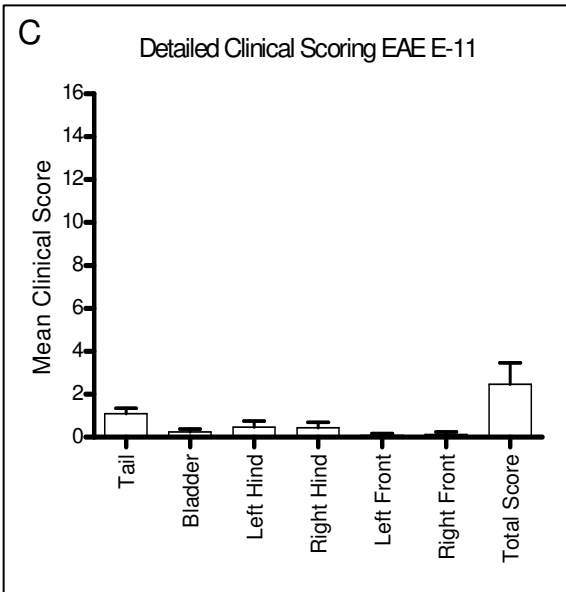
Disability scores range from a mean clinical disability score of 0 (no disability) to 15 (maximal disability). The bell shaped distribution outlining peak neurological disability in response to EAE induction occurred at day 12 post-disease induction.



**Figure 18 (A-G): Detailed Neurological Disability Scores for active EAE animals.**

( $N_T=18$ ) at days 9 ( $n=6$ ), 12 ( $n=6$ ) & 15 ( $n=6$ ), spanning the 6 specific domains of clinical disability assessment that include: *tail*, *bladder*, *left hind*, *right hind*, *left front* and *right front*. Total score represents the mean of the individual summated scores ( $n=6$ ) of each specified time point for each of the 6 individual domains of clinical disability assessment. The mean clinical disability scores obtained at each predetermined time point range from 0 (no disability) to 15 (maximal disability).





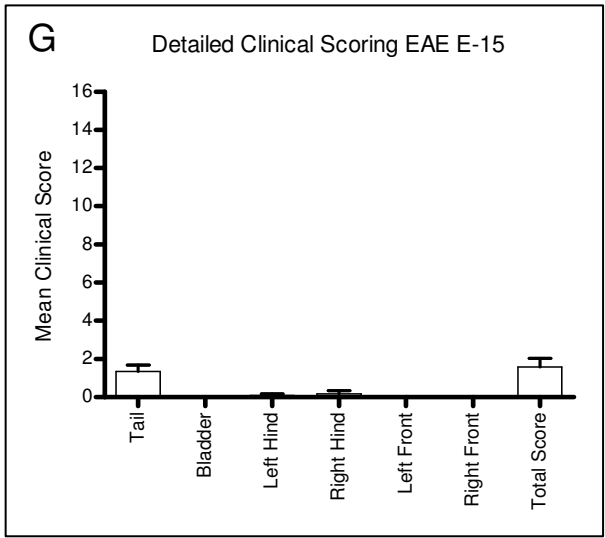


**Figure 19: Normalized thermal withdrawal latencies in EAE15 rats for tail relative to time of disease onset.**

Values are normalized to average baseline responses (Days -4 to 1) and displayed as means +/- standard deviations. Data are aligned to day of onset of clinical disease; Day 0 is the first day of clinical symptoms/signs for each individual animal. Withdrawal latencies were significantly increased at day 0 compared to baseline responses (p=0.002, Tukey's honest significance test).

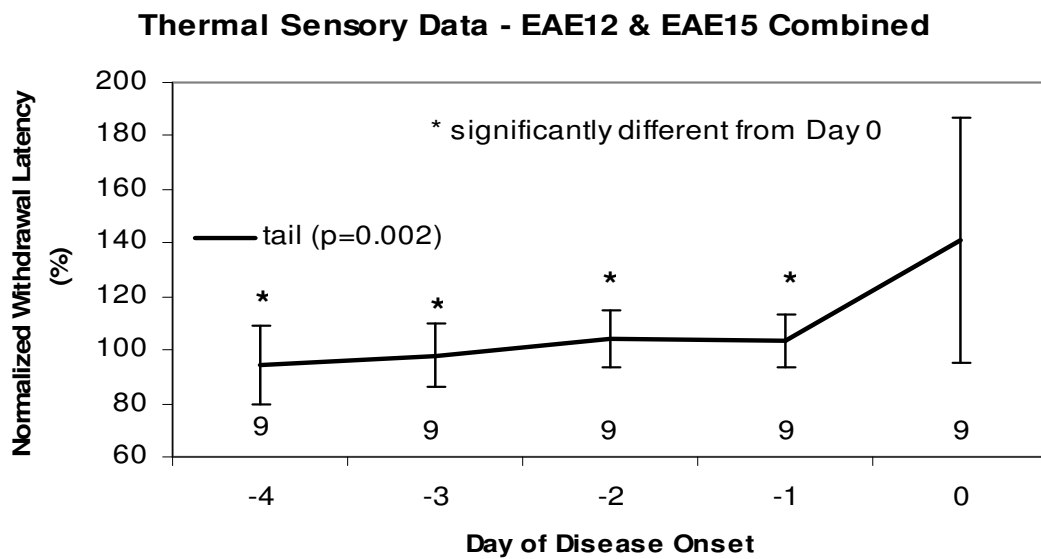


**Figure 20: Thermal withdrawal latencies normalized to baseline responses (average of Day -4 to Day -1).**

Data are aligned to day of onset of clinical disease; Day 0 is the first day of clinical symptoms/signs for each individual animal. Withdrawal latencies were significantly elevated at day 4 compared to all days before except Day 3 (Repeated measures ANOVA,  $p > 0.05$ , Tukey's posthoc test ). ANOVA by SITE for DAY effect is significant for front right, front left and rear left.

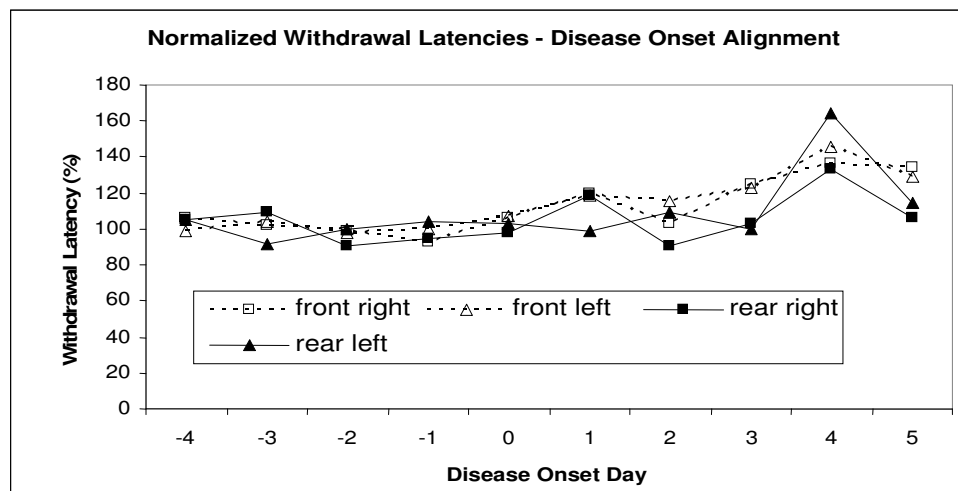


**Figure 21: Mechanical withdrawal thresholds normalized to baseline responses (average of Day -4 to Day -1).**

Data are aligned to day of onset of clinical disease; ie, Day 0 is the first day of clinical symptoms/signs for each individual animal. No significant effects using repeated measures ANOVA for SITE x DAY.

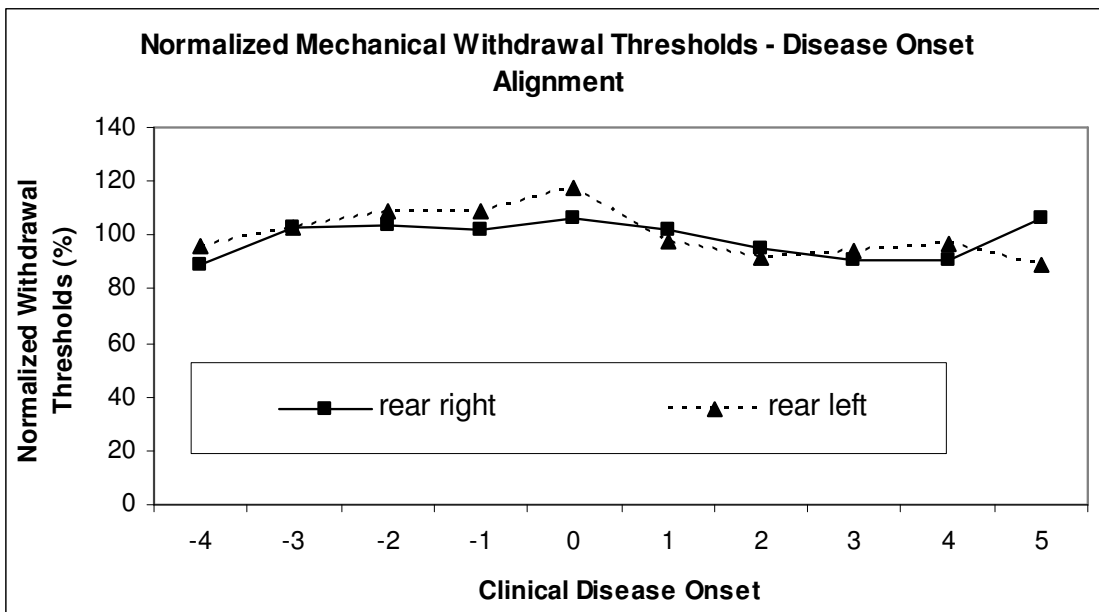


**Figure 22: Percentage of TNF- $\alpha$  positive neurons in DRG.**

Significantly increased proportions of TNF- $\alpha$  positive sensory neurons were identified in the active EAE group which appeared to peak at 12 dpi. ( $P < 0.05$ , Anova). NC= Naïve control, AC= Active control, EAE=Active EAE.

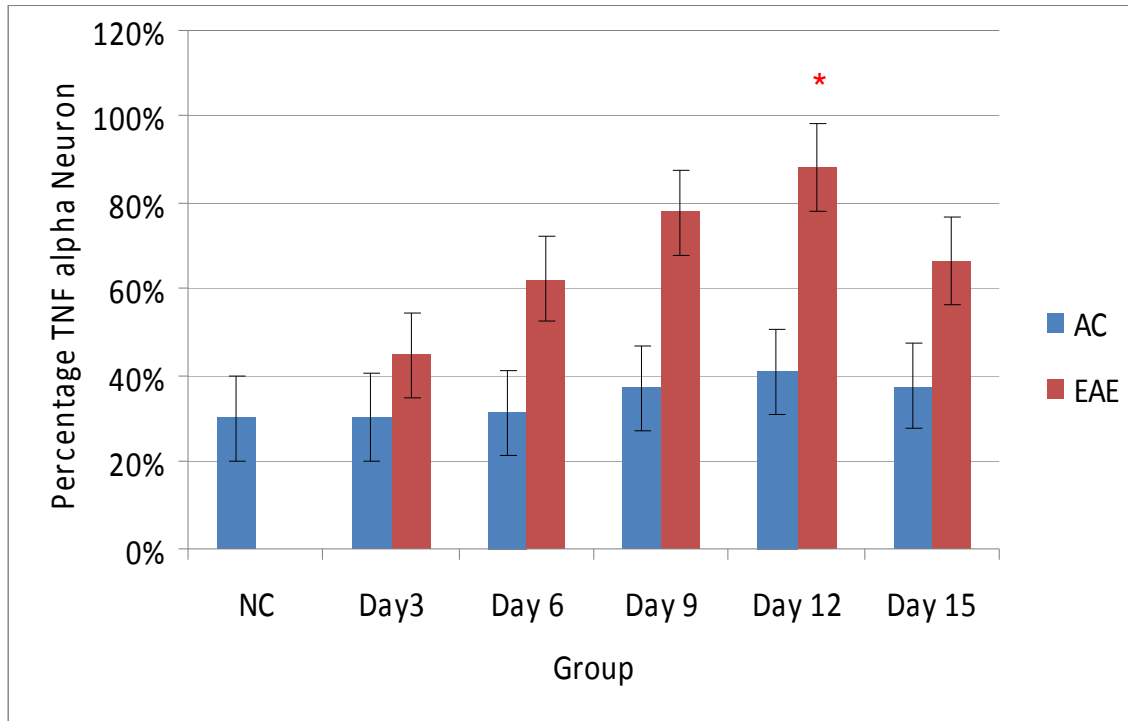


**Figure 23: Cell size distribution of TNF- $\alpha$  positive neurons in DRG.**

Analysis of size of the TNF- $\alpha$  positive neurons identified from DRG obtained from the active EAE and active control group revealed a predominant cell size distribution that is reflective of small to medium diameter (<25  $\mu\text{m}$ , mean=22.30  $\mu\text{m}$ , SD $\pm$ 4.47  $\mu\text{m}$ ) sensory neurons which corresponds to C and A $\delta$  fibers, respectively. (\*P <0.01, Anova). NC= Naïve control, AC= Active control, EAE=Active EAE.

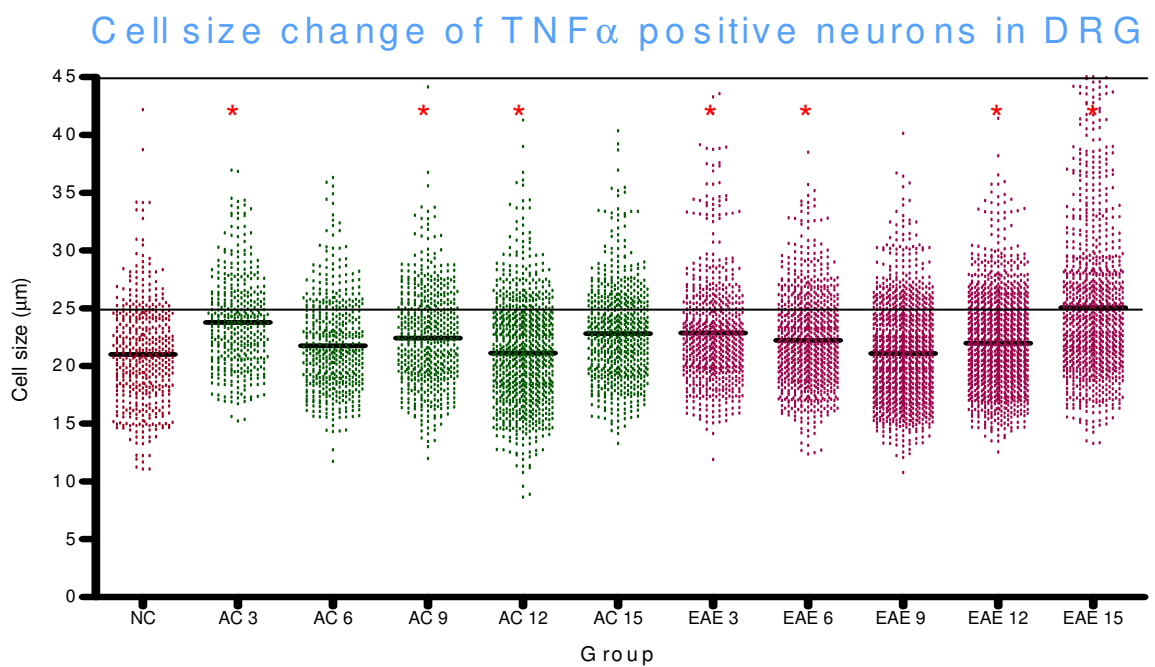


**Table 1: Afferent fibers innervation into the spinal cord laminae (Based on facts from Millan, 1999).**

Afferent fibers	Laminae
A $\beta$ fibers (non nociceptive)	*(III –IV) less in V/VI limited extent in Iii, I
A $\delta$ fibres ( nociceptive )	*I, sparse extent in IIo less X
C fibers (nociceptive)	*IIo, less in I, weak in V, X

\*predominant innervations

**Table 2: Animal usage: N=66.**

	Naïve control	Active control					Active EAE				
No. of animals	6	6	6	6	6	6	6	6	6	6	6
Sacrifice day	15	3	6	9	12	15	3	6	9	12	15

**Table 3: Neurological Disability Clinical Scoring System for animals induced to a state of EAE.**

The total score is the **sum** of the following individual scores obtained for each of the 6 specified clinical domains:

<b><u>Tail:</u></b>	<b><u>Bladder:</u></b>
0 – normal	0 – normal
1 – partially paralyzed, weakness	1 - incontinence
2 – completely paralyzed, limp	

<b><u>Right hind limb:</u></b>	<b><u>Left hind limb:</u></b>
0 – normal	0 – normal
1 – weakness	1 - weakness
2 – dragging with partial paralysis	2 - dragging with partial paralysis
3 – complete paralysis	3 – complete paralysis

<b><u>Right forelimb:</u></b>	<b><u>Left forelimb:</u></b>
0 – normal	0 - normal
1 – weakness	1 - weakness
2 – dragging, not able to support weight	2 – dragging, not able to support weight
3 – complete paralysis	3 – complete paralysis

**Table 4: Summary of tissue analysis.**

Tissue analysis	Fresh extract	Tissue sections
DRG	qRT-PCR Protein	In situ hybridization Immunohistochemistry
Spinal cord	qRT-PCR Protein	In situ hybridization Immunohistochemistry

## **CHAPTER 5: DISCUSSION**

The results of this study are the first to our knowledge to provide supportive evidence in regard to the advanced cellular mechanisms involved in MS induced neuropathic pain. We show that TNF- $\alpha$  gene and protein expression in the DRG and spinal cord tissue is increased in the active EAE day 12 dpi compared to control groups. In addition, our findings show TNF- $\alpha$  mRNA expression in the dorsal root entry point which supports our hypothesis that antigen induced DRG derived TNF- $\alpha$  can undergo axoplasmic anterograde transport from the periphery to the spinal cord via the dorsal roots. Our evidence that TNF- $\alpha$  mRNA translocates from the DRG to the dorsal horn of the spinal cord after CNS antigen induced inflammation is strong supportive evidence for the role of TNF- $\alpha$  in the signaling events that accompany DRG mediated CNS inflammation.

In the active EAE group sensory abnormalities assessed by thermal sensory testing, were also observed. Neurological disability assessments also demonstrate that the peak clinical score for active EAE animals is at day 12 which correlates with the findings of elevated TNF- $\alpha$  protein and gene expression in active EAE at day 12.

### ***TNF- $\alpha$ PROTEIN AND GENE EXPRESSION***

To assess the underlying cellular mechanism of MS induced neuropathic pain, we analyzed TNF- $\alpha$  protein and gene expression in the DRG, dorsal roots, and spinal cord. TNF- $\alpha$  protein expression was measured using IHC analysis. TNF- $\alpha$  mRNA expression was measured using qRT PCR and ISH analysis.

Previous studies have provided unequivocal evidence that pro-inflammatory cytokines mediate cellular and/or molecular changes in the DRG that manifest as hyperexcitability

of the primary sensory neurons. Thus these cytokines contribute to both induction and maintenance of neuropathic pain (Jancalek et al.; Wagner and Myers, 1996; Sommer and Schafers, 1998; Sommer et al., 1998a; Schafers et al., 2003a). Specifically, TNF- $\alpha$  has a critical role in the development and maintenance of neuropathic pain (Kiguchi et al., 2009). In addition, TNF- $\alpha$  plays a pivotal role in both peripheral and central mechanisms of neuropathic pain (Leung and Cahill). Traditional chronic constriction injury (CCI) of sciatic nerve in rats results in increased TNF- $\alpha$  immunoreactivity in DRG of both injured and uninjured ipsilateral adjacent afferents (Schafers et al., 2003c). Unilateral axotomy of the sciatic nerve in rats also demonstrates transient up regulation of TNF- $\alpha$  in both ipsi and contralateral DRG (Miao et al., 2008). On the other hand, inhibiting the synthesis of TNF- $\alpha$  with thalidomide or treatment with anti- TNF neutralizing antibodies at the time of nerve injury blocked the development of hyperalgesia and allodynia in animal models (Sommer et al., 1998b; Sommer et al., 1998a; Sommer et al., 2001). TNF- $\alpha$  act via two receptors: TNFR1 and TNFR2. TNFR1 is activated by binding of soluble TNF- $\alpha$ , whereas TNFR2 is activated by binding preferentially to transmembrane TNF- $\alpha$  (McCoy and Tansey, 2008). Previous study reported that elevated soluble TNF- $\alpha$  is a hallmark of acute and chronic neuroinflammation as well as number of neurodegenerative conditions, including MS (McCoy and Tansey, 2008). Therefore, further experiments are required to determine which form of TNF- $\alpha$  is present in our model.

Besides the injury induced causes of neuropathic pain, disease has also been associated with the development of neuropathic pain (Namaka et al., 2004). Research suggests that neuropathic pain is becoming a common problem in diabetes, and cancer, as well as in MS patients (Nurmikko et al.; Blumenthal, 2009; Wasan et al., 2009). A recent study

indicates that a common mechanism of neuropathic pain is the presence of inflammation at the site of injury which ultimately activates the immune system and release of immune active substances (Vallejo et al.). This concept is similar to the concept which focuses on the neuroimmune activation of chronic neuropathic pain (Mata et al., 2008).

Based on our published immune activation DRG and Spinal cord model for MS induced NPP (Melanson et al., 2009), antigen (MBP) induced activation of Th1 cells in the peripheral blood results in the elevated production of inflammatory cytokines such as TNF- $\alpha$ . Therefore we hypothesize that this blood derived inflammatory cytokine gains access to the DRG via the highly permeable capillaries that vascularize the DRG membrane. Entry of inflammatory cytokines into the DRG facilitates the activation of sensory neurons housed within the ganglia. This results in the release of neurotrophins such as BDNF and NGF. As a result, the newly synthesized cytokines and neurotrophins within the DRG can undergo axoplasmic transport directly into the CNS via the dorsal root port of entry to the spinal cord and directly act on dorsal horn neurons. This critical cytokine-neurotrophin interaction in the DRG followed by transport to the dorsal horn represents a plausible mechanism for MS-induced neuropathic pain involving the pathological activation of dorsal horn neurons. In addition, we hypothesize that Th1 cells may migrate to the DRG via and invasion through the BBB resulting from increased ICAM-1 expression on the endothelial cells, activated by the Th1 cell-derived TNF- $\alpha$ . The dual invasion of inflammatory cytokines and/or Th1 in the DRG would then continue to facilitate a positive feedback loop between DRG and the activated immune system (Melanson et al., 2009).

In our lab, a previous study was primarily focused on the TNF- $\alpha$  expression within DRG to determine its potential role in facilitating the intracellular signaling pathways involved in MS-induced neuropathic pain (Melanson et al., 2009). Thus, in order to identify possible mechanisms and temporal stages of central signaling pathways involved in neuropathic pain, this research was extended to include the analysis of TNF- $\alpha$  expression in the spinal cord tissue. In addition, this study was also designed to correlate the changes of TNF- $\alpha$  expression with the neurological disability symptoms and neuropathic behavior symptoms.

Anterograde and retrograde transport mechanisms for the neurotrophins BDNF and NGF between DRG and spinal cord support the theory that anterograde TNF- $\alpha$  protein transport also occurs (Richardson and Riopelle, 1984; Yip and Johnson, 1986; Zweifel et al., 2005; Miao et al., 2008). In addition to protein transport, other research has shown established transport mechanisms for the mRNA of BDNF and NT-3 as well as other substances, providing support for our findings of anterograde transport of TNF- $\alpha$  mRNA between DRG and spinal cord (Qiao et al., 2008; Wang et al., 2008). These findings support the bi-directional axonal transport of TNF- $\alpha$  protein and mRNA between DRG and spinal cord and correlate well with our experimental findings. Our IHC results demonstrate a significant increase of TNF- $\alpha$  protein in the DRG and spinal cord of active EAE day 12 dpi compared to control groups. The qRT-PCR and in situ hybridization findings also showed significant changes mRNA expression both in DRG and spinal cord of rats with active EAE group. Our experiments also showed TNF- $\alpha$  mRNA expression in the dorsal root. This finding also supported our hypothesis that TNF- $\alpha$  is capable of anterograde transport from the DRG to the spinal cord via dorsal root for local translation

at the pre-synaptic terminus essential for the release and interaction with the post-synaptic dorsal horn neurons, facilitating its involvement in the central mechanism of chronic neuropathic pain.

### ***NEUROLOGICAL DISABILITY ASSESSMENTS***

Similar to the human presentation of MS, animal EAE models may have relapsing remitting or a chronic relapsing course of disease (Olechowski et al., 2009). Prior studies have demonstrated that the MBP induced EAE model typically requires 8-11 days before clinical onset of symptoms with peak symptoms occurring between days 12-13 post-induction followed by complete remission (Gold et al., 2000). Our animal model demonstrated clinical symptoms appearing at day 6 after immunization with the peak symptoms at day 12 followed by remission which corresponds with previous results (Gold et al., 2000; Melanson et al., 2009). Clinical symptoms began in the tail and progressed to bladder and hind feet. This also corresponds with the findings from the behavioral assessments where we noticed hypoalgesia largely involving the tail and hind feet. This result parallels the human condition, with the highest percentage of MS patients complaining of chronic NPP in their lower extremities (Ehde et al., 2006). In addition, the results of the neurological disability scoring correlate with the results of IHC, qRT-PCR, and ISH which showed elevated TNF- $\alpha$  protein and gene expression in active EAE at day 12 dpi.

### ***BEHAVIORAL ASSESSMENTS***

Chronic pain is a major symptom associated with MS (Nurmikko et al.; Olechowski et al., 2009). The typical symptoms of neuropathic pain include hyperalgesia, allodynia and spontaneous pain (Marchand et al., 2005; Kiguchi et al., 2009). We first assessed changes

to the sensitivity to noxious heat in five specific domains of the animals using radiant heat stimulus. Results of our study showed significantly increased thermal withdrawal latencies that indicate the development of thermal hypoalgesia following clinical onset of EAE disease. Studies using a PLP induced relapsing remitting model of EAE in the SJL/J strain of mice showed thermal hypoalgesia followed by thermal hyperalgesia (Aicher et al., 2004). The same study also reported that hyperalgesia is not typically seen until resolution of the acute phase of the disease (Aicher et al., 2004). Our data correspond with their results for the same time period. The MBP induced EAE model is the acute inflammatory model. Therefore, the observed hypoalgesia is most likely explained by inflammation, axonal swelling, and constriction, which ultimately slows down nerve impulse conduction. Either way, the observed sensory changes are clear indicators that sensory function is altered in this animal model. To assess mechanical allodynia, we used von frey filament. No significant changes were observed in withdrawal latencies in the active EAE or control groups of animals resulting from mechanical stimulus. This finding can be explained by the role of cutaneous afferent fibers. In the chronic stage of disease, there is a degeneration and loss of A $\delta$  and C fiber projections in laminae II. Subsequently, the central projections of surviving A $\beta$  fibers in lamina III and IV may sprout into the territory vacated by the A $\delta$  and C-fiber terminals and make contact with second order pain transmission neurons in laminae II (Lekan et al., 1996; Nakamura and Myers, 1999). Thus, non-noxious information, such as proprioceptive information or touch may be interpreted as being of noxious origin. As our animal model is the acute inflammatory model, therefore it could be possible that there is no degeneration or loss of A $\delta$  and C-

fiber. As a result, there will be no sprouting of A $\beta$  fibers in laminae II which may be involved in the mechanism of allodynia.

### ***CELLULAR SOURCE OF TNF- $\alpha$ EXPRESSION***

The 3 main categories of cutaneous sensory afferent fibers, A $\beta$ , A $\delta$  and C fibers, keep the body in touch with the diverse stimuli received from the external environment (Namaka et al., 2004). Under normal conditions, A $\delta$  and C fibers, the main fibers for nociceptive transmission, contain medium and small diameter sensory axons, respectively, whereas A $\beta$  fibers are involved in signaling non-nociceptive information and contain large diameter sensory axons. Studies show that in the intact nervous system small diameter neurons are TNF- $\alpha$  immunoreactive, but after chronic constriction injury medium to large DRG neurons increase their expression of TNF- $\alpha$  (Schafers et al., 2002). We therefore needed to identify the specific cellular source of TNF- $\alpha$  in the DRG. Based on the additional detailed analysis of DRG sensory neurons, our results demonstrate that active EAE day 12 group has the highest percentage of TNF- $\alpha$  positive neurons compared to other groups. In addition, the specific cellular source of TNF- $\alpha$  appears to be predominantly small to medium diameter with an average diameter of 22.30  $\mu$ m which correspond to C and A $\delta$  nociceptive neurons. The findings that we have presented depicting the specific cellular source of TNF- $\alpha$  due to inflammation are consistent with other studies (Schafers et al., 2002; Schafers et al., 2003c; Miao et al., 2008) This finding of the specific cellular source correlates with qRT-PCR data that clearly demonstrate a statistically significant increase in TNF- $\alpha$  expression at active EAE day 12 compared to other groups.

## **CHAPTER 6: LIMITATIONS AND FUTURE RESEARCH**

### **CONSIDERATIONS**

Thermal hyperalgesia and mechanical allodynia were the two major indicators used to confirm neuropathic pain behaviors in animal models of pain. In our animal model of MS, we were not able to observe these indicators. Instead we observed thermal hypoalgesia. As has been shown in previous studies, this is a clear indicator that sensory function is altered in our animal model. This thermal hypoalgesia may be the result of axonal swelling due to inflammation, which we expected in the monophasic rat model. Since a previous study reported that hyperalgesia is preceded by hypoalgesia, and hyperalgesia is not typically seen until resolution of the initial acute phase of the disease (Aicher et al., 2004), we have plan in a future study to move from the monophasic rat model to the biphasic mouse model using MOG as an immunogen (Aicher et al., 2004). By using monophasic mouse model, we hope to correlate the TNF- $\alpha$  expression with the specific neuropathic pain behaviors. Like MS, the MOG mouse EAE animal model also follows a different phase of the disease which is characterized by inflammation, demyelination and loss of axons. Using the biphasic model we will be able to analyze the role to inflammatory cytokines in different stages of the disease process, spanning from the early antigenic induction of inflammation as confirmed in our rat MPB model, to the later stages of de-myelination in accordance with the mouse model of MS.

Besides thermal hyperalgesia and mechanical allodynia, cold allodynia is often reported to be the sensory disturbances in MS patients (Svendsen et al., 2005) and appears early in the disease process prior to any apparent neurological deficits (Olechowski et al., 2009).

Therefore in our future study we will use the acetone test to detect changes in the sensitivity to innocuous cold stimuli.

TNF- $\alpha$  is a proinflammatory cytokine and plays a pathogenic role in many autoimmune disease such as MS (McCoy and Tansey, 2008; Takei and Laskey, 2008b) Studies show that TNF- $\alpha$  signaling depends on the function of NGF (Takei and Laskey, 2008b). In the presence of NGF, TNF- $\alpha$  promotes neuronal cell survival via TNFR2 (Takei and Laskey, 2008a). Another study showed that endogenous TNF- $\alpha$  contributes to neuronal cell death via TNFR1 after withdrawal of NGF (Barker et al., 2001). BDNF is also a member of the neurotrophin family and important modulator of neuronal function and survival (Saha et al., 2006). In support of the relationship between TNF- $\alpha$  and BDNF, TNF- $\alpha$  mediates neuroprotection indirectly by promoting astroglial BDNF expression (Saha et al., 2006). Therefore, in our DRG/spinal cord model (Figure 7), we suggested a correlation between TNF- $\alpha$ , BDNF, and NGF. BDNF causes OL differentiation and proliferation and promote myelin formation and repair. In the presence of NGF, TNF- $\alpha$  promotes neuronal survival via TNFR2. Conversely, TNF- $\alpha$  causes OL death via TNFR1 in the absence of NGF. Failure to maintain the adequate balance of these three key factors (TNF- $\alpha$ , BDNF and NGF) may contribute to MS pathophysiology. Therefore in our future study we hope to find out the TNF- $\alpha$  signaling pathways and how they contribute in MS pathophysiology via two receptors. In addition, we will also analyze NGF expression in the DRG as well as Spinal cord tissue and correlate with TNF- $\alpha$  signaling pathways.

## **CHAPTER 7: SUMMARY AND CONCLUSIONS**

The result of our current research shows that following EAE induction TNF- $\alpha$  protein and gene expression was increased in the DRG as well as in the spinal cord tissue of active EAE groups at day 12 compared to control groups. Using our novel cryostat technique our results also demonstrated that axoplasmic anterograde transport of TNF- $\alpha$  is possible between DRG and spinal cord via dorsal root, confirmed by ISH. In situ results indicate increased TNF- $\alpha$  mRNA expression in the DRG, dorsal root entry point and spinal cord tissue. In addition, analysis of specific cellular source of TNF- $\alpha$  reveal that active EAE day 12 groups has the highest percentage of TNF- $\alpha$  positive neurons than other groups and majority of the TNF- $\alpha$  positive neurons appeared small to medium sized, corresponding to A $\delta$  and C nociceptive neurons.

In addition, our findings also demonstrated that the animal developed clinical symptoms after antigen induction. The clinical symptoms appear at day 6 (dpi), peak at day 12 followed by remission. Behavioral assessments also demonstrate the sensory abnormalities in the active EAE group, whereas the control group did not show any signs of neurological disability or sensory abnormalities. These findings correspond with the findings that increased TNF- $\alpha$  protein and gene expression at day 12 of active EAE group.

Neuropathic pain is a well known characteristic of MS. As a result neuropathic pain can be a valuable pre-diagnostic marker for MS. The results presented in this study support our hypothesis that antigen induced production of inflammatory cytokine TNF- $\alpha$  in the DRG can undergo axoplasmic anterograde transport to the spinal cord in the early stages of MS, which could trigger the induction of neurotrophins (BDNF and NGF) that

regulate downstream effects on myelin. Because of the involvement in facilitating the development of neuropathic pain, the DRG and/or spinal cord represent plausible targets for early treatment strategies aimed at attenuating the effects of inflammatory cytokines during the initial active stages of MS.

Earlier diagnosis leads to the earlier application of therapeutic strategies, which results in decreased disease progression. MS is a disease that affects not just the person diagnosed with MS but the entire family. Its impact is felt through out the entire family system, affecting communication, relationships and daily functioning. Dealing with such an unpredictable chronic disease, the changes it can bring, its costs and the many choices to be made, put a lot of stress on all family members. If we can diagnose the disease by addressing primary symptomatic concern of neuropathic pain it will not only increase the patient health and well being but also help their family restoring quality of life aspects to the entire family unit.

## CHAPTER 8:REFERENCES

- Aicher SA, Silverman MB, Winkler CW, Bebo BF, Jr. (2004) Hyperalgesia in an animal model of multiple sclerosis. *Pain* 110:560-570.
- Aloe L, Properzi F, Probert L, Akassoglou K, Kassiotis G, Micera A, Fiore M (1999) Learning abilities, NGF and BDNF brain levels in two lines of TNF-alpha transgenic mice, one characterized by neurological disorders, the other phenotypically normal. *Brain Res* 840:125-137.
- Amato MP, Ponziani G, Siracusa G, Sorbi S (2001) Cognitive dysfunction in early-onset multiple sclerosis: a reappraisal after 10 years. *Arch Neurol* 58:1602-1606.
- Archibald CJ, McGrath PJ, Ritvo PG, Fisk JD, Bhan V, Maxner CE, Murray TJ (1994) Pain prevalence, severity and impact in a clinic sample of multiple sclerosis patients. *Pain* 58:89-93.
- Argov Z, Mastaglia FL (1979) Drug-induced peripheral neuropathies. *Br Med J* 1:663-666.
- Arnett HA, Mason J, Marino M, Suzuki K, Matsushima GK, Ting JP (2001) TNF alpha promotes proliferation of oligodendrocyte progenitors and remyelination. *Nat Neurosci* 4:1116-1122.
- Ascherio A, Munger KL (2007a) Environmental risk factors for multiple sclerosis. Part I: the role of infection. *Ann Neurol* 61:288-299.
- Ascherio A, Munger KL (2007b) Environmental risk factors for multiple sclerosis. Part II: Noninfectious factors. *Ann Neurol* 61:504-513.
- Aurilio C, Pota V, Pace MC, Passavanti MB, Barbarisi M (2008) Ionic channels and neuropathic pain: physiopathology and applications. *J Cell Physiol* 215:8-14.
- Azevedo FA, Carvalho LR, Grinberg LT, Farfel JM, Ferretti RE, Leite RE, Jacob Filho W, Lent R, Herculano-Houzel S (2009) Equal numbers of neuronal and nonneuronal cells make the human brain an isometrically scaled-up primate brain. *J Comp Neurol* 513:532-541.
- Bakshi R, Shaikh ZA, Miletich RS, Czarnecki D, Dmochowski J, Henschel K, Janardhan V, Dubey N, Kinkel PR (2000) Fatigue in multiple sclerosis and its relationship to depression and neurologic disability. *Mult Scler* 6:181-185.
- Baloh RH, Enomoto H, Johnson EM, Jr., Milbrandt J (2000) The GDNF family ligands and receptors - implications for neural development. *Curr Opin Neurobiol* 10:103-110.
- Banfield MJ, Naylor RL, Robertson AG, Allen SJ, Dawbarn D, Brady RL (2001) Specificity in Trk receptor:neurotrophin interactions: the crystal structure of TrkB-d5 in complex with neurotrophin-4/5. *Structure* 9:1191-1199.
- Banwell BL (2004) Pediatric multiple sclerosis. *Curr Neurol Neurosci Rep* 4:245-252.
- Barcellos LF, Sawcer S, Ramsay PP, Baranzini SE, Thomson G, Briggs F, Cree BC, Begovich AB, Villoslada P, Montalban X, Uccelli A, Savettieri G, Lincoln RR, DeLoa C, Haines JL, Pericak-Vance MA, Compston A, Hauser SL, Oksenberg JR (2006) Heterogeneity at the HLA-DRB1 locus and risk for multiple sclerosis. *Hum Mol Genet* 15:2813-2824.

- Barker V, Middleton G, Davey F, Davies AM (2001) TNFalpha contributes to the death of NGF-dependent neurons during development. *Nat Neurosci* 4:1194-1198.
- Barnes MP, Kent RM, Semlyen JK, McMullen KM (2003) Spasticity in multiple sclerosis. *Neurorehabil Neural Repair* 17:66-70.
- Begum F, Zhu W, Namaka MP, Frost EE (2010) A novel decalcification method for adult rodent bone for histological analysis of peripheral-central nervous system connections. *Journal of Neuroscience Methods* 187:59-66.
- Blumenthal DT (2009) Assessment of neuropathic pain in cancer patients. *Curr Pain Headache Rep* 13:282-287.
- Boiko A, Vorobeychik G, Paty D, Devonshire V, Sadovnick D (2002) Early onset multiple sclerosis: a longitudinal study. *Neurology* 59:1006-1010.
- Boucher TJ, Okuse K, Bennett DL, Munson JB, Wood JN, McMahon SB (2000) Potent analgesic effects of GDNF in neuropathic pain states. *Science* 290:124-127.
- Bowersox SS, Gadbois T, Singh T, Pettus M, Wang YX, Luther RR (1996) Selective N-type neuronal voltage-sensitive calcium channel blocker, SNX-111, produces spinal antinociception in rat models of acute, persistent and neuropathic pain. *J Pharmacol Exp Ther* 279:1243-1249.
- Caldwell JH, Schaller KL, Lasher RS, Peles E, Levinson SR (2000) Sodium channel Na(v)1.6 is localized at nodes of ranvier, dendrites, and synapses. *Proc Natl Acad Sci U S A* 97:5616-5620.
- Callen DJ, Shroff MM, Branson HM, Li DK, Lotze T, Stephens D, Banwell BL (2008) Role of MRI in the differentiation of ADEM from MS in children. *Neurology*.
- Cameron AA, Leah JD, Snow PJ (1986) The electrophysiological and morphological characteristics of feline dorsal root ganglion cells. *Brain Res* 362:1-6.
- Campagnoni AT, Skoff RP (2001) The pathobiology of myelin mutants reveal novel biological functions of the MBP and PLP genes. *Brain Pathol* 11:74-91.
- Cantorna MT (2008) Vitamin D and multiple sclerosis: an update. *Nutr Rev* 66:S135-138.
- Chang YS, Wang L, Suh YA, Mao L, Karpen SJ, Khuri FR, Hong WK, Lee HY (2004) Mechanisms underlying lack of insulin-like growth factor-binding protein-3 expression in non-small-cell lung cancer. *Oncogene* 23:6569-6580.
- Chaplan SR, Guo HQ, Lee DH, Luo L, Liu C, Kuei C, Velumian AA, Butler MP, Brown SM, Dubin AE (2003) Neuronal hyperpolarization-activated pacemaker channels drive neuropathic pain. *J Neurosci* 23:1169-1178.
- Chatel M, Lanteri-Minet M, Lebrun-Frenay C (2001) [Pain in multiple sclerosis]. *Rev Neurol (Paris)* 157:1072-1078.
- Chitnis T (2006) Pediatric multiple sclerosis. *Neurologist* 12:299-310.
- Chitnis T (2007) The role of CD4 T cells in the pathogenesis of multiple sclerosis. *Int Rev Neurobiol* 79:43-72.
- Christensen T (2007) Human herpesviruses in MS. *Int MS J* 14:41-47.
- Cohen S, Levi-Montalcini R, Hamburger V (1954) A Nerve Growth-Stimulating Factor Isolated from Sarcomas 37 and 180. *Proc Natl Acad Sci U S A* 40:1014-1018.
- Compston A, Coles A (2008) Multiple sclerosis. *Lancet* 372:1502-1517.
- Crayton H, Heyman RA, Rossman HS (2004) A multimodal approach to managing the symptoms of multiple sclerosis. *Neurology* 63:S12-18.
- Cunha FQ, Lorenzetti BB, Poole S, Ferreira SH (1991) Interleukin-8 as a mediator of sympathetic pain. *Br J Pharmacol* 104:765-767.

- Dasari VR, Spomar DG, Gondi CS, Sloffer CA, Saving KL, Gujrati M, Rao JS, Dinh DH (2007) Axonal remyelination by cord blood stem cells after spinal cord injury. *J Neurotrauma* 24:391-410.
- Delarasse C, Daubas P, Mars LT, Vizler C, Litzemberger T, Iglesias A, Bauer J, Della Gaspera B, Schubart A, Decker L, Dimitri D, Roussel G, Dierich A, Amor S, Dautigny A, Liblau R, Pham-Dinh D (2003) Myelin/oligodendrocyte glycoprotein-deficient (MOG-deficient) mice reveal lack of immune tolerance to MOG in wild-type mice. *J Clin Invest* 112:544-553.
- Dhib-Jalbut S, Jiang H, Williams GJ (1996) The effect of interferon beta-1b on lymphocyte-endothelial cell adhesion. *J Neuroimmunol* 71:215-222.
- Ding M, Hart RP, Jonakait GM (1995) Tumor necrosis factor-alpha induces substance P in sympathetic ganglia through sequential induction of interleukin-1 and leukemia inhibitory factor. *J Neurobiol* 28:445-454.
- Dogrul A, Gardell LR, Ossipov MH, Tulunay FC, Lai J, Porreca F (2003) Reversal of experimental neuropathic pain by T-type calcium channel blockers. *Pain* 105:159-168.
- Donaghy M (2002) Assessing the risk of drug-induced neurologic disorders: statins and neuropathy. *Neurology* 58:1321-1322.
- Dopp JM, Mackenzie-Graham A, Otero GC, Merrill JE (1997) Differential expression, cytokine modulation, and specific functions of type-1 and type-2 tumor necrosis factor receptors in rat glia. *J Neuroimmunol* 75:104-112.
- Duce IR, Keen P (1976) A light and electron microscope study of changes occurring at the cut ends following section of the dorsal roots of rat spinal nerves. *Cell Tissue Res* 170:491-505.
- Duce IR, Keen P (1977) An ultrastructural classification of the neuronal cell bodies of the rat dorsal root ganglion using zinc iodide-osmium impregnation. *Cell Tissue Res* 185:263-277.
- Duquette P, Murray TJ, Pleines J, Ebers GC, Sadovnick D, Weldon P, Warren S, Paty DW, Upton A, Hader W, et al. (1987) Multiple sclerosis in childhood: clinical profile in 125 patients. *J Pediatr* 111:359-363.
- Dyer CA (2002) The structure and function of myelin: from inert membrane to perfusion pump. *Neurochem Res* 27:1279-1292.
- Dyment DA, Ebers GC, Sadovnick AD (2004) Genetics of multiple sclerosis. *Lancet Neurol* 3:104-110.
- Ehde DM, Osborne TL, Hanley MA, Jensen MP, Kraft GH (2006) The scope and nature of pain in persons with multiple sclerosis. *Mult Scler* 12:629-638.
- Ehde DM, Jensen MP, Engel JM, Turner JA, Hoffman AJ, Cardenas DD (2003) Chronic pain secondary to disability: a review. *Clin J Pain* 19:3-17.
- Feiguin F, Ferreira A, Kosik KS, Caceres A (1994) Kinesin-mediated organelle translocation revealed by specific cellular manipulations. *J Cell Biol* 127:1021-1039.
- Fernyhough P, Smith DR, Schapansky J, Van Der Ploeg R, Gardiner NJ, Tweed CW, Kontos A, Freeman L, Purves-Tyson TD, Glazner GW (2005) Activation of nuclear factor-kappaB via endogenous tumor necrosis factor alpha regulates survival of axotomized adult sensory neurons. *J Neurosci* 25:1682-1690.

- Ferreira SH, Lorenzetti BB, Cunha FQ, Poole S (1993) Bradykinin release of TNF-alpha plays a key role in the development of inflammatory hyperalgesia. *Agents Actions* 38 Spec No:C7-9.
- Fields HL, Basbaum AI (1978) Brainstem control of spinal pain-transmission neurons. *Annu Rev Physiol* 40:217-248.
- Fields KL, Brookes JP, Mirsky R, Wendon LM (1978) Cell surface markers for distinguishing different types of rat dorsal root ganglion cells in culture. *Cell* 14:43-51.
- Figiel I, Dzwonek K (2007) TNFalpha and TNF receptor 1 expression in the mixed neuronal-glial cultures of hippocampal dentate gyrus exposed to glutamate or trimethyltin. *Brain Res* 1131:17-28.
- Frisen J, Verge VM, Fried K, Risling M, Persson H, Trotter J, Hokfelt T, Lindholm D (1993) Characterization of glial trkB receptors: differential response to injury in the central and peripheral nervous systems. *Proc Natl Acad Sci U S A* 90:4971-4975.
- Frohman E, Phillips T, Kokel K, Van Pelt J, O'Leary S, Gross S, Hawker K, Racke M (2002) Disease-modifying therapy in multiple sclerosis: strategies for optimizing management. *Neurologist* 8:227-236.
- Furlan R, Cuomo C, Martino G (2009) Animal models of multiple sclerosis. *Methods Mol Biol* 549:157-173.
- Gabay E, Tal M (2004) Pain behavior and nerve electrophysiology in the CCI model of neuropathic pain. *Pain* 110:354-360.
- Gasser HS (1950) Unmyelinated fibers originating in dorsal root ganglia. *J Gen Physiol* 33:651-690.
- George A, Buehl A, Sommer C (2004) Wallerian degeneration after crush injury of rat sciatic nerve increases endo- and epineurial tumor necrosis factor-alpha protein. *Neurosci Lett* 372:215-219.
- Girault JA, Peles E (2002) Development of nodes of Ranvier. *Curr Opin Neurobiol* 12:476-485.
- Gold R, Hartung HP, Toyka KV (2000) Animal models for autoimmune demyelinating disorders of the nervous system. *Mol Med Today* 6:88-91.
- Greenstein JI (2007) Current concepts of the cellular and molecular pathophysiology of multiple sclerosis. *Dev Neurobiol* 67:1248-1265.
- Groves MJ, Christopherson T, Giometto B, Scaravilli F (1997) Axotomy-induced apoptosis in adult rat primary sensory neurons. *J Neurocytol* 26:615-624.
- Hargus NJ, Patel MK (2007) Voltage-gated Na<sup>+</sup> channels in neuropathic pain. *Expert Opin Investig Drugs* 16:635-646.
- Hensiek AE, Sawcer SJ, Feakes R, Deans J, Mander A, Akesson E, Roxburgh R, Corradu F, Smith S, Compston DA (2002) HLA-DR 15 is associated with female sex and younger age at diagnosis in multiple sclerosis. *J Neurol Neurosurg Psychiatry* 72:184-187.
- Hermann GE, Rogers RC, Bresnahan JC, Beattie MS (2001) Tumor necrosis factor-alpha induces cFOS and strongly potentiates glutamate-mediated cell death in the rat spinal cord. *Neurobiol Dis* 8:590-599.
- Hofmann K, Tschopp J (1995) The death domain motif found in Fas (Apo-1) and TNF receptor is present in proteins involved in apoptosis and axonal guidance. *FEBS Lett* 371:321-323.

- Huang EJ, Reichardt LF (2003) Trk receptors: roles in neuronal signal transduction. *Annu Rev Biochem* 72:609-642.
- Imitola J, Chitnis T, Khoury SJ (2005) Cytokines in multiple sclerosis: from bench to bedside. *Pharmacol Ther* 106:163-177.
- Jahn O, Tenzer S, Werner HB (2009) Myelin proteomics: molecular anatomy of an insulating sheath. *Mol Neurobiol* 40:55-72.
- Jancalek R, Dubovy P, Svizenska I, Klusakova I Bilateral changes of TNF-alpha and IL-10 protein in the lumbar and cervical dorsal root ganglia following a unilateral chronic constriction injury of the sciatic nerve. *J Neuroinflammation* 7:11.
- Jensen TS (2002) Anticonvulsants in neuropathic pain: rationale and clinical evidence. *Eur J Pain* 6 Suppl A:61-68.
- Ji RR, Woolf CJ (2001) Neuronal plasticity and signal transduction in nociceptive neurons: implications for the initiation and maintenance of pathological pain. *Neurobiol Dis* 8:1-10.
- Ji RR, Strichartz G (2004) Cell signaling and the genesis of neuropathic pain. *Sci STKE* 2004:reE14.
- Johnson ES, Ludwin SK (1981) The demonstration of recurrent demyelination and remyelination of axons in the central nervous system. *Acta Neuropathol (Berl)* 53:93-98.
- Junger H, Sorkin LS (2000) Nociceptive and inflammatory effects of subcutaneous TNFalpha. *Pain* 85:145-151.
- Kantarci O, Wingerchuk D (2006) Epidemiology and natural history of multiple sclerosis: new insights. *Curr Opin Neurol* 19:248-254.
- Katz N (2000) Neuropathic pain in cancer and AIDS. *Clin J Pain* 16:S41-48.
- Kiguchi N, Maeda T, Kobayashi Y, Saika F, Kishioka S (2009) Involvement of inflammatory mediators in neuropathic pain caused by vincristine. *Int Rev Neurobiol* 85:179-190.
- Kim GM, Xu J, Song SK, Yan P, Ku G, Xu XM, Hsu CY (2001) Tumor necrosis factor receptor deletion reduces nuclear factor-kappaB activation, cellular inhibitor of apoptosis protein 2 expression, and functional recovery after traumatic spinal cord injury. *J Neurosci* 21:6617-6625.
- Kinouchi K, Brown G, Pasternak G, Donner DB (1991) Identification and characterization of receptors for tumor necrosis factor-alpha in the brain. *Biochem Biophys Res Commun* 181:1532-1538.
- Kitahata LM (1993) Pain pathways and transmission. *Yale J Biol Med* 66:437-442.
- Kole MH, Ilschner SU, Kampa BM, Williams SR, Ruben PC, Stuart GJ (2008) Action potential generation requires a high sodium channel density in the axon initial segment. *Nat Neurosci* 11:178-186.
- Kornek B, Lassmann H (2003) Neuropathology of multiple sclerosis-new concepts. *Brain Res Bull* 61:321-326.
- Krupp L (2006) Fatigue is intrinsic to multiple sclerosis (MS) and is the most commonly reported symptom of the disease. *Mult Scler* 12:367-368.
- Lassmann H (2008) Models of multiple sclerosis: new insights into pathophysiology and repair. *Curr Opin Neurol* 21:242-247.
- Lassmann H, Bruck W, Lucchinetti CF (2007) The immunopathology of multiple sclerosis: an overview. *Brain Pathol* 17:210-218.

- Lekan HA, Carlton SM, Coggeshall RE (1996) Sprouting of A beta fibers into lamina II of the rat dorsal horn in peripheral neuropathy. *Neurosci Lett* 208:147-150.
- Leung L, Cahill CM TNF-alpha and neuropathic pain--a review. *J Neuroinflammation* 7:27.
- Lewin GR, Ritter AM, Mendell LM (1993) Nerve growth factor-induced hyperalgesia in the neonatal and adult rat. *J Neurosci* 13:2136-2148.
- Lewin GR, Rueff A, Mendell LM (1994) Peripheral and central mechanisms of NGF-induced hyperalgesia. *Eur J Neurosci* 6:1903-1912.
- Li L, Xian CJ, Zhong JH, Zhou XF (2003) Lumbar 5 ventral root transection-induced upregulation of nerve growth factor in sensory neurons and their target tissues: a mechanism in neuropathic pain. *Mol Cell Neurosci* 23:232-250.
- Li Y, Ji A, Weihe E, Schafer MK (2004) Cell-specific expression and lipopolysaccharide-induced regulation of tumor necrosis factor alpha (TNFalpha) and TNF receptors in rat dorsal root ganglion. *J Neurosci* 24:9623-9631.
- Lu VB, Biggs JE, Stebbing MJ, Balasubramanian S, Todd KG, Lai AY, Colmers WF, Dawbarn D, Ballanyi K, Smith PA (2009) Brain-derived neurotrophic factor drives the changes in excitatory synaptic transmission in the rat superficial dorsal horn that follow sciatic nerve injury. *J Physiol* 587:1013-1032.
- Lublin FD (2005) Clinical features and diagnosis of multiple sclerosis. *Neurol Clin* 23:1-15, v.
- Ludwin SK (2006) The pathogenesis of multiple sclerosis: relating human pathology to experimental studies. *J Neuropathol Exp Neurol* 65:305-318.
- Lunemann JD, Kamradt T, Martin R, Munz C (2007) Epstein-barr virus: environmental trigger of multiple sclerosis? *J Virol* 81:6777-6784.
- Lykissas MG, Batistatou AK, Charalabopoulos KA, Beris AE (2007) The role of neurotrophins in axonal growth, guidance, and regeneration. *Curr Neurovasc Res* 4:143-151.
- MacEwan DJ (2002) TNF receptor subtype signalling: differences and cellular consequences. *Cell Signal* 14:477-492.
- Madsen LS, Andersson EC, Jansson L, krogsgaard M, Andersen CB, Engberg J, Strominger JL, Svejgaard A, Hjorth JP, Holmdahl R, Wucherpfennig KW, Fugger L (1999) A humanized model for multiple sclerosis using HLA-DR2 and a human T-cell receptor. *Nat Genet* 23:343-347.
- Marchand F, Perretti M, McMahon SB (2005) Role of the immune system in chronic pain. *Nat Rev Neurosci* 6:521-532.
- Martin M, Weber-Varzegi J, Flammer J (2005) [Toxic optic neuropathy due to cisplatin therapy: a case report]. *Klin Monbl Augenheilkd* 222:244-247.
- Martinez-Sanchez M, Striggow F, Schroder UH, Kahlert S, Reymann KG, Reiser G (2004) Na(+) and Ca(2+) homeostasis pathways, cell death and protection after oxygen-glucose-deprivation in organotypic hippocampal slice cultures. *Neuroscience* 128:729-740.
- Martino G, Hartung HP (1999) Immunopathogenesis of multiple sclerosis: the role of T cells. *Curr Opin Neurol* 12:309-321.
- Martino G, Grohovaz F, Brambilla E, Codazzi F, Consiglio A, Clementi E, Filippi M, Comi G, Grimaldi LM (1998) Proinflammatory cytokines regulate antigen-independent T-cell activation by two separate calcium-signaling pathways in multiple sclerosis patients. *Ann Neurol* 43:340-349.

- Mata M, Hao S, Fink DJ (2008) Gene therapy directed at the neuroimmune component of chronic pain with particular attention to the role of TNF alpha. *Neurosci Lett* 437:209-213.
- McCoy MK, Tansey MG (2008) TNF signaling inhibition in the CNS: implications for normal brain function and neurodegenerative disease. *J Neuroinflammation* 5:45.
- McLaughlin KA et al. (2009) Age-dependent B cell autoimmunity to a myelin surface antigen in pediatric multiple sclerosis. *J Immunol* 183:4067-4076.
- McMahon SB, Bennett DL, Priestley JV, Shelton DL (1995) The biological effects of endogenous nerve growth factor on adult sensory neurons revealed by a trkA-IgG fusion molecule. *Nat Med* 1:774-780.
- Melanson M, Miao P, Eisenstat D, Gong Y, Gu X, Au K, Zhu W, Begum F, Frost E, Namaka M (2009) Experimental autoimmune encephalomyelitis-induced upregulation of tumor necrosis factor-alpha in the dorsal root ganglia. *Mult Scler*.
- Mense S (1990) Structure-function relationships in identified afferent neurones. *Anat Embryol (Berl)* 181:1-17.
- Miao P, Madec K, Gong Y, Shen H, Eisenstat D, Melanson M, Gu X, Leong C, Klowak M, Namaka M (2008) Axotomy-induced up-regulation of tumor necrosis factor-alpha in the dorsal root ganglia. *Neurol Res* 30:623-631.
- Miletic G, Miletic V (2002) Increases in the concentration of brain derived neurotrophic factor in the lumbar spinal dorsal horn are associated with pain behavior following chronic constriction injury in rats. *Neurosci Lett* 319:137-140.
- Millan MJ (1999) The induction of pain: an integrative review. *Prog Neurobiol* 57:1-164.
- Minagar A, Alexander JS (2003) Blood-brain barrier disruption in multiple sclerosis. *Mult Scler* 9:540-549.
- Moalem G, Tracey DJ (2006) Immune and inflammatory mechanisms in neuropathic pain. *Brain Res Rev* 51:240-264.
- Moller KA, Johansson B, Berge OG (1998) Assessing mechanical allodynia in the rat paw with a new electronic algometer. *J Neurosci Methods* 84:41-47.
- Muto T, Tsuchiya D, Morikawa K, Jingami H (2007) Structures of the extracellular regions of the group II/III metabotropic glutamate receptors. *Proc Natl Acad Sci U S A* 104:3759-3764.
- Myers RR, Sekiguchi Y, Kikuchi S, Scott B, Medicherla S, Protter A, Campana WM (2003) Inhibition of p38 MAP kinase activity enhances axonal regeneration. *Exp Neurol* 184:606-614.
- Naidu S, Kaufmann WE, Abrams MT, Pearlson GD, Lanham DC, Fredericksen KA, Barker PB, Horska A, Golay X, Mori S, Wong DF, Yablonski M, Moser HW, Johnston MV (2001) Neuroimaging studies in Rett syndrome. *Brain Dev* 23 Suppl 1:S62-71.
- Nakamura S, Myers RR (1999) Myelinated afferents sprout into lamina II of L3-5 dorsal horn following chronic constriction nerve injury in rats. *Brain Res* 818:285-290.
- Nakazawa T, Nakazawa C, Matsubara A, Noda K, Hisatomi T, She H, Michaud N, Hafezi-Moghadam A, Miller JW, Benowitz LI (2006) Tumor necrosis factor-alpha mediates oligodendrocyte death and delayed retinal ganglion cell loss in a mouse model of glaucoma. *J Neurosci* 26:12633-12641.
- Namaka M, Gramlich CR, Ruhlén D, Melanson M, Sutton I, Major J (2004) A treatment algorithm for neuropathic pain. *Clin Ther* 26:951-979.

- Nelson DA (1993) Dorsal root ganglia may be reservoirs of viral infection in multiple sclerosis. *Med Hypotheses* 40:278-283.
- Niino M, Fukazawa T, Kikuchi S, Sasaki H (2008) Therapeutic potential of vitamin D for multiple sclerosis. *Curr Med Chem* 15:499-505.
- Noctor SC, Martinez-Cerdeno V, Kriegstein AR (2007) Contribution of intermediate progenitor cells to cortical histogenesis. *Arch Neurol* 64:639-642.
- Nurmikko TJ, Gupta S, MacIver K Multiple sclerosis-related central pain disorders. *Curr Pain Headache Rep* 14:189-195.
- Obata K, Noguchi K (2006) BDNF in sensory neurons and chronic pain. *Neurosci Res* 55:1-10.
- Ohtori S, Takahashi K, Moriya H, Myers RR (2004) TNF-alpha and TNF-alpha receptor type 1 upregulation in glia and neurons after peripheral nerve injury: studies in murine DRG and spinal cord. *Spine* 29:1082-1088.
- Olechowski CJ, Truong JJ, Kerr BJ (2009) Neuropathic pain behaviours in a chronic-relapsing model of experimental autoimmune encephalomyelitis (EAE). *Pain* 141:156-164.
- Osterberg A, Boivie J (2009) Central pain in multiple sclerosis - Sensory abnormalities. *Eur J Pain*.
- Osterberg A, Boivie J, Thuomas KA (2005) Central pain in multiple sclerosis--prevalence and clinical characteristics. *Eur J Pain* 9:531-542.
- Ozenci V, Kouwenhoven M, Link H (2002) Cytokines in multiple sclerosis: methodological aspects and pathogenic implications. *Mult Scler* 8:396-404.
- Poliak S, Peles E (2003) The local differentiation of myelinated axons at nodes of Ranvier. *Nat Rev Neurosci* 4:968-980.
- Pollock J, McFarlane SM, Connell MC, Zehavi U, Vandenabeele P, MacEwan DJ, Scott RH (2002) TNF-alpha receptors simultaneously activate Ca<sup>2+</sup> mobilisation and stress kinases in cultured sensory neurones. *Neuropharmacology* 42:93-106.
- Portenoy RK, Yang K, Thornton D (1988) Chronic intractable pain: an atypical presentation of multiple sclerosis. *J Neurol* 235:226-228.
- Prineas JW, Barnard RO, Kwon EE, Sharer LR, Cho ES (1993) Multiple sclerosis: remyelination of nascent lesions. *Ann Neurol* 33:137-151.
- Prineas JW, Kwon EE, Goldenberg PZ, Ilyas AA, Quarles RH, Benjamins JA, Sprinkle TJ (1989) Multiple sclerosis. Oligodendrocyte proliferation and differentiation in fresh lesions. *Lab Invest* 61:489-503.
- Qiao LY, Gulick MA, Bowers J, Kuemmerle JF, Grider JR (2008) Differential changes in brain-derived neurotrophic factor and extracellular signal-regulated kinase in rat primary afferent pathways with colitis. *Neurogastroenterol Motil* 20:928-938.
- Quintao NL, Santos AR, Campos MM, Calixto JB (2008) The role of neurotrophic factors in genesis and maintenance of mechanical hypernociception after brachial plexus avulsion in mice. *Pain* 136:125-133.
- Rae-Grant AD, Eckert NJ, Bartz S, Reed JF (1999) Sensory symptoms of multiple sclerosis: a hidden reservoir of morbidity. *Mult Scler* 5:179-183.
- Raine CS, Wu E (1993) Multiple sclerosis: remyelination in acute lesions. *J Neuropathol Exp Neurol* 52:199-204.
- Raine CS, Moore GR, Hintzen R, Traugott U (1988) Induction of oligodendrocyte proliferation and remyelination after chronic demyelination. Relevance to multiple sclerosis. *Lab Invest* 59:467-476.

- Rambourg A, Clermont Y, Beaudet A (1983) Ultrastructural features of six types of neurons in rat dorsal root ganglia. *J Neurocytol* 12:47-66.
- Ramer MS, Bisby MA (1999) Adrenergic innervation of rat sensory ganglia following proximal or distal painful sciatic neuropathy: distinct mechanisms revealed by anti-NGF treatment. *Eur J Neurosci* 11:837-846.
- Rasband MN, Park EW, Vanderah TW, Lai J, Porreca F, Trimmer JS (2001) Distinct potassium channels on pain-sensing neurons. *Proc Natl Acad Sci U S A* 98:13373-13378.
- Raskin J, Smith TR, Wong K, Pritchett YL, D'Souza DN, Iyengar S, Wernicke JF (2006) Duloxetine versus routine care in the long-term management of diabetic peripheral neuropathic pain. *J Palliat Med* 9:29-40.
- Ratcliffe CF, Westenbroek RE, Curtis R, Catterall WA (2001) Sodium channel beta1 and beta3 subunits associate with neurofascin through their extracellular immunoglobulin-like domain. *J Cell Biol* 154:427-434.
- Richardson PM, Riopelle RJ (1984) Uptake of nerve growth factor along peripheral and spinal axons of primary sensory neurons. *J Neurosci* 4:1683-1689.
- Rose NR (1998) The role of infection in the pathogenesis of autoimmune disease. *Semin Immunol* 10:5-13.
- Sah DW, Ossipo MH, Porreca F (2003) Neurotrophic factors as novel therapeutics for neuropathic pain. *Nat Rev Drug Discov* 2:460-472.
- Saha RN, Liu X, Pahan K (2006) Up-regulation of BDNF in astrocytes by TNF-alpha: a case for the neuroprotective role of cytokine. *J Neuroimmune Pharmacol* 1:212-222.
- Schafers M, Svensson CI, Sommer C, Sorkin LS (2003a) Tumor necrosis factor-alpha induces mechanical allodynia after spinal nerve ligation by activation of p38 MAPK in primary sensory neurons. *J Neurosci* 23:2517-2521.
- Schafers M, Sorkin LS, Geis C, Shubayev VI (2003b) Spinal nerve ligation induces transient upregulation of tumor necrosis factor receptors 1 and 2 in injured and adjacent uninjured dorsal root ganglia in the rat. *Neurosci Lett* 347:179-182.
- Schafers M, Geis C, Brors D, Yaksh TL, Sommer C (2002) Anterograde transport of tumor necrosis factor-alpha in the intact and injured rat sciatic nerve. *J Neurosci* 22:536-545.
- Schafers M, Geis C, Svensson CI, Luo ZD, Sommer C (2003c) Selective increase of tumour necrosis factor-alpha in injured and spared myelinated primary afferents after chronic constrictive injury of rat sciatic nerve. *Eur J Neurosci* 17:791-804.
- Scheltens P, Barkhof F, Valk J, Algra PR, van der Hoop RG, Nauta J, Wolters EC (1992) White matter lesions on magnetic resonance imaging in clinically diagnosed Alzheimer's disease. Evidence for heterogeneity. *Brain* 115 ( Pt 3):735-748.
- Siebert RJ, Abernethy DA (2005) Depression in multiple sclerosis: a review. *J Neurol Neurosurg Psychiatry* 76:469-475.
- Simone IL, Carrara D, Tortorella C, Liguori M, Lepore V, Pellegrini F, Bellacosa A, Ceccarelli A, Pavone I, Livrea P (2002) Course and prognosis in early-onset MS: comparison with adult-onset forms. *Neurology* 59:1922-1928.
- Snutch TP (2005) Targeting Chronic and Neuropathic Pain: The N-type Calcium Channel Comes of Age. *NeuroRx* 2:662-670.
- Soderstrom M (2001) Optic neuritis and multiple sclerosis. *Acta Ophthalmol Scand* 79:223-227.

- Sohn YH, Kim JS (1998) The influence of white matter hyperintensities on the clinical features of Parkinson's disease. *Yonsei Med J* 39:50-55.
- Sommer C, Schafers M (1998) Painful mononeuropathy in C57BL/Wld mice with delayed wallerian degeneration: differential effects of cytokine production and nerve regeneration on thermal and mechanical hypersensitivity. *Brain Res* 784:154-162.
- Sommer C, Kress M (2004) Recent findings on how proinflammatory cytokines cause pain: peripheral mechanisms in inflammatory and neuropathic hyperalgesia. *Neurosci Lett* 361:184-187.
- Sommer C, Schmidt C, George A (1998a) Hyperalgesia in experimental neuropathy is dependent on the TNF receptor 1. *Exp Neurol* 151:138-142.
- Sommer C, Marziniak M, Myers RR (1998b) The effect of thalidomide treatment on vascular pathology and hyperalgesia caused by chronic constriction injury of rat nerve. *Pain* 74:83-91.
- Sommer C, Lindenlaub T, Teuteberg P, Schafers M, Hartung T, Toyka KV (2001) Anti-TNF-neutralizing antibodies reduce pain-related behavior in two different mouse models of painful mononeuropathy. *Brain Res* 913:86-89.
- Sorkin LS, Xiao WH, Wagner R, Myers RR (1997) Tumour necrosis factor-alpha induces ectopic activity in nociceptive primary afferent fibres. *Neuroscience* 81:255-262.
- Sotelo J (2007) On the viral hypothesis of multiple sclerosis: participation of varicella-zoster virus. *J Neurol Sci* 262:113-116.
- Svendsen KB, Jensen TS, Hansen HJ, Bach FW (2005) Sensory function and quality of life in patients with multiple sclerosis and pain. *Pain* 114:473-481.
- Takahashi N, Kikuchi S, Shubayev VI, Campana WM, Myers RR (2006) TNF-alpha and phosphorylation of ERK in DRG and spinal cord: insights into mechanisms of sciatica. *Spine* 31:523-529.
- Takei Y, Laskey R (2008a) Tumor necrosis factor alpha regulates responses to nerve growth factor, promoting neural cell survival but suppressing differentiation of neuroblastoma cells. *Mol Biol Cell* 19:855-864.
- Takei Y, Laskey R (2008b) Interpreting crosstalk between TNF-alpha and NGF: potential implications for disease. *Trends Mol Med* 14:381-388.
- Temburni MK, Jacob MH (2001) New functions for glia in the brain. *Proc Natl Acad Sci U S A* 98:3631-3632.
- Theodosiou M, Rush RA, Zhou XF, Hu D, Walker JS, Tracey DJ (1999) Hyperalgesia due to nerve damage: role of nerve growth factor. *Pain* 81:245-255.
- Trapp BD, Ransohoff R, Rudick R (1999) Axonal pathology in multiple sclerosis: relationship to neurologic disability. *Curr Opin Neurol* 12:295-302.
- Trinchieri G (1995) Interleukin-12: a proinflammatory cytokine with immunoregulatory functions that bridge innate resistance and antigen-specific adaptive immunity. *Annu Rev Immunol* 13:251-276.
- Tsai EC, Dalton PD, Shoichet MS, Tator CH (2004) Synthetic hydrogel guidance channels facilitate regeneration of adult rat brainstem motor axons after complete spinal cord transection. *J Neurotrauma* 21:789-804.
- Tsuda M, Masuda T, Kitano J, Shimoyama H, Tozaki-Saitoh H, Inoue K (2009) IFN-gamma receptor signaling mediates spinal microglia activation driving neuropathic pain. *Proc Natl Acad Sci U S A* 106:8032-8037.

- Ugolini G, Marinelli S, Covaceuszach S, Cattaneo A, Pavone F (2007) The function neutralizing anti-TrkA antibody MNAC13 reduces inflammatory and neuropathic pain. *Proc Natl Acad Sci U S A* 104:2985-2990.
- Ulmann L, Hatcher JP, Hughes JP, Chaumont S, Green PJ, Conquet F, Buell GN, Reeve AJ, Chessell IP, Rassendren F (2008) Up-regulation of P2X4 receptors in spinal microglia after peripheral nerve injury mediates BDNF release and neuropathic pain. *J Neurosci* 28:11263-11268.
- Umapathi T, Chaudhry V (2005) Toxic neuropathy. *Curr Opin Neurol* 18:574-580.
- Vallejo R, Tilley DM, Vogel L, Benyamin R The role of glia and the immune system in the development and maintenance of neuropathic pain. *Pain Pract* 10:167-184.
- Van't Veer A, Du Y, Fischer TZ, Boetig DR, Wood MR, Dreyfus CF (2009) Brain-derived neurotrophic factor effects on oligodendrocyte progenitors of the basal forebrain are mediated through trkB and the MAP kinase pathway. *J Neurosci Res* 87:69-78.
- van Dorp R, Jalink K, Oudega M, Marani E, Ypey DL, Ravesloot JH (1990) Morphological and functional properties of rat dorsal root ganglion cells cultured in a chemically defined medium. *Eur J Morphol* 28:430-444.
- Wagner R, Myers RR (1996) Endoneurial injection of TNF-alpha produces neuropathic pain behaviors. *Neuroreport* 7:2897-2901.
- Wall PD (1967) The laminar organization of dorsal horn and effects of descending impulses. *J Physiol* 188:403-423.
- Wang R, Guo W, Ossipov MH, Vanderah TW, Porreca F, Lai J (2003) Glial cell line-derived neurotrophic factor normalizes neurochemical changes in injured dorsal root ganglion neurons and prevents the expression of experimental neuropathic pain. *Neuroscience* 121:815-824.
- Wang TH, Meng QS, Qi JG, Zhang WM, Chen J, Wu LF (2008) NT-3 expression in spared DRG and the associated spinal laminae as well as its anterograde transport in sensory neurons following removal of adjacent DRG in cats. *Neurochem Res* 33:1-7.
- Wang X, Ratnam J, Zou B, England PM, Basbaum AI (2009) TrkB signaling is required for both the induction and maintenance of tissue and nerve injury-induced persistent pain. *J Neurosci* 29:5508-5515.
- Wasan AD, Ossanna MJ, Raskin J, Wernicke JF, Robinson MJ, Hall JA, Edwards SE, Lipsius S, Meyers AL, McCarberg BH (2009) Safety and efficacy of duloxetine in the treatment of diabetic peripheral neuropathic pain in older patients. *Curr Drug Saf* 4:22-29.
- Waubant E (2006) Biomarkers indicative of blood-brain barrier disruption in multiple sclerosis. *Dis Markers* 22:235-244.
- Waxman SG, Ritchie JM (1993) Molecular dissection of the myelinated axon. *Ann Neurol* 33:121-136.
- Wiendl H, Kieseier BC (2003) Disease-modifying therapies in multiple sclerosis: an update on recent and ongoing trials and future strategies. *Expert Opin Investig Drugs* 12:689-712.
- Wilson-Gerwing TD, Stucky CL, McComb GW, Verge VM (2008) Neurotrophin-3 significantly reduces sodium channel expression linked to neuropathic pain states. *Exp Neurol* 213:303-314.

- Won R, Lee BH, Park S, Kim SH, Park YG, Chung SS (2000) Role of different peripheral components in the expression of neuropathic pain syndrome. *Yonsei Med J* 41:354-361.
- Woolf CJ, Mannion RJ (1999) Neuropathic pain: aetiology, symptoms, mechanisms, and management. *Lancet* 353:1959-1964.
- Woolf CJ, Ma QP, Allchorne A, Poole S (1996) Peripheral cell types contributing to the hyperalgesic action of nerve growth factor in inflammation. *J Neurosci* 16:2716-2723.
- Woolf CJ, Allchorne A, Safieh-Garabedian B, Poole S (1997) Cytokines, nerve growth factor and inflammatory hyperalgesia: the contribution of tumour necrosis factor alpha. *Br J Pharmacol* 121:417-424.
- Xu JT, Xin WJ, Zang Y, Wu CY, Liu XG (2006) The role of tumor necrosis factor-alpha in the neuropathic pain induced by Lumbar 5 ventral root transection in rat. *Pain* 123:306-321.
- Yajima Y, Narita M, Usui A, Kaneko C, Miyatake M, Yamaguchi T, Tamaki H, Wachi H, Seyama Y, Suzuki T (2005) Direct evidence for the involvement of brain-derived neurotrophic factor in the development of a neuropathic pain-like state in mice. *J Neurochem* 93:584-594.
- Yang HW, Lemon RN (2003) An electron microscopic examination of the corticospinal projection to the cervical spinal cord in the rat: lack of evidence for cortico-motoneuronal synapses. *Exp Brain Res* 149:458-469.
- Yang J, Siao CJ, Nagappan G, Marinic T, Jing D, McGrath K, Chen ZY, Mark W, Tessarollo L, Lee FS, Lu B, Hempstead BL (2009) Neuronal release of proBDNF. *Nat Neurosci* 12:113-115.
- Yao H, Donnelly DF, Ma C, LaMotte RH (2003) Upregulation of the hyperpolarization-activated cation current after chronic compression of the dorsal root ganglion. *J Neurosci* 23:2069-2074.
- Yip HK, Johnson EM, Jr. (1986) Comparative dynamics of retrograde transport of nerve growth factor and horseradish peroxidase in rat lumbar dorsal root ganglia. *J Neurocytol* 15:789-798.
- Yoshida S, Matsuda Y (1979) Studies on sensory neurons of the mouse with intracellular-recording and horseradish peroxidase-injection techniques. *J Neurophysiol* 42:1134-1145.
- Zelenka M, Schafers M, Sommer C (2005) Intraneural injection of interleukin-1beta and tumor necrosis factor-alpha into rat sciatic nerve at physiological doses induces signs of neuropathic pain. *Pain* 116:257-263.
- Zhang W, Liu HT (2002) MAPK signal pathways in the regulation of cell proliferation in mammalian cells. *Cell Res* 12:9-18.
- Zhou XF, Rush RA (1996) Endogenous brain-derived neurotrophic factor is anterogradely transported in primary sensory neurons. *Neuroscience* 74:945-953.
- Zimmermann M (2001) Pathobiology of neuropathic pain. *Eur J Pharmacol* 429:23-37.
- Zweifel LS, Kuruvilla R, Ginty DD (2005) Functions and mechanisms of retrograde neurotrophin signalling. *Nat Rev Neurosci* 6:615-625.

## CHAPTER 9: APPENDIX

### RECEIPES

#### A. ANIMAL PERFUSION

##### **-100ml of pre-fix solution**

NaCl	0.9g
NaNO <sub>3</sub>	0.1g
Heparin	1 IU
Water	80ml

Bring up to 100ml with ddH<sub>2</sub>O

##### **-1 L 0.5M phosphate stock solution**

**Sodium phosphate dibasic anhydrous (Na<sub>2</sub>HPO<sub>4</sub>, MW=141.96)** 70.97g

ddH<sub>2</sub>O 900 ml

Warm to dissolve well, cool to room temperature,

Bring to 1 L with ddH<sub>2</sub>O

**Sodium phosphate monobasic monohydrate (NaH<sub>2</sub>PO<sub>4</sub>·H<sub>2</sub>O, MW=137.99)** 17.33g

ddH<sub>2</sub>O 200ml

Bring to 250 ml with ddH<sub>2</sub>O

Add above dibasic Na<sub>2</sub>HPO<sub>4</sub> solution to monobasic NaH<sub>2</sub>PO<sub>4</sub> solution until pH is 7.4, store at room temperature.

##### **-100ml of fixative solution**

Paraformaldehyde 4g

ddH<sub>2</sub>O 50 ml

Heat to 65°C while stirring

Turn heat off and continue to stir

Clear the solution with 1-2 drops of 10N NaOH

Cool to room temperature

Add 20ml 0.5M phosphate buffer solution

Filter with #1 filter paper

Adjust pH to 7.0 with 1N HCl

Bring up to 100ml with ddH<sub>2</sub>O

## **B. IN SITU HYBRIDIZATION**

### **-1 L of DEPC water**

DEPC 1ml

Autoclaved water 1 L

Shake vigorously and keep overnight (12hrs) at 37°C in a RNase free flask

Autoclave the DEPC treated water.

### **-1L of DEPC treated PBS (pH 7.4)**

140mM of NaCl (Sigma# S9888) 8.18 g

2.7mM of KCl (Sigma#P8041) 0.20 g

10mM of Na<sub>2</sub>HPO<sub>4</sub> (Fisher #S374) 1.41g

1.8mM of KH<sub>2</sub>PO<sub>4</sub> (Sigma# P9791) 0.24 g

Bring up to 1L with DEPC treated water

### **-100 ml of DEPC treated PBS containing 100mM Glycine (Sigma#G8898)**

Glycine 0.75 g

Bring up to 100 ml with DEPC treated PBS

### **- 100 ml of DEPC treated PBS containing 0.3% of Triton –X-100 (Sigma# X-100)**

Triton (x-100) 0.3 ml

Bring up to 100ml with DEPC treated PBS

### **-100 ml of DEPC treated PBS containing 4% Paraformaldehyde (Fisher, cat# 04042)**

Paraformaldehyde 4g

DEPC treated PBS 80 ml

Stir and heat up to 65°C

Turn off the heat and continue to stir

Add 10N NaOH to clear the solution

Cool to room temperature

Filter with filter paper  
 Adjust pH (7.4) with 1N HCl  
 Bring up to 100 ml with DEPC H<sub>2</sub>O  
**- 100 ml of 20x SSC**  
 Sodium citrate (Sigma# S1804) 8.82 g  
 Sodium chloride (Sigma# S9625) 17.53 g  
 DEPC H<sub>2</sub>O 80 ml  
 Adjust pH 7.0  
 Bring up to 100ml with DEPC H<sub>2</sub>O  
**-100 ml of 2x SSC**  
 20xSSC 10 ml  
 Bring up to 100 ml with DEPC H<sub>2</sub>O  
**-100 ml of 1x SSC**  
 20x SSC 5 ml  
 Bring up to 100 ml with DEPC H<sub>2</sub>O  
**-Buffer 1 (100mM Tris HCl, 150 mM NaCl)**  
 1 M stock Tris-HCl (7.5) 10 ml  
 NaCl 0.88 g  
 Bring up to 100 ml with autoclaved H<sub>2</sub>O  
**-Buffer 2 (100 mM Tris-HCl, 100 mM NaCl, 50 mM MgCl<sub>2</sub>)**  
 1 M stock Tris-HCl (9.5) 10 ml  
 NaCl 0.58 g  
 MgCl<sub>2</sub> 1.01 g  
 Bring up to 100 ml with autoclaved H<sub>2</sub>O  
**-Buffer 3 (10 mM Tris-HCl, 1 mM EDTA)**  
 1 M stock Tris-HCl (8.1) 1ml  
 0.5 M stock EDTA 0.2 ml  
**-100 ml of TE buffer (100mM Tris- HCl, 50 mM EDTA , pH 8.0)**  
 1M stock Tris HCl (pH 8.0) 10 ml  
 0.5 M stock of EDTA 10 ml  
 Top up to 100 ml with DEPC H<sub>2</sub>O

**-50 ml of 50% Dextran Sulphate (Sigma, Cat#8906)**

Dextran Sulphate 25 g

Bring to 50 ml with DEPC H<sub>2</sub>O

Warm to 65° C

Aliquot and keep into -80°C

When ready to use warm to 65°C

**-6.5 ml of 1M DTT (Sigma, Cat#D0632)**

DTT 1 gm

DEPC H<sub>2</sub>O 6.5 ml

Vortex properly

Aliquot and store at -80°C